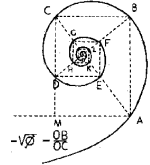# UNIVERSITÀ DEGLI STUDI DI MILANO

SCUOLA DI DOTTORATO IN MEDICINA MOLECOLARE

CICLO XXVIII
Anno Accademico 2014/2015

TESI DI DOTTORATO DI RICERCA
MED/04

Myc-driven epigenetic memory maintains Embryonic Stem cell identity

Dottorando: Alessandro Cherubini
Matricola N° R10202

TUTORE: Ch.mo Prof. Mario Clerici
CO-TUTORE: Dr. Alessio Zippo

DIRETTORE DEL DOTTORATO: Ch.mo Prof. Mario Clerici

ABSTRACT

Stem cells balance their self-renewal and differentiation potential by integrating environmental signals with the Transcriptional Regulatory Network (TRN). Moreover, the integration between extrinsic and intrinsic signals affects the maintenance of their epigenetic state, establishing an accurate cells identity. Although c-Myc transcription factors plays a major role in stem cells self-renewal and pluripotency, their mechanisms of actions and their ability to establish an epigenetic memory remains poorly defined. We addressed this point by profiling the epigenetic pattern and gene expression in Embryonic Stem (ES) cells, whose growth depends on conditional c-Myc activity. Here we show that c-Myc potentiates the Wnt/β-Catenin signaling pathway, which cooperates with the transcriptional regulatory network in sustaining ES cells self-renewal. c-Myc activation results in the transcriptional repression of Wnt antagonists Dkk1 and Sfrp1 through the direct recruitment of PRC2 on these targets. We found that, through these molecular mechanisms, c-Myc promotes pluripotency and self-renewal of ES cells by activating an alternative epigenetic program. Finally our data suggest that the consequent potentiation of the autocrine Wnt/β-Catenin signaling induces the transcriptional activation of the endogenous Myc family members, which in turn activates a Myc-driven self-reinforcing circuit. Thus, our data unravel a Myc-dependent self-propagating epigenetic memory in the maintenance of ES cell identity.

SOMMARIO

Le cellule staminali bilanciano la loro capacità di fare self-renewal e il loro potenziale di differenziamento integrando segnali ambientali con il Network di Regolazione Trascrizionale (TRN). Inoltre, l'integrazione tra segnali estrinseci e intrinseci influenza il mantenimento dello stato epigenetico, stabilendo una precisa identità cellulare. Sebbene il fattore di trascrizione c-Myc abbia un ruolo fondamentale nel mantenimento del self-renewal e della pluripotenza delle cellule staminali, i suoi meccanismi di azione e la sua capacità di stabilire una memoria epigenetica sono poco conosciuti. Abbiamo investigato su questo aspetto, analizzando il pattern epigenetico e l'espressione genica di cellule Staminali Embrionali (ES) cresciute in modo dipendente dall'attività di c-Myc. Mostriamo che c-Myc potenzia la via di segnalazione Wnt/β-Catenina, che coopera con il TRN, sostenendo il self-renewal delle cellule staminali embrionali. L'attivazione di c-Myc causa la repressione trascrizionale degli antagonisti del Wnt, tramite il reclutamento diretto di PRC2 a livello di questi target. Il conseguente potenziamento della via Wnt/β-Catenina autocrina induce l'attivazione trascrizionale dei geni endogeni della famiglia Myc, i quali a loro volta attivano un circuito auto-regolatorio dipendente da Myc. I nostri dati descrivono un meccanismo di mantenimento della capacità di self-renewal delle cellule staminali embrionali basato su una memoria epigenetica indotta da Myc, in grado di auto-propagarsi.

TABLE OF CONTENTS

List of figures

List of Abbreviations

4-OHT	4-Hydroxytamoxifen
AEBP2	Adipocyte Enhancer-Binding Protein 2
AKT	RAC-alpha serine/threonine-protein kinase
AP	Alkaline Phosphatase
bHLH	basic Helix Loop Helix
BSA	Bovine Serum Albumin
CFP	Cyan Fluorescence Protein
ChIP	Chromatin immunoprecipitation
c-Myc	vMyc avian myelocytomatosis viral oncogene homolog
CSCs	Cancer Stem Cells
Dkk1	Dickkopf homolog 1
DMEM	Dulbecco's Modified Eagles Medium
DMSO	Dymethyl sulfoxide
DNA	Deoxyribonucleic acid
EBs	Embryoid Bodies
EDTA	ethylenediamininetetraacetic
EED	Embryonic Ectoderm Development
eGFP	Green Fluorescence Protein
EpiSC	Epiblast Stem Cells
ER	Estrogen Receptor
ES cells	Embryonic Stem cells
EZH1/2	Enhancer of Zeste Homolog 1/2
FACS	Fluorescence Activated Cell Sorting
FBS	Fetal Bovine Serum
FRET	Fluorescence Resonance Energy Transfer
GSK3β	Glycogen Synthase Kinase 3 b
h	hours

HRP	Horseradish peroxidase
ICM	Inner Cell Mass
IMEC	Immortalized Mammary Epithelial Cells
KSR	Knockout Serum Replacement
LIF	Leukaemia Inhibitory Factor
Lrp6	Low density lipoprotein receptor-related protein 6
MBII	Myc Box II
MEBM	Mammary Epithelial Basal Medium
min	minutes
MOI	Multiplicity Of Infection
NEAA	Non-Essential Amino Acids
ON	Over Night
PBS	Phosphate-Buffered Saline
PcG	Polycomb group
PCR	Polymerase Chain Reaction
Pen/Strep	Penicillin/Streptomycin
PFA	Paraformaldehyde
PI	Propidium Iodide
PMSF	Phenylmethyl sulfonyl fluoride
PRC 1/2	Polycomb Repressive Complex 1/2
RNA	Ribonucleic acid
RT	Room Temperature
Sfrp1	Secreted frizzled-related protein 1
shRNA	Short hairpin interfering RNA
SUZ12	Suppressor of Zeste 12
TAD	Trans Activation Domain
TFs	Transcription factors
Wnt3a	Wingless-type member 3A
YFP	Yellow Fluorescence Protein

1. INTRODUCTION

1.1 Epigenetics

The development of a complex organism requires a single genome to generate a multitude of cell phenotypes. The term "epigenetic" appeared in 1942, along with the idea that genetics and developmental biology should be related each other. Conrad Waddington, by using the prefix epi- ("above" in Greek), suggested the existence of mechanisms besides the gene sequence that participate to the acquisition and maintenance of a specific cell identity [Holliday, 2006]. In addition to differentiation processes, a cell will be exposed to multiple events including mitotic and apoptotic signals, DNA repair, metabolite availability, drug exposure or the general chemical environment. All those events require more or less rapid activation or silencing of specific genes and these changes have to be maintained for a short or long term. Thus, the cell has to sense its environment in order to adapt the transcriptional levels of important genes and to maintain proper functions [Bird and Tweedie, 1995] (Figure 1.1). In the nucleus, the DNA is associated with histone proteins, RNAs and non-histone proteins, in an organized structure named "chromatin fiber". Chromatin components are subjected to chemical modifications, which are then interpreted by the transcriptional machinery for appropriate gene expression. Importantly, the activities of enzymes that add and remove those chemical "marks" have been shown to directly or indirectly depend on the environment. It has been proposed that the chromatin fiber, through modifying enzymes, acts as an environmental sensor and a signaling unit for the alteration of gene expression. Thus, it is of general interest to understand how environmental agents can impact on the activity of the genome in a short or long-term manner [Turner, 2009].
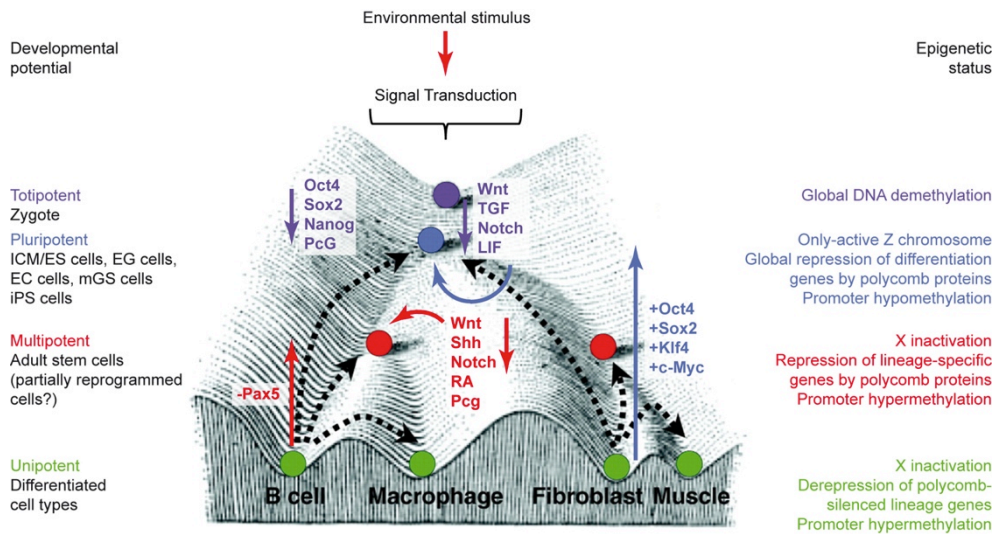
Figure 1.1 Waddington model.
Developmental restrictions can be illustrated as marbles rolling down from the hill into one of several valleys. In response to environmental stimuli, a particular signal transduction is activated, which leads to a defined epigenetic state, corresponding to different developmental potentials. [Modified from Mohammad and Baylin, 2010].

1.1.1 Chromatin organization and dynamics

In eukaryotic cells, chromatin has a highly complex structure with several levels of organization (Figure 1.2). The nucleosome, basic unit of chromatin, consists of a histone octamer, which contains a pair of each of the core histone proteins: H2A, H2B, H3 and H4 [Luger et al., 1997], around which 147 base pairs of DNA are wrapped. A fifth histone protein, the lysine-rich histone H1, was found to sit on top of the nucleosome, outside the core octamer, and to associate with the DNA at the entry/exit sites of the nucleosome. Finally, the portion of free DNA between adjacent nucleosomes was called "linker DNA". The length of linker DNA partly dictates nucleosome positioning and is considered as an important factor in chromatin function. In fact, it is likely that the position of nucleosomes in the chromatin fiber is a key determinant for the accessibility of various DNA-

binding proteins and therefore affects gene regulation. However, how high levels of DNA compaction are established is not fully understood yet.

A series of modifications to the DNA itself and to histone proteins have been characterized and termed "epigenetic modifications". Many studies have correlated these "marks" with gene activity and several mechanisms describe how specific modifications induce transcriptional activation or silencing. Thus, it seems that the chromatin is not a simple packaging tool but also a platform for signaling that regulates gene expression.
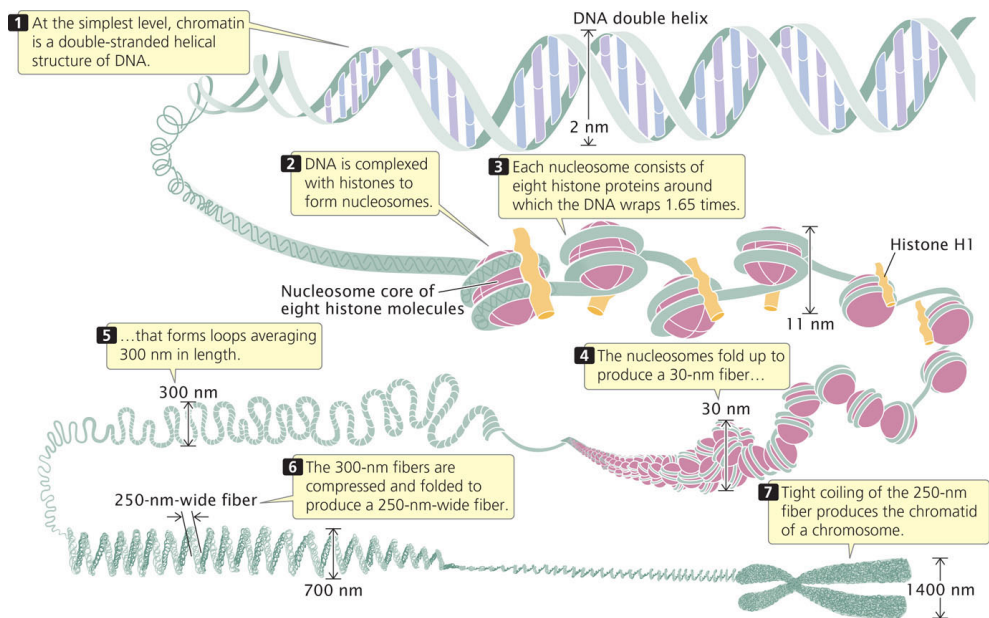
Figure 1.2 The different levels of chromatin compaction.
Chromosomal DNA is packaged inside nuclei with the help of histones, forming complexes called nucleosomes. Each nucleosome is composed of DNA wound 1.65 times around eight histone proteins. Nucleosomes fold up to form a 30-nanometer chromatin fiber, which forms loops averaging 300 nanometers in length. The fibers are compressed and folded into the chromatids of a chromosome.

1.1.2 Histone modifications

All histone proteins possess unstructured N-terminal tails that extend out from the nucleosome core. These exposed tails are subjected to a wide variety of post-translational modifications such as acetylation, methylation, phosphorylation, ubiquitination or ADP-ribosylation (Figure 1.3). Specific histone modifications are deposited on specific residues. For instance lysine (K) can be acetylated, ubiquitinated or sumoylated, while serine (S) are phosphorylated. Methylation occurs on both lysine and arginine (R) and at different levels, as a residue can be mono-, di- or tri-methylated [Kouzarides, 2007]. Histone modifications alter transcription via direct or indirect effects. For instance, acetylation was shown to loose the chromatin fiber by neutralizing the positive charge of lysines. Thereby, the association of histones with DNA is weakened, allowing transcription factors and RNA polymerase to bind to regulatory sequences [Tse et al., 1998]. Histone modifications can also indirectly lead to changes in gene expression, as they are specifically recognized by proteins that will then impact on the function of the adjacent chromatin [Taverna et al., 2007].
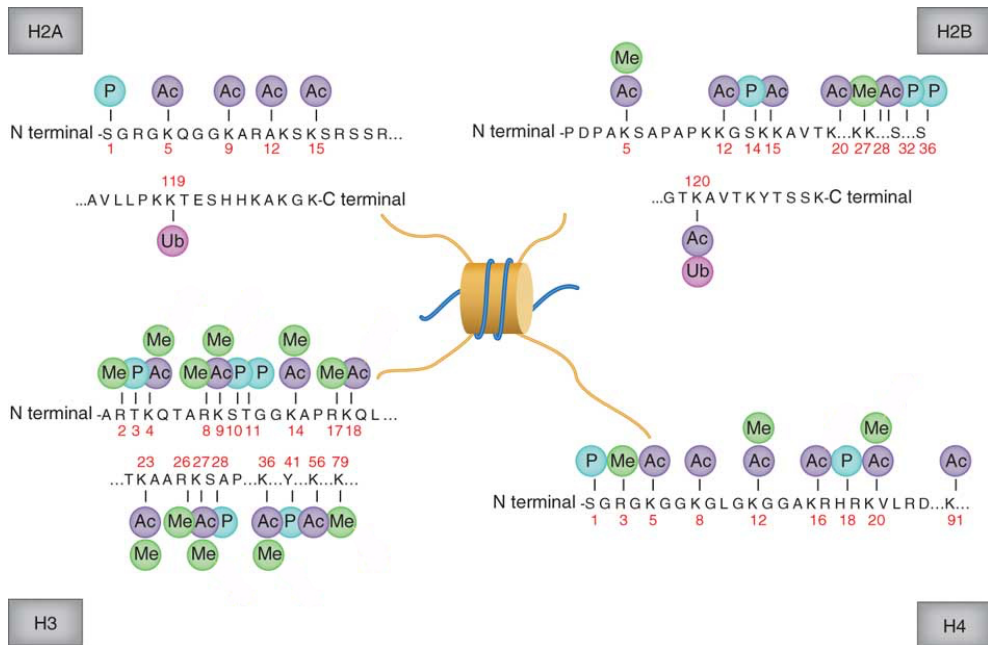
Figure 1.3 Histone modification patterns.
Histone tails are subjected to many post-translational modifications that occur on specific residues. In the right combination, these modifications determine gene expression, therefore establishing the global and local, condensed or de-condensed chromatin states.

1.1.3 DNA methylation

DNA methylation is another epigenetic modification that has been consistently associated with transcriptional silencing. The covalent addition of a methyl (CH3) group occurs at the 5-carbon of the cytosine ring, resulting in 5-methylcytosine (5-mC). The addition of methyl groups is affected at different levels in cells and is carried out by a family of enzymes called DNA methyltransferases (DNMTs), which contain DNMT1, DNMT3a and DNMT3b. In mammals, DNA methylation occurs almost exclusively in the symmetric CG context. However, evidence of non-CG methylation was found in ES cells [Ramsahoye et al., 2000]. In mammals, the CG dinucleotides are mostly found near gene promoters in dense clusters,

called CpG islands. However, the distribution of DNA methylation in the genome is uneven, as a significant number of CG dinucleotides are unmethylated [Suzuki and Bird, 2008]. Slightly less than half of all genes are associated with CpG islands, and they are either housekeeping or tissue-restricted genes [Cross and Bird, 1995]. Although most of the CpG islands remain unmethylated, there are some important exceptions such as the methylation of the inactive X-chromosome or the CpG islands associated with imprinted genes [Ideraabdullah et al., 2008].

1.1.4 Histone modifications depositions

Large families of specific enzymes are responsible for the deposition or removal of histone modifications. The enrichment of each mark is therefore the results of a dynamic process involving the activity of two enzymes that catalyze opposite reactions.

The methylation state of histone tails also depends on the antagonistic actions of large families of enzymes. Lysine residues are methylated by lysine methyl-transferases (KMTs), that contain a conserved SET-domain responsible for the transfer of a methyl group from S-adenosyl-L-methionin (SAM), leading to the production of S-adenosyl-L-homocysteine (SAH). SET-domain containing enzymes have been classified into seven principal families (SUV39, SET1, SET2, EZ, RIZ, SMYD and SUV4) according to sequence homology and function. All KMTs are residue-specific, for instance the EZ family induce methylation of lysine 27 of histone H3.

Lysine methylation has been considered as a dynamic modification since the discovery of lysine demethylases (KDMs), although not all residues have had a demethylases identified so far.

As previously mentioned, histone proteins are subjected to a wide variety of post-translational modifications, in addition to methylation. Kinases and phosphatases respectively add and remove phosphate groups on serine,

threonine and tyrosine residues. Acetylases and deacetylases respectively add and remove acetyl groups on lysine residues. While ubiquitin-ligases and de-ubiquitin enzymes control lysine ubiquitination levels on H2A and H2B [Bannister and Kouzarides, 2011].

1.1.5 Binding histone modifications

Many chromatin-associated proteins possess particular domains able to recognize and bind specific modifications. For instance, bromodomains are capable of interaction with acetyl residues, while a wide range of domains including chromodomains, Tudor domains or PHD fingers, recognizes methyl marks. Along with the diversity of histone modifications, the diversity of "reader" domains provides a new explanation for the multiple outcomes of chromatin marks [Taverna et al., 2007]. In fact, reader domains give a chance for modifying enzymes and chromatin-binding proteins to communicate. Thereby, a series of modifications can act together to regulate transcription in a specific manner [Jenuwein and Allis, 2001; Spotswood and Turner, 2002]. All chromatin-remodeling complexes, which move nucleosome to regulate DNA accessibility, recognize histone modifications and interact with chromatin modifiers [Clapier and Cairns, 2009]. This complexity supports the idea of cross-talk between different histone marks and a code for transcription (Figure 1.4), called "histone code" [Jenuwein and Allis, 2001].
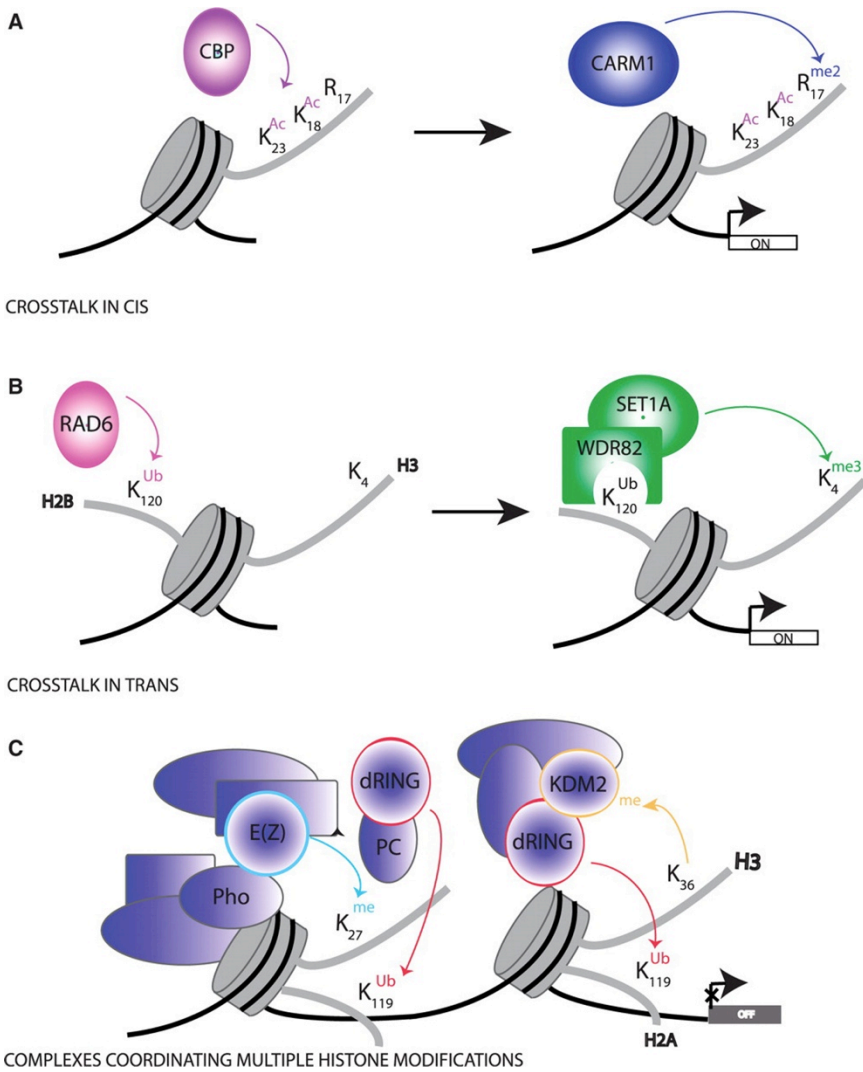
Figure 1.4 Cross-talk between different histone modifications.
Histone modifications are recognized by specific motifs of binding proteins. Therefore, when protein readers interact each other, they lead to cross-talk between histone marks. [Izzo and Schneider, 2010].

1.2 Embryonic Stem cells

Embryonic Stem (ES) cells derive from the inner cell mass (ICM) of early blastocyst. Gene targeting experiments in ES cells have become a major tool to determine gene function in mammals [Capecchi, 2005]. Two main features characterize Embryonic Stem cells: the capacity for prolonged self-renewal and the potential to give rise to any cell type comprising the adult organism. In fact, ES cells injected into blastocyst are able to generate a chimeric animal, confirming their pluripotent nature. Since then, many studies have monitored ES cells differentiation pathway and identifying specific marker. Based on those studies, protocols that involve the spatial rearrangement of cells in culture and exposure to specific environmental factors were described, in order to drive differentiation of ES cells into defined lineages (Figure 1.5) [Murry and Keller, 2008]. Hence, differentiation of ES cells in culture constitutes a precious tool to study the establishment and long-term maintenance of specific gene expression programs that define cell identity. A full understanding of pluripotency and cell fate is crucial for the development of regenerative medicine and to speculate on the mechanisms of tumorigenesis, as cancer cells can present a stem cell-like phenotype.
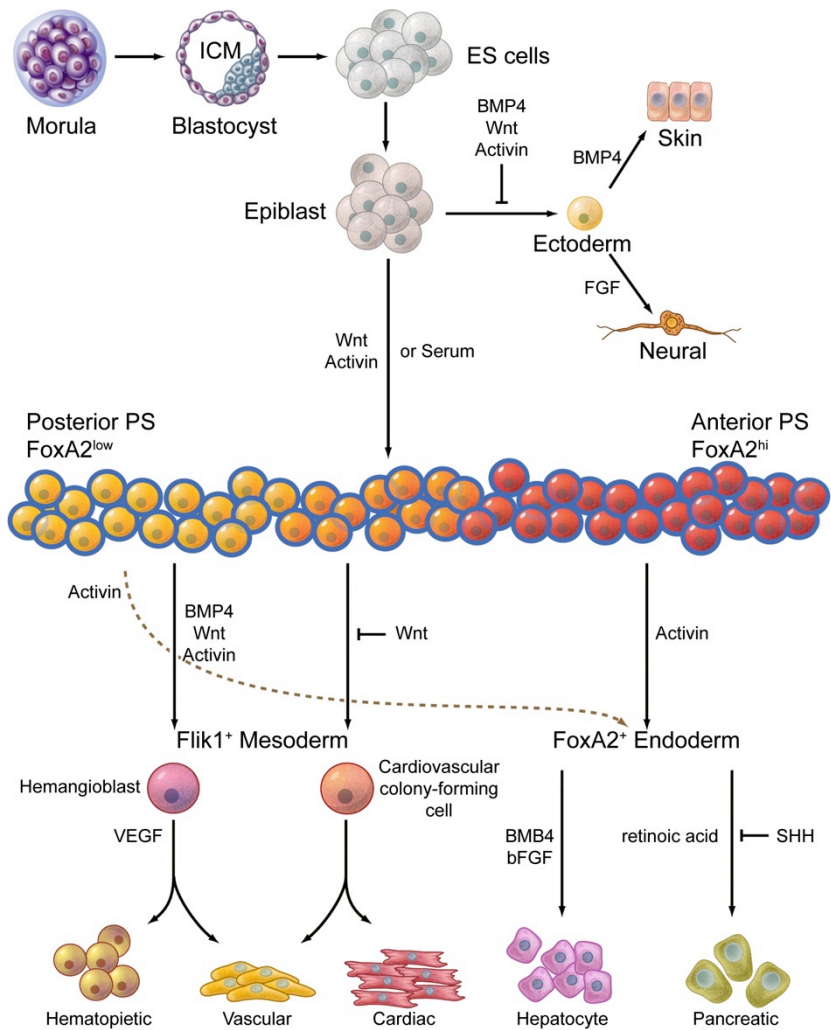
Figure 1.5 ES cells differentiation in culture.
It is possible to maintain ES cells in a pluripotent state with the addition of LIF into the medium. On the bases of specific environmental stimuli, they also can differentiate *in vitro* in the cells of the three embryonic layers [Modified from Murry and Keller, 2008].

1.2.1 Genetic regulation of pluripotency

In vivo, pluripotency is a transitional state, since in development most of the cells that compose an embryo are engaged in a differentiation pathway at a very early stage. However, during this short period of time, cells have to maintain the pluripotent state together with a high rate of proliferation. Many studies have shown that gene expression in ES cells is very variable, leading to heterogeneous populations poised for a range of lineage specification [Silva and Smith, 2008]. However, in 2006 Yamanaka and co. work showed that only four transcription factors were indispensable to generate induced Pluripotent Stem (iPS) cells: Oct4, Sox2, Klf4 and c-Myc [Takahashi and Yamanaka, 2006]. Finally, also Nanog was identified as another major player in pluripotency maintenance [Mitsui et al., 2003].

The cross-talk between these essential transcription factors and chromatin regulators is required to maintain ES cells identity, through activation of ES cells-specific genes and repression of lineage-specific developmental genes [Orkin and Hochedlinger, 2011]. Since then, many studies have established three distinct ES cells regulatory module: Transcriptional regulatory network (TRN), c-Myc and Polycomb Repressive Complexes (PRCs), that are able to interact with one another and sustain ES cells pluripotency [Chen et al., 2008; Kim et al., 2010]. The TRN is composed of ES cells factors Oct4, Sox2 and Nanog, which activate the transcription of ES cells-specific genes and repress the developmental genes [Kim et al., 2010; Young, 2011]. c-Myc, which is part of the four TFs involved in iPS cells generation, seems to work separately from the TRN [Sridharan et al., 2009; Soufi et al., 2012]. Finally, the Polycomb Repressive Complexes, composed by PRC1 and PRC2, repress lineage-specific genes [Margueron and Reinberg, 2011].

1.2.2 Chromatin structure in ES cells

Since it is now well accepted that chromatin structures are associated with the transcriptional activity of genes, the purpose of many recent studies has been to describe a putative epigenetic signature of ES cells. The challenge for those cells is to maintain pluripotency while preparing for differentiation, to repress developmental genes but keep them poised for transcription. Hence, the genome in ES cells must be in a highly plastic state so as to have the capacity to enter any one distinct differentiation pathway [Meshorer et al., 2006]. However, until now the molecular mechanisms for self-renewal, maintenance of pluripotency and lineage specification are poorly understood.

ES cells seem to be characterized by a distinct higher order global chromatin structure. Their nuclei are larger than those of differentiated cells and are more riche in less compact euchromatin and particular epigenetic features. Once the differentiation program starts, a gradual and organized redistribution of the genome occurs inside the nucleus, resulting in a rapid reorganization of the genome that accumulates highly condensed, transcriptionally inactive heterochromatin [Arney and Fisher, 2004].

In order to guarantee such a dynamic chromatin structure, ES cells are characterized by the existence of an unusual chromatin signature represented by the so called "bivalent domains" [Bernstein et al., 2006]. They are large regions of chromatin in which the repressive mark H3K27me3 co-localizes with peaks of the activating mark H3K4me3. Bivalent domains were often associated with low expression and were rapidly switched on according to differentiation program, reinforcing again the concept of "poised chromatin". In addition to H3K27me3 marks, the Polycomb complex deposits also monoubiquitination on lysine 119 of H2A (H2AK119ub), in order to retain the poised polymerase on bivalent domain [Stock et al., 2007]. In addition to histones, many other DNA-binding proteins, such as Transcription Factors (TFs) could affect the chromatin

structure, in order to rapidly switch the gene expression on or off, by creating transient interactions with chromatin, with residence times that can range from few minutes to few seconds [Meshorer et al., 2006].

1.3 Myc genes

One of the most studied groups of genes is the Myc oncogene family, comprising c-Myc, N-Myc and L-Myc. c-Myc gene was discovered in the beginning of the 1980s and its protein was originally discovered as the homolog to the viral oncogene of the avian myelocytomatosis retrovirus (*v-myc*) [Vennstrom et al., 1982]. Regulation of c-Myc expression is crucial in order to obtain normal cell functions and, since it regulates the transcription of a wide range of genes, even small changes in its expression can influence cell growth, proliferation, apoptosis, differentiation and transformation [Meyer and Penn 2008; Levens, 2010]. Furthermore, targeted gene disruption of both Myc alleles in ES cells leads to embryonic lethality at day 9.5-10.5, which highlights the crucial role of Myc in normal growth control during mammalian development [Davis et al., 1993].

1.3.1 Conserved regions and the interaction with cofactors

The C-terminal part of c-Myc contains a basic helix-loop-helix-leucine zipper (bHLH-LZ) motif (Figure 1.6). Myc protein can bind to DNA through its bHLH domain, while the LZ domain allows the dimerization with its partner Max (Figure 1), another bHLH transcription factor [Eilers and Eisenman, 2008]. Myc/Max heterodimers are capable of binding specific DNA sequences such as the E-box sequence (5'-CACGTG-3') and subsequently activate transcription of target genes [Adhikary and Eilers 2005]. Furthermore, Max association and DNA binding are required for transcriptional activation of many genes involved in cell proliferation, metabolism, stemness and apoptosis [Blackwell et al., 1990; Amati et al., 1993]. In addition to the bHLH-LZ domain, c-Myc is composed of a basic region involved in determining sequence-specific DNA binding [Ryan and Birnie, 1996].
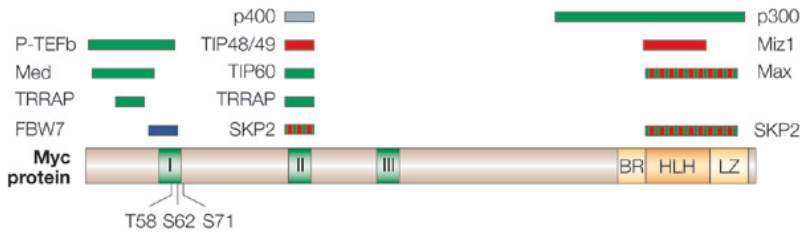
Figure 1.6 Schematic illustration of c-Myc showing the conserved regions and the interaction with co-factors.
The N-terminal Transactivation Domain (TAD) includes MBI and MBII domains. The C-terminal region contains the bHLH-LZ motif. [Adapted from Adhikary et al., 2005].

Finally, c-Myc presents a Trans Activation Domain (TAD), located at the N-terminal region, which is composed of two Myc homology Boxes, named Myc Box I-II (MBI-II). The so called "MB domains" are highly conserved between c-Myc, N-Myc and L-Myc and across species [Cowling and Cole, 2006] and are essential for c-Myc transforming activity, transcriptional activation and repression, since they are necessary for the interaction with a wide range of co-factors. Among those, chromatin remodelling complexes, such as Histone Acetylation complexes (HAT) or Polycomb Repressive Complexes, play an important role.

1.3.2 c-Myc-mediated transcriptional activation and repression

1.3.2.1 Transcriptional activation

c-Myc can facilitate chromatin opening by recruitment of HAT complexes to chromatin. TRRAP and GCN5 are part of the HAT complex STAGA and the TAD domain of c-Myc is shown to bind TRRAP, which in turn binds GCN5 and acetylates histone [McMahon et al., 2000]. Moreover, other chromatin remodelling protein complexes, such as TIP60, interact with c-Myc and

TRRAP, which in turn recruit the TIP60 complex subunits TIP48, TIP49 and p400 to the chromatin [Frank et al., 2003].

RNA polymerase III (Pol III) transcription is necessary for cell growth and it has been shown that c-Myc binds to the Pol III-specific Transcription Factor TFIIIB, therefore activating Pol III transcription. Pol III plays a pivotal role in the cell cycle, since it is involved in the transcription of ribosomal protein genes and in the synthesis of transfer RNA (tRNA) and 5S ribosomal RNA (5S rRNA), in order to favour protein expression in a growing cell.

Cells overexpressing c-Myc show altered expression of Pol II target genes. The c-Myc TAD domain is shown to induce Pol II phosphorylation through the interaction with C-Terminal Domain (CTD) kinases that phosphorylate Pol II CTD domain [Eberhard and Farnham 2001]. Moreover, recent works shown that transcriptional activation can be affected by Myc/Max complex-mediated recruitment of Pim1 to the chromatin of target genes, where it phosphorylates histone H3 at Ser 10 [Zippo et al., 2007].

1.3.2.2 Transcriptional repression

In addition to transcriptional activation, c-Myc is able to repress specific target genes. So far, the repressive mechanisms were not well elucidated, even if c-Myc seems to be responsible of the repression of at least 15% of target genes [Meyer and Penn 2008]. One of the mechanisms described until now argues that c-Myc interacts with Miz-1, therefore interfering with the formation of a Miz1-p300 complex and inhibiting Miz1-mediated transcriptional activation [Staller et al., 2001]. However, so far no studies have elucidated the direct interaction between c-Myc and chromatin modifiers in order to inhibit the expression of target genes. Our results describe the binding between c-Myc and PRC2 complex, leading to repression of c-Myc/PRC2 co-bound genes.

1.3.3 Regulation of c-Myc stability

The cellular half-life of the c-Myc protein is very short, approximately 20-30 minutes [Hann and Eisenman, 1984] before it is targeted for proteosome degradation. The role of post-translational modifications in c-Myc stability and activity has been studied extensively during the years, and several different modifications, such as phosphorylation, ubiquitination, glycosylation and acetylation have been described. Up to today, studies on phosphorylated c-Myc clearly show a role in the regulation of c-Myc biological activities, whereas the biological effects of the other modifications are still more ambiguous [Hann, 2006].

1.3.3.1 Phosphorylation at Ser62 and Thr58

The phosphorylation at Ser62 and Thr58 in MBI is sequential (Figure 3) and initial phosphorylation of Ser62 is required for Thr58 phosphorylation [Lutterbach and Hann, 1994]. Gsk3β is shown to phosphorylate Thr58 [Gregory et al., 2003]. The activity of Gsk3β is regulated by the PI3K pathway: phosphorylation of Gsk3β by PI3K-induced Akt kinase inhibits Gsk3β. *In-vivo* phosphorylation of Ser62 stabilizes c-Myc [Sears et al., 2000] and phosphorylation of Ser62 is mediated by MEK-activated ERK and Cdk2 [Hydbring et al., 2010].

The tumour suppressor Axin1 has been proposed to facilitate the formation of a degradation complex for c-Myc, by favouring the interaction between c-Myc and Gsk3β, PPA2 and Pin1 [Arnold et al., 2009].

1.4 The Polycomb Group Family

The Polycomb Group (PcG) represents a family of transcriptional repressors that play an important role in maintaining the repressed state of genes in the developmental regulatory transcriptional programs. PcG genes were discovered in the fruitfly *Drosophila melanogaster* more than 30 years ago as regulators of anterior-posterior body patterning through repression of the homeotic genes [Lewis, 1978]. Consequent identification of the trithorax group (trxG), that activate homeotic genes, led to a concept of a balance between silencing and activating factors that together provide cellular memory at different stages of development [Shao et al., 1999]. Subsequent work has shown that PcG and trxG groups form large multiprotein complexes that directly interact with the chromatin at their target genes [Schuettengruber et al., 2007]. In *Drosophila*, specific DNA regulatory elements, named "Polycomb" and "Trithorax response elements" (PRE and TRE respectively), were found to be necessary and sufficient for recruitment of both PcG and trxG complexes [Schwartz and Pirrotta, 2007]. Recently, PcG and trxG genes have also been identified in vertebrates, where they are involved in many biological functions: cell proliferation [Martinez and Cavalli, 2006], stem cell identity maintenance, cancer [Sparmann and van Lohuizen, 2006], genomic imprinting and X inactivation [Delaval and Feil, 2004; Heard, 2005].

1.4.1 Polycomb Complexes

The composition of these complexes is context-dependent. However, in vertebrates the PcG-mediated repression is performed through the combined activity of two Polycomb Repressive Complexes (PRCs): the initiator complex PRC2, and the maintenance complex PRC1. Although biochemical analysis showed that PRC1 and PRC2 are independent

entities with separate function and timing [Shao et al., 1999; Ng et al., 2000], a transient interaction between components of both complexes has been observed. Furthermore, it has been reported that complex formation is important for PcG proteins stability [Schwartz and Pirrotta, 2008].

1.4.1.1 The PRC1 complex

The core of the PRC1 complex includes one subunit of the PCGF (BMI1, MEL18 or NSPC1), CBX, HPH, and RING1 paralog groups (Figure 1.7) [Levine et al., 2002; Whitcomb et al., 2007]. The RING1 protein has monoubiquitylation E3 ligase activity specific for the lysine 119 of H2A (H2AK119ub), a mark associated to repressive chromatin structure [Wang et al., 2004]. In addition to the four core subunits of PRC1, a number of other proteins have been reported to associate with the complex.
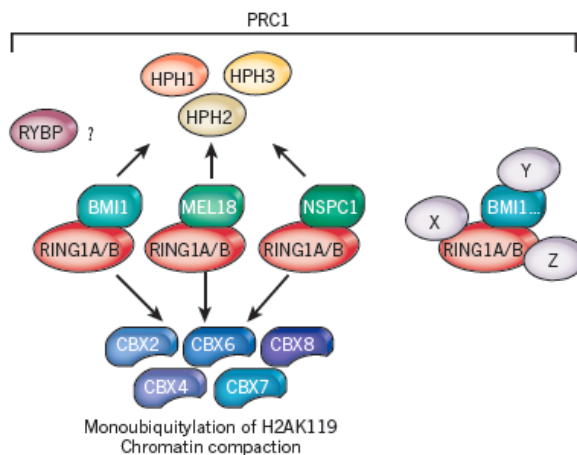
Figure 1.7 PRC1 complex.
The diagram shows on the left the classical PRC1 complexes, while on the right the so-called PRC1-like complexes. RING1A/B is the subunit endowed with catalytic activity. The "pocket" shape of the CBX proteins represents the chromodomain that recognize H3K27me3. X, Y and Z denote various proteins, such as SCMH1/2, FBXL10, E2F6 and JARID1D, that could contribute to the formation of PRC1-like complexes. [Modified from Margueron and Reinberg, 2011].

1.4.1.2 The PRC2 complex

The core of PRC2 comprises two homologous of the Enhancer of Zeste (EZH1/2), the homologue of Embryonic Ectoderm Development (EED) and the homologue of Suppressor of Zeste (SUZ12) (Figure 1.8). The EZH1 and EZH2 proteins catalyze the trimethylation at lysine 27 of histone H3 (H3K27me3), another typical epigenetic silencing mark [Cao et al., 2002]. Genetic experiments in mice have shown how the integral PRC2 complex plays a key role during development, since the absence of the PRC2 genes was found to induce early embryonic lethality [Pasini et al., 2004]. Additional components associated with the PRC2 complex are the Retinoblastoma Binding Protein 4 (RBBP4) and 7 (RBBP7). Together with SUZ12, these two proteins were shown to be required for the association of EZH2 with nucleosomes [Cao et al., 2002; Nekrasov et al., 2005]. A recent work showed that PRC2 requires a particular protein co-factor, called AEBP2, to tri-methylate Lysine 27 of histone H3 [Ciferri et al., 2012]. Finally, additional variation in the complex formation is induced by the different expression level of EZH2 or EED isoforms, which play a pivotal role in directing the enzimatyc activity of the complex [Kuzmichev et al., 2002; Kuzmichev et al., 2005].
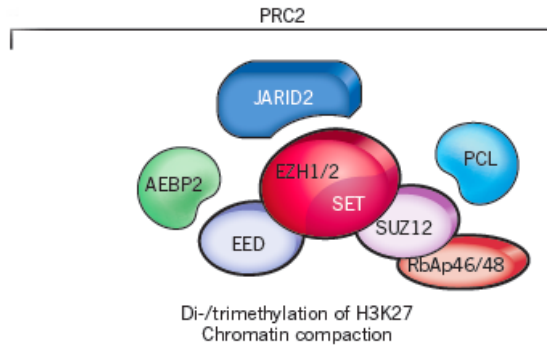
Figure 1.8 PRC2 cmplex.
The diagram shows the three core subunits of PRC2. The catalytic subunit EZH2, that contains a SET domain for histone H3K27 methylation, and two non-catalytic subunits SUZ12 and EED. In addition, different co-factors may be associated with the core of PRC2 in order to increase the histone methyltransferase activity. [Modified from Margueron and Reinberg, 2011].

1.4.2 Mechanism of PcG-mediated Repression

The current model of gene silencing by PcG complexes is summarized in Figure 1.9. Following recruitment of the PRC2 complex to chromatin, the histone methyltransferases activity of EZH2 converts the lysine 27 of histone H3 to a trimethylated form (H3K27me3) [Cao et al., 2002; Czermin et al., 2002]. This mark is then recognized by the chromodomain of the PRC1 complex, which catalyzes the ubiquitination of histone H2A on lysine 119 (H2AK119ub). In mice, it has been shown that the Ring1B E3 ligase protein is the catalytic subunit, while both Ring1A and Bmi1 have been identified as important enhancers of enzymatic activity [Cao et al., 2005; Buchwald et al., 2006]. However, this model has been challenged by the fact that it does not explain how PRC2 is recruited to chromatin and how the binding of PRC1 results in stable repression. For this reason, a complete understanding of their functions in gene silencing remains to be deciphered.
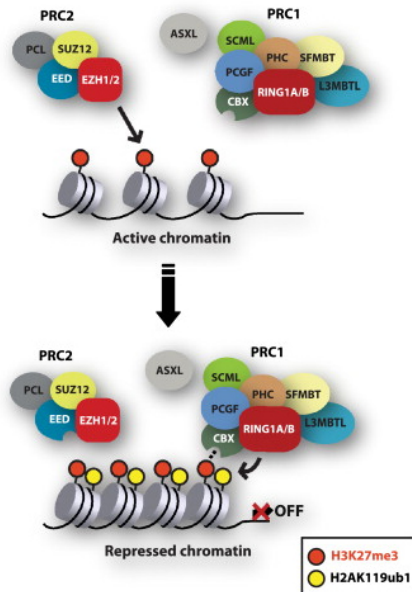
Figure 1.9 Classical model of PcG-mediated repression.
Following recruitment of the PRC2 complex to chromatin, EZH2/1 catalyzes the trymethylation of H3K27 (H3K27me3). In the next step, the PRC1 complex recognizes and binds the H3K27me3 mark. The ubiquitin E3 ligase activity of the complex mediates the ubiquitination of H2AK119 (H2AK119ub). These events result in the stable repression of transcription. [Modified from Sauvageau and Sauvageau, 2010].

1.4.3 PcG in Stem Cells and Cancer

Recent genome-wide screens of PcG protein binding sites in mouse ES cells identified more than a thousand potential target genes [Boyer et al., 2006; Bracken et al., 2006]. The most important concept that emerge from this analysis is that PcG proteins are important for maintaining pluripotency of ES cells and the identity and self-renewal capacity of somatic stem cells [Ringrose and Paro, 2007], while their disrupted levels have been increasingly linked to aberrant proliferation in cancer [Sparmann and van Lohuizen, 2006].

1.4.3.1 PcG proteins in stem cell self-renewal

Even though the lack of core PRC2 components leads to the global loss of H3K27 methylation, H3K27me3 and PcG-mediated gene silencing were maintained at a select number of key developmental genes, thanks to the activity of Ezh1 [Shen et al., 2008]. Indeed, the interaction between Ezh1 and Eed can maintain ES cell self-renewal, but not pluripotency, which additionally requires Ezh2 and Suz12 [Pasini et al., 2004; Ezhkova et al., 2009].

Thus, PcG-mediated repression has an important role in the maintenance of ES cells self-renewal and pluripotency and in the priming of differentiation, whereas they are required in the maintenance of somatic stem cells identity and self-renewal. The significance of PcG proteins in pluripotency is further supported by the fact that Sox2, Oct4 and Nanog co-localize with PcG proteins on the promoters of target genes [Boyer et al., 2006; Lee et al., 2006]

1.4.3.2 PcG in cancer

Aberrant expression of PcG proteins were found to be implicated in tumorigenesis. Human BMI1 has been found to be highly expressed in leukaemia and lymphoma, colorectal cancer, liver cancer, breast cancer, medulloblastoma and glioma [Bruggeman et al., 2007]. CBX7 have been found to be involved in lymphomas and prostate cancer [Gil et al., 2005], whereas EZH2 is commonly found to be overexpressed in various types of cancer, including leukaemia, prostate cancer and breast cancer and it is considered a marker of aggressive cancer [Bracken et al., 2006; Kleer et al., 2003]. SUZ12 is also found to be deregulated in various cancers, including colon, breast and liver cancer [Kirmizis et al., 2003].

During last years emerging evidences indicated that tumors contain a subset of cancer cells that display properties of stem cells, such as the

ability to self-renew and to spawn differentiated progeny. In this context, the dual role of PcG proteins in cancer and stem cells is unlikely to be coincidental. Rather it could fit with the cancer stem cell hypothesis, which holds that the origin of tumours is based on stem cell properties. The emerging understanding of what governs cellular identity plasticity has shed light on processes involved in reversing differentiation and acquiring self-renewal capacity. The role of PcG proteins in resetting the repression of differentiation-specific genes is likely to be an important topic [Jaenisch and Young, 2008].

2. AIMS OF THE STUDY

Mouse ES cells are derived and maintained by using various empirical combinations of feeder cells, cytokine leukaemia inhibitory factor (LIF) and fetal calf serum, which lead mainly to the activation of Stat3 signalling. [Niwa et al., 1998]. However the ES cells dependency on LIF/Stat3 signalling could be circumvented by either the inhibition of pro-differentiation regulators [Kaji et al., 2006; Ying et al., 2008] or by the enforced expression of pluripotency factors [Chambers et al., 2003; Niwa et al., 2009]. Among these, the Myc family members c-Myc and N-Myc have been described to modulate self-renewal and pluripotency of ES cells [Cartwright et al., 2005]. However the molecular mechanisms underlying their action are poorly understood. In this work we aimed to distinguish and characterize the molecular mechanisms through which c-Myc transcription factor maintains self-renewal and pluripotency of ES cells.

Recent works showed that transcription factors networks, activated by environmental stimuli, represent the basic building block for the formation of cellular memory. However, the molecular mechanisms were poorly investigated so far. Here we undertook to elucidate the role of c-Myc in the establishment of an epigenetic memory in ES cells.

3. MATERIALS AND METHODS

3.1 Cell Culture

All the cell lines used are listed in Table 2.1 and were kept under conventional cell culture conditions at 37°C and 5% CO_2.

Cells	Description	Source
mES cells line R1	Mouse Embryonic Stem cells	Cartwright et al., 2005
mES cells line R1 Myc^{T58A}ER	Mouse Embryonic Stem cells expressing c-Myc fused with Estrogen Receptor	Cartwright et al., 2005
HEK-293T	Human embryonic kidney fibroblast immortalized by hTERT	ATCC
EpiSC	Epiblast stem cells carrying an Oct4GiP transgene	Guo et al., 2009
NIH-3T3	Mouse embryonic fibroblast	ATCC
IMEC	Human immortalized mammary epithelial cells	DiRenzo et al., 2002

Table 3.1 cell lines

3.1.1 Cell culture and treatment

<u>**mouse Embryonic Stem cells:**</u> are an adherent male ES cells line grown on 0.1% gelatine-coated plate (Sigma, cat. N°G1393) in Dulbecco's modified eagles medium (DMEM) (Euroclone, cat. N°ECB7501L). The culture medium was supplemented with 15% fetal bovine serume (FBS) (Millipore, cat. N°ES-009-B), 1% penicillin/streptomycin (Pen/Srep) (Euroclone), 1% Glutamax (Gibco, cat. N°35050), 1x non-essential amino acids (NEAA) (Euroclone, cat. N°ECB3054D), 100 μM 2-mercaptoethanol (Gibco, cat. N°31350) and 10U/μl Leukaemia inhibitory factor (LIF/ESGRO) (Millipore, cat. N°ESG1107). Cells were split every two days, usually $5x10^3$ cells/cm^2. Briefly, after three washes in PBS the cells were detached from the plate using trypsin-EDTA 1x (Euroclone, cat. N°ECB3052D). Medium was then added to neutralise the trypsin and pipetted in order to divide at single cell, centrifuged for 5 minutes at 300g and resuspended in warm fresh medium. The medium was changed every day.

<u>**HEK-293T and NIH-3T3:**</u> were grown in DMEM medium supplemented wit 10% FBS (Euroclone, cat. N°ECS0180L), 1% Pen/Strep, 1% L-glutamine (Euroclone), 1x NNEA. Cells were split with ratio 1:10 every three days as previous described.

<u>**Epiblast stem cells:**</u> EpiSCs were grown on plate coated with 15 μg/ml of fibronectin (Sigma, cat. N°F1141) in DMEM-F12/Neurobasal medium 1:1 (Gibco, cat. N°21103) supplemented with 1x N2 supplement (Gibco, cat. N°17502), 1x B27 supplement (Gibco, cat. N°17504), 0,033% BSA (Millipore), 1% Pen/Strep, 1x L-glutamine, 12 ng/ml bFGF (Peprotech, cat. N°100-18B) and 20 ng/ml ActivinA (R&D, cat. N°338-AC). Cells were split every three days, usually in a 1 to 10 ratio but this varied according to cell density. Cells were detached from the plate using Collagenase IV 5 mg/ml

(Gibco, cat. N°17104). Medium was then added and cells were slightly pipetted in order to obtain small clumps, centrifuged for 5 minutes at 300g and resuspended in warm fresh medium. On alternate days, cells were supplemented with warm fresh medium.

IMEC: are a human cell line derived from epithelial cells of the mammary gland, immortalized through the overexpression of hTERT [DiRenzo et al., 2002]. IMEC cells were grown in MEBM (Mammary Epithelial Basal Medium) (Lonza, cat. N°LOCC4136) supplemented with 13 mg/ml of bovine pituitary extract (BPE), 20 ng/ml of Epidermal Growth Factor (EGF), 10 μg/ml of Insulin, 0.5 μg/ml of Hydrocortisone and 1% Pen/Strep. For mammosphere culture, 4×10^3 IMEC cells were seeded onto plate Ultra Low Attachment (Corning Costar) in MEBM medium supplemented with 20 ng/ml of EGF, 10 μg/ml of insulin, 0.5 μg/ml of hydrocortisone, 1% Pen/Strep, 1x B27 supplement, 20 ng/ml of bFGF and 5 μg/ml of heparin (Sigma, cat. N°H3149).

Reagents:

All cells were treated with the following reagents in the described experimental procedures: 4-OHT 50 nM (Sigma, cat. N°H6278); Dkk1 100 ng/ml (R&D, cat. N°5897-DK); Sfrp1 100 ng/ml (R&D, cat. N°1384-SF); Wnt-3a 100 ng/ml (R&D, cat. N°5036-WN); CHIR99021 3μM (abcam, cat. N°Ab120890); PD 0325901 1 μM (Sigma, cat. N°PZ0162); EPZ005687 1μM (BioVision, cat. N°2364); GSK126 2μM (BioVision, cat. N°2282); AG490 5μM (Invivogen, cat. N°tlrl-ag4); Jak1 1μM (Millipore, cat. N°420099); XAV939 3μM (abcam, cat. N°ab120897).

3.1.2 Freezing and recovery of cells

All cells were grown to ~80% confluency and detached as described above. After centrifugation the pellet cells were resuspended into 1 ml of pre-cooled freezing solution (50% FBS, 40% medium and 10% DMSO). The cells were afterwards transferred into a cryotube (Nunc) and frozen gradually in a freezing container (Nalgene) at -80°C. After about 24h, the tubes were transferred in the liquid nitrogen cell storage (-180°C).

For recovery of the cells after freezing, the frozen cells were swiftly transferred from liquid nitrogen to a 37°C waterbath and incubated until just thawed and then transferred to a culture dish containing pre-warm medium.

3.1.4 Alkaline phosphatase assay

Alkaline phosphatase activity is a specific marker of undifferentiated cells. The enzyme activity was detected by histochemical staining of fixed adherent cells. Briefly, medium was removed from the plate and cells were fixed for 5 min with 4% PFA. Cells were then rinsed three times in 100 mM TrisHCl ph 8 and incubated for 30 min in staining solution using VECTOR Red Alkaline Phosphatase (AP) Substrate Kit (Vector Lab, cat. N°SK-5100) according to manufacturer's guidelines and scanned with Nikon Eclipse Ti instrument to score positive colonies.

3.1.5 Differentiation of ES cells

3.1.5.1 EBs differentiation

Cells were trypsinised and replated 100 cells/well in non-adherent 96-well plates in DMEM supplemented with 10% KSR (Invitrogen,), 1x NNEA, 2mM L-glutamine and 1mM sodium pyruvate (Euroclone) without LIF. After 4 days of differentiation EBs were transferred onto petri dishes in order to continue differentiation without the EBs could attach the plate.

3.1.5.2 EpiLC transition

ES cells were induced to differentiate by following a method previous published [Hayashi et al., 2011]. Briefly, cells were trypsinised and replated $2x10^4$ cells/cm^2 onto plate coating with 16.7 μg/ml in N2B27 medium containing Activin A (20 ng/ml), bFGF (12 ng/ml) and KSR (1%). The medium was changed every day

3.1.6 Transfection with DNA (plasmids)

The cells were counted and seeded in plate 24h prior to transfection. The number of cells seeded varied among the cell lines and was calculated such that the cells would be ~80% confluent on the day of the transfection. The transfection mix was prepared using Lipofectamine 2000 (Invitrogen, cat. N°11668) with a ratio of 3 μl of Lipofectamine 2000 for every 1 μg of total DNA transfected.

3.1.7 Production of lentivirus and retrovirus

Lentivirus and retrovirus were produced by transient calcium phosphate transfection of HEK-293T cells with viral plasmids (shRNA, pBABE-Myc^{T58A}ER or PGK-H2BeGFP) and the corresponding packaging plasmids (pREV, VSV-G and pMDLg/pRRE). Additional information regarding the plasmids has been included in Table 2.2. The day before transfection, $7.5x10^6$ HEK-293T cells were seeded in 150 mm culture dish in complete DMEM. 2 h before transfection the medium from the plate was removed and replenished with ISCOVE's DMEM (Euroclone, cat. N°) medium supplemented with 10% of FBS, 1% Pen/Strep, 2mM of L-glutamine, 1 mM sodium pyruvate and 1x NEAA. The transfection mix was prepared by adding 32 μg of transfer plasmid, 6.25 μg of pREV and 9 μg of the VSV-G plasmid and 12.5 μg of pMDLg/pRRE. The final volume of the plasmid mix

was adjusted to 1.125 ml with ddH$_2$O. 0.125 ml of 2.5 M CaCl$_2$ solution was added to the plasmid mix and the mixture was vortexed gently. The final transfection mixture was prepared by drop wise addition of the CaCl$_2$-DNA mix to 1.250 ml of HEPES-buffered saline (HBSS) while vortexing the solution. The mixture was incubated at room temperature for 15 min to allow formation of DNA precipitates. Three millilitre aliquots were distributed into each 150 mm culture dish and the dishes were gently swirled. Cells were incubated for 18 h at 37°C. The next day the medium was changed with complete DMEM. Virus-containing supernatant was harvested at 48 h after transfection and concentrated using ultracentrifugation.

Supernatant containing virus particle were distributed into SW32 Ti open-top conical tubes (Beckman). The tubes were centrifuged at 50.000g for 2 h at 4°C in a Beckman ultracentrifuge using a SW32 Ti ultracentrifuge rotor (Beckman). When centrifugation was completed the supernatants was removed and the tubes were inverted and left to dry for 5 minutes. The pellet from each centrifuge tube was resuspended in 80 μl of PBS by gently pipetting up and down and kept for 30 min at 4°C in gently agitation. Virus-containing solution was aliquot in sterile microcentrifuge tubes and stored at -80°C.

Plasmid	Description	Source of reference
pBABE-Myc^{T58A}ER	Retroviral expression vector encoding Myc^{T58A} fused with hormone binding domain 4-OHT	Addgene
pLKO.1 shc-Myc	TRCN0000042515	Open Biosystem
pLKO.1 shN-Myc	TRCN0000020694	Open Biosystem
pLKO.1 shβ-Catenin	TRCN0000012690	Open Biosystem
pLKO.1 shEed	TRCN0000095722	Open Biosystem
pLKO.1 shEzh2	TRCN0000039042	Open Biosystem
PGK-H2beGFP	Lentiviral expression vector encoding H2B histone fused with GFP	Addgene
pREV	Expresses the protein to activate nuclear export of viral mRNAs	Addgene
VSV-G	Expresses the glycoprotein of the vescicular stomatitis virus	Addgene
pMDLg/pRRE	Contains Gag and Pol proteins	Addgene

Table 3.2 Viral plasmids

3.1.8 Retrovirus or Lentivirus Transduction

ES cells were counted and seeded in 6 well culture dishes in complete DMEM medium (section 2.1.1) 8h before infection. Subsequently, the medium from wells containing the cells to be infected was changed with fresh growth medium containing polybrene (Sigma, cat. N°107689), a cationic polymer used to increase the efficiency of transduction.

Concentrated virus suspension was added to individual wells containing target cells at an MOI of 1 and the cells were incubated at 37°C for 24 h. The following day the medium was removed and replenished with fresh growth medium containing appropriate antibiotic for selection (Puromycin, 1 μg/ml).

3.1.9 Cell cycle analysis with a FACS machine

For analysing the cell cycle distribution, cells were harvested by trypsinization for approximately 10 min to minimize clump formation, and all the cells (including the floating cells) were collected and pelleted by centrifugation at 300g for 5 min. The cell pellet was resuspended in 300 μl of PBS and fixed by the addition of 700 μl cold ethanol, overnight at 4°C. The next day the fixed cells were pelleted by centrifugation at 300g and the cell pellet was washed once with cold PBS. The cell pellets were then resuspended for 40 min in 200 μl of staining solution composed of 10 μl RNAse A and 2 μl of propidium iodide (100mg/ml) per 100 μl of PBS. Propidium iodide (PI) is an intercalating dye that fluoresces more strongly when bound to DNA. Therefore the amount of DNA present in the cell would be proportional to the PI signal. RNAse A was used to degrade RNA for the DNA only to be quantified. The cells were then sorted according to their size and DNA content using a FACScan flow cytometer (BD FACSCanto). The FACS data were further analysed using the software FlowJo (FlowJo inc.) to measure the percentage of cells in each cell cycle phase.

3.1.10 Time-lapse video microscopy

For live imaging analysis ES cells were seeded in 24 well plate (Ibidi, cat. N°82406) coated with 15 μg/ml Fibronectin. Time-lapse video

microscopy and single cell tracking of ES cells expressing H2B-eGFP were carried out continuously for 48h at 37° C and 5% CO_2 using the Eclipse T*i* fully automated system (Nikon). Images of fluorescent cells were acquired every 20 minutes with 20x Plan Apo l objective (Nikon) using a LED illumination system combined with a CMOS camera (Andor) for the detection. Single cell tracking was performed using the TTT software as described previously [Rieger and Schroeder, 2009] and movies were assembled using Image J software.

3.1.11 Teratoma Assay

Teratoma formation was assessed by injecting intracranial ES cells (LIF, Myc, -Myc) in immuno-compromised mice (CD1 nude). Briefly, $2x10^5$ cells suspended in 2 ml of DMEM were delivered into the right striatum by stereotactic injection. The following coordinates were used: antero-posterior = 0; mediolateral = 2.5 mm; dorso-ventral = 3 mm. Mice were sacrificed at different times from 2 to 4 weeks post-injection, according to the cell line originally injected. Hematoxylin and eosin staining were performed on 5 mm-thick paraffin sections.

3.2 Molecular Biology

3.2.1 Cloning

The coding sequence of PRC2 members and c-Myc was amplified from total cDNA of hES cells (was kindly provided by Salvatore Oliviero), using primers designed to contain appropriate restriction enzymes (Appendix A). The PCR was assembled as described in Table 2.3 using the AccuPrime *Pfx* kit (Invitrogen) for its high fidelity. The cycling is shown in table 2.4.

Reagent	Final concentration
AccuPrime *Pfx* Reaction mix	1x
Primer forward	0.2 μM
Primer reverse	0.2 μM
Template	10-100 ng
AccuPrime *Pfx* DNA Polymerase	1 u
H$_2$O	to 50 μl

Table 3.3 Reaction setup for the PCR amplification

Temperature	Time	Cycling
95°C	2 min	1x
95°C	15 sec	
55-64°C	30 sec	30 cycles
68°C	1 min per Kb	
68°C	2 min	1x
4°C	Cooling	

Table 3.4 Cycling conditions for the PCR amplification

The PCR reactions were then loaded into a 1% Agarose gel containing 0.5 µg/ml ethidium bromide (made with TAE buffer). After sufficient resolution was achieved, the DNA fragments were visualized using a UV transilluminator (UVITEC, Cambridge) and the relevant pieces of DNA were excised and recovered using the Wizard SVGel Clean-Up system (Promega, cat. N°A9282), according to manufacturer's instructions. Concentrations of PCR products were measured using NanoDrop spectrophotometer (Thermo Scientific).

Digestion of the purified products and the vector backbone were performed for 2h at 37°C with appropriate enzymes (NEB) (Table 2.5). Subsequently, the vector was dephosphorylated by incubating the reaction with 1 unit of calf alkaline phosphatase (NEB,) for 1h at 37°C. The PCR fragment and the vector were then once more purified using Wizard and their concentrations were measured using a NanoDrop spectrophotometer.

Reagent	Final amount
10x Buffer NEB	1x
Enzymes	4 u per µg of DNA
DNA	2 µg
ddH$_2$O	to 20 µl

Table 3.5 Setup of the restriction digestion reaction

Generally, ligations were performed using two different ratio of insert DNA to vector (Table 2.6) at 16°C overnight. A control reaction, using water instead of insert, was also performed. *E. coli* chemical competent bacteria (generated from the DB1035 bacteria as described in Molecular cloning: a laboratory manula) were transformed with 5 µl of each ligation reaction. Briefly the bacteria were incubated with DNA for 30 min on ice, the heat-

shock at 42°C for 2 min and on ice for 2 min was performed. Then the bacteria were incubated in 200 μl of 2xYT medium at 37°C for 1h and plated on LB plates with 50 μg/ml Kanamycin (Sigma, cat. N°K1377).

Reagent	Ratio 1:1	Ratio 1:3	negative
vector	100 ng	100 ng	100 ng
Insert	100 ng	300 ng	-
T4 buffer (10x)	2 μl	2 μl	2 μl
T4 ligase	1 μl	1 μl	1 μl
H$_2$O	to 20 μl	to 20 μl	to 20 μl

Table 3.6 Setup of the ligation reaction
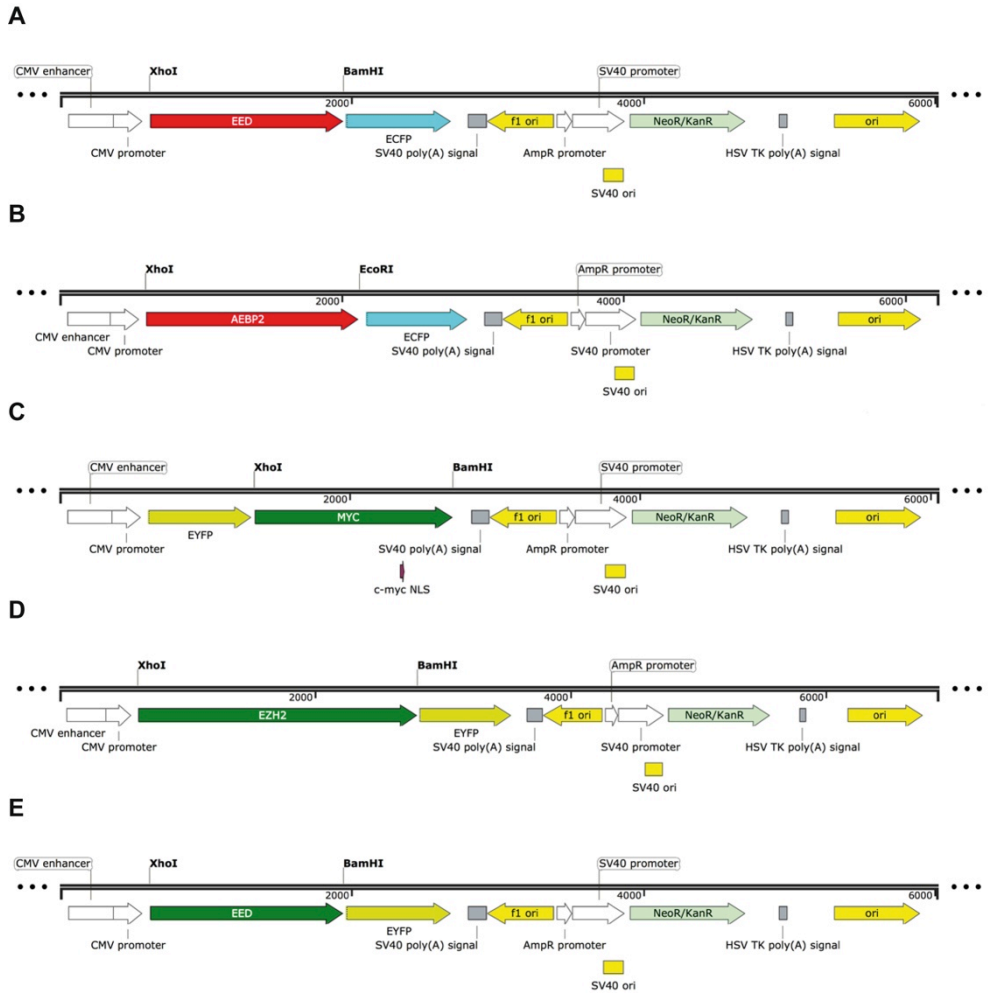
Figure 3.1 List of construct used in Fluorescence Resonance Energy Transfer (FRET).
For each vector plasmid are shown the restriction sites used for cloning: (A) pECFP-EED. (B) pECFP-AEBP2. (C) pEYFP-MYC. (D) pEYFP-EZH2. (D) pEYFP-EED.

3.2.2 Gene transcription analysis

3.2.2.1 RNA extraction

For extraction of total RNA the cells were harvested by scrapping directly in the Trizol reagent (Ambion, cat. N°15596018) and lysed by pipetting. 200 μl of chloroform for each 1 ml of Trizol were added to the samples followed by vigorous shaking by hand for 15 sec and incubation for 2-3 min at RT. Phase separation was done by centrifugation at 12.000g for 15 min at 4°C and the water phase was transferred in a fresh eppendorf tube. Equal volume of isopropanol was added and the RNA was left to precipitate for 10 min at RT. The RNA was recovered by centrifugation at 12.000g for 15 min at 4°C and washed with 75% ethanol. The RNA pellets were dried on a RT and resuspended in 30 μl RNAse free water. The concentration of RNA was measured using NanoDrop spectrophotometer. Moreover we analysed the 260/280 (Nucleic acid/Protein) and 260/230 (Nucleic acid/Polysaccharide) ratios per sample. Ratios, indicating the degree of nucleic acid purification, should be in a range of 1.8-2.1.

3.2.2.2 Quantitative real-time PCR (qPCR)

qPCR is a technique based on the general standard PCR principle, but using different fluorescent dyes and detection methods with better sensitivity. For the qPCR reaction we used SuperScript III One-Step SYBR Green kit (Invitrogen, cat. N° 11746). Briefly, 1 μl of each RNA or water (as negative control) was mixed with 19 μl of the primer-specific qPCR mix (Table 2.7) in the wells of a qPCR 96-well plate. The primer used to detach each gene product were designed using *Universal ProbeLibrary Assay Design Center* (Roche) and are listed in Appendix A. The amplification reaction was done using the StepOne Plus system (Applied Biosystem) and the cycling conditions are reported in Table 2.8. To ensure specificity

of amplification, melting curve analysis was performed. Relative gene expression levels were determined using calculated concentration values, normalized to ERCC Spike-In Control RNA (Ambion, cat. N°4456740).

Component	Final concentration
SuperScript III RT Taq Mix	1 μl
2X SYBR Green Reaction Mix	25 μl
Forward primer, 10 μl	1 μl
Reverse primer, 10 μl	1 μl
Total RNA	1 μl
H$_2$O	to 20 μl

Table 3.7 Reaction setup for the qPCR amplification

Temperature	Time	Cycling
50°C	15 min	1x
95°C	5 min	
95°C	15 sec	40 cycles
60°C	30 sec	
From 60°C to 95°C	Melting curve	

Table 3.8 Cycling conditions for the qPCR amplification

3.2.3 Chromatin Immunoprecipitation (ChIP)

The following procedure is based on [Zippo et al., 2007]. Briefly, the cells to be used for chromatin immunoprecipitation (ChIP) were treated with a cross-linking reagent before they were harvested. To this end, 37% formaldehyde (Sigma, cat. N°F8775) was added to the medium for a final concentration of 1% for 10 min at RT. The formaldehyde was the quenched by addition of 125 mM glycine and incubation for 5 min at RT. The fixed cells were subsequently washed twice with cold PBS, harvested by

scrapping in 1 ml cold PBS and centrifuged for 5 min at 1500g. Cell pellets were lysed in ice-cold ChIP buffer and incubated on ice for 10 min and nuclear pellets were obtained by centrifugation at 14000 g at 4°C for 10 min. The nuclear pellet was washed with 1 ml ChIP buffer and resuspended in 300 μl of ChIP buffer per 10^6 cells. The chromosomal DNA was then sheared using BioRuptor waterbath sonicator (Diagenode) at high setting for 10 min. Samples were sonicated in pulse of 30 sec with 30 sec intervals. Following sonication, the samples were cleared by centrifugation at 15000g for 10 min at 4°C.

For the immunoprecipitation of specific proteins on the chromatin, 100 μg of chromatin was used per IP and a 10% input sample was retained. The IP samples were adjusted to 500 μl and 2.5 μg of antibody was added. As a negative control rabbit unspecific IgG was used. Following addition of antibody, the samples were incubated on a rotating wheel at 4°C O/N. The next day, samples were cleared by centrifugation to remove unspecific complexes and the top of the samples was transferred to a new Eppendorf tube containing 20 μl Protein A/G beads pre-washed in ChIP buffer. Samples were incubated on a rotating wheel at 4°C for 3h. The beads were then centrifuged at 500g for 5 min at 4°C and washed three times with 1 ml of ChIP buffer for 10 min at 4°C. The antibody/protein/DNA complexes were eluted from the beads by adding 50 μl of Elution Buffer at RT and shaking on a vortexer for 15 min at highest speed. The input samples were included at this stage and adjusted to 100 μl with elution buffer. NaCl was added to a final concentration of 0.2 M and the samples were incubated at 65°C O/N to reverse the cross-linking. Next, RNase A was added to a final concentration of 0.1 mg/ml and samples were incubated for 30 min at 37°C. The relative enrichment for specific DNA sequences was determined by qPCR, as described in section 2.2.2.2 using a SYBR GreenER qPCR SuperMix (Invitrogen, cat. N°11762).

3.2.4 Microarray analysis

BeadChip Arrays were scanned with HiScan Array Scanner (Illumina) using the iScan Control Software (Illumina). Genes and probes transcript levels were obtained from Illumina Intensity Data (.idat) files, applying quantile normalization and background subtraction implemented by the GenomeStudio Gene Expression Module v1.0 Software (Illumina). All experiments in each condition reported were performed on triplicate biological samples, except for the Eed knocked down ES grown in LIF withdrawal and in presence of 4-OHT, for which a single replicate was analyzed on the array. Cut-offs for up- and down-regulation of gene expression were set to 1.5 fold change threshold in all the analyses performed.

Single microarray replicates were subjected to dendograms cluster analysis performed with the GenomeStudio Gene Expression Module v1.0 Software (Illumina), using Euclidean distance matrix. The top 200 genes up- or down-regulated in the comparison between LIF maintained ES and EpiSC were selected to generate a heatmap reporting a hierarchical clustering analysis of both genes and single microarray replicates (complete linkage, Euclidean distance matrix), using the TM4 MeV v4.9 software.

Differentially expressed genes in the LIF- versus Myc-maintained ES comparison were checked for biological and functional enrichment using both Ingenuity Pathway Analysis (IPA, Qiagen Redwood City, www.qiagen.com/ingenuity) based online tool PANTHER Classification System.

3.3 Biochemistry

3.3.1 Immunoblotting analysis

3.3.1.1 Total protein extraction

The cells were washed twice with cold PBS, harvested by scrapping in 1 ml cold PBS and centrifuged for 5 min at 1500g. Harvested cell pellets were lysed by the addition of 5X v/v ice-cold F-buffer. Lysing was allowed to proceed for 30 min on a rotating wheel at 4°C. The chromosomal binding proteins were then separated using BioRuptor waterbath sonicator (Diagenode) at low setting for 5 min. Samples were sonicated in pulse of 30 sec with 30 sec intervals. Lysates were cleared by centrifugation for 10 min at 15000g at 4°C and supernatant was collected on ice.

The protein concentration of lysates was determined using Pierce^{TM} BCA Protein Assay Kit (Thermo Scientific, cat. N°23227), according to manufacturer's instructions. The absorbance was measured at λ=595 using SAFAS spectrophotometer (SAFAS, Monaco). Values were compared to a standard curve obtained from the BSA dilution series.

Protein fractionation was performed by using Subcellular Protein Fractionation Kit (Thermo Scientific, cat. N°78840) according to manufacturer's instruction.

3.3.1.2 Western Blot

Generally, 20 μg of protein samples were prepared by adding 4X Bolt LDS Sample Buffer (Novex, cat. N°B0007) and 10X Bolt Sample Reducing Agent (Novex, cat. N°B0009) to a 1X final concentration and samples were adjusted to an equivalent final volume by using ddH$_2$O. The samples were then boiled at 95°C for 10 min. SeeBlue Plus 2 (Invitrogen, cat. N°LC5925) markers were used for monitoring fractionation and size estimation. For separating the samples the Novex system (life technologies) was used and

the samples were loaded onto a pre-cast Bolt 4-12% Bis-Tris Plus gels (Novex, cat. N°NW04122BOX) and run in Bolt MES running buffer (Novex, cat. N°B0002). Electrophoresis was performed at 110 V until desired fractionation was achieved.

3.3.1.3 Immunoblotting

After separation by electrophoresis, proteins were transferred to a nitrocellulose membrane (novex, cat. N°IB301001) using the iBlot transfer system (life technologies). Proteins were transferred at a 300 V for 7 min. Following this, the membrane was blocked in freshly prepared WB blocking buffer for 1 h at RT with constant agitation. The primary antibody commonly used in this work are listed in Appendix B. Generally, the primary antibodies were diluted at 1:1000 in WB blocking buffer and used for incubation of the membrane ON at 4°C with agitation. The membrane was then washed three times with WB washing buffer, each time for 5 min. Depending on the primary antibody used, the membrane was incubated with secondary antibody HRP-conjugated diluted in WB blocking buffer for 1 h at RT (Appendix B). Following this incubation, the membrane was washed again three times for 5 min in WB washing buffer and then incubated with a 1:1 mix of ECL reagents (GE Healthcare, cat. N°RPN2232) for 5 min to initiate the chemiluminescence of HRP. The chemiluminescent signal was captured using LAS3000 system (GE Healthcare).

3.3.2 Immunofluorescence

ES cells were grown on a coverslip coated with 0.1% gelatin in a 24 well plate. The culture medium was removed carefully from the wells and cells fixed in 4% PFA for 20 min at RT. Subsequently the coverslips were

washed twice with PBS and permeabilized with IF permeabilization buffer for 10 min at RT. After permeabilization the coverslips were washed three times with PBS and blocked with IF blocking buffer for 30 min at RT. The primary antibody was diluted in IF blocking buffer (Appendix B) and a minimum of 150 µl was applied on cells. Following incubation at RT for 2 h, cells were washed three times with IF washing buffer and incubated for 1 h at RT with the secondary antibody diluted in IF blocking buffer. Finally, after three washes in IF washing buffer, the nuclei were counterstained with DAPI in PBS for 10 min at RT. The coverslips were carefully lifted from the well using fine tweezers and mounted on microscope slides using ProLong antifade medium (Invitrogen).

Proximity ligation assay was performed using in situ PLA Technology (O-link Bioscence) according to manufacturer's instruction.

Images were acquired using a Leica TCS SP5 confocal microscope with HCX PL APO 63x/1.40 objective. The data were analysed using Volocity software ().

3.3.4 Fluorescence Resonance Energy Transfer (FRET)

The technique of FRET permits to determine the interaction between two molecules within several nanometers in a cellular context. The mechanism of FRET involves a donor fluorophore in an excited electron state, which may transfer its energy to an acceptor group through a non-radiative process. The distance over which energy can be transferred is dependent on the spectral characteristic of the fluorophores, but is generally in the range 10-100A°.

Briefly, NIH3T3 cells were transfected with the appropriate ratio between the fluorescence tagged proteins to optimize protein distribution. Myc-interaction experiments were performed by co-expressing the MAX protein (Myc:Max ratio 4:1) and the protein of interest. FRET acceptor

photobleaching was carried out using the Leica TCS SP5 confocal microscope and apFRET software (Leica) according to the manufacturer's instructions. Fixed cells were analysed with a HCX PL APO lbd.BL 63.0x1.40 oil objective and 8x zoom. The argon laser was tuned to 458 nm to excite CFP (PMT window 465-495nm) and to 514 nm to excite YFP (PMT window 555-630 nm). The region of interest was bleached until intensity of 20% in the YFP channel using the 514 argon laser line.

3.4 Solutions

<u>Bacterial culture</u>

Luria broth (LB)   1% (w/v) NaCl
0.5% (w/v) yeast extract
1% (w/v) bacto-tryptone

SOC medium   2% (w/v) tryptone
0.05% (w/v) yeast extract
0.006% (w/v) NaCl
0.002% (w/v) KCl
0.002% (w/v) $MgCl_2$
0.036% (w/v) D-glucose

<u>Cell culture</u>

2x HBS   140 mM NaCl
1.5 mM Na_2PO_4
50 mM HEPES (pH 7.1)

Biochemistry

F-buffer	10 mM HEPES
	50 mM KCl
	50 mM NaF
	5 μM $ZnCl_2$
	0.1 mM Na_3VO_4
	1% Triton X-100
	10 mM Sodium butyrate
	1x Anti-protease
	1x Anti-phosphatase
	1 mM PMSF
WB washing buffer	PBS
	0.1% (v/v) Tween-20
WB blocking buffer	WB washing buffer
	5% dried milk (BIO-RAD, cat. N°170-6404)
IF permeabilization buffer	PBS
	0.1% Triton X-100
IF washing buffer	PBS
	0.1% Tween-20
IF blocking buffer	IF washing buffer
	5% BSA

Immunoprecipitation

ChIP buffer   50 mM HEPES pH 7.9
                               140 mM NaCl
                               1 mM EDTA
                               1% (v/v) Triton X-100
                               0.1% DOC
                               0.1% SDS
                               1 mM PMSF
                               1x anti-protease

ChIP elution buffer   50 mM TrisHCl pH 8
                               1 mM EDTA
                               5 mM DTT
                               1% SDS

DNA analysis

TAE buffer   40 mM Tris Base
                               20 mM Acetic acid
                               1 mM EDTA

4. RESULTS

4.1 c-Myc sustains self-renewal and pluripotency of ES Cells

4.1.1 Enforced expression of c-Myc sustains ES cells self-renewal

In order to evaluate the ability of c-Myc to sustain ES cells self-renewal, we used ES Myc^{T58A}ER cells (line R1) [Cartwright et al., 2005], which express an exogenous MycER fusion protein activated by 4-hydroxytamoxifen (4-OHT) induction. This tool has the potential to monitor the kinetics of action of c-Myc activation through 4-hydroxytamoxifen (4-OHT) induction. In fact, the carboxyl terminus of MycER protein is fused to the ligand-binding domain of a mutant estrogen receptor (ER) [Danielian et al., 1993]. It is constitutively expressed, but remains inactive until the 4-OHT is supplied. Moreover, the T58A mutation prevents c-Myc phosphorylation and subsequent ubiquitination, therefore extending the half-life of c-Myc.

Then, we compared ES cells grown in medium containing LIF or in a Myc-dependent manner, in absence of LIF and with 4-OHT induction (Myc-maintained) (Figure 4.1A). Colony morphology and alkaline phosphatase (AP) activity were used as initial readouts for ES cell maintenance. In agreement with previous studies [Cartwright et al., 2005], we show that activation of MycER is sufficient for the cells to grow with an uniform dome-shaped colony morphology and elevated alkaline phosphatase activity (AP+) for the first three days (Figure 4.1B). On the contrary, cells grown in absence of LIF and 4-OHT, showed evident signs of differentiation and a dramatic reduction of AP+ colonies (Figure 4.1B). Moreover, Myc-dependent cells maintained the same efficiency in giving rise to round and AP+ colony in a single cell clonogenic assay, similar to LIF-maintained cells (Figure 4.1C). To exclude that 4-OHT treatment could affect their

stemness, we treated ES cells without MycER transgene with tamoxifen for three days. As shown in Figure 4.1D, we observed that without MycER activity ES cells were unable to proliferate and self-renew. These data suggest the specific role of c-Myc to sustain ES cells self-renewal, and this is not due to an exchange of growth factor secreted from the colonies, as the Myc-dependent cells were able to proliferate even when grown as single cells.
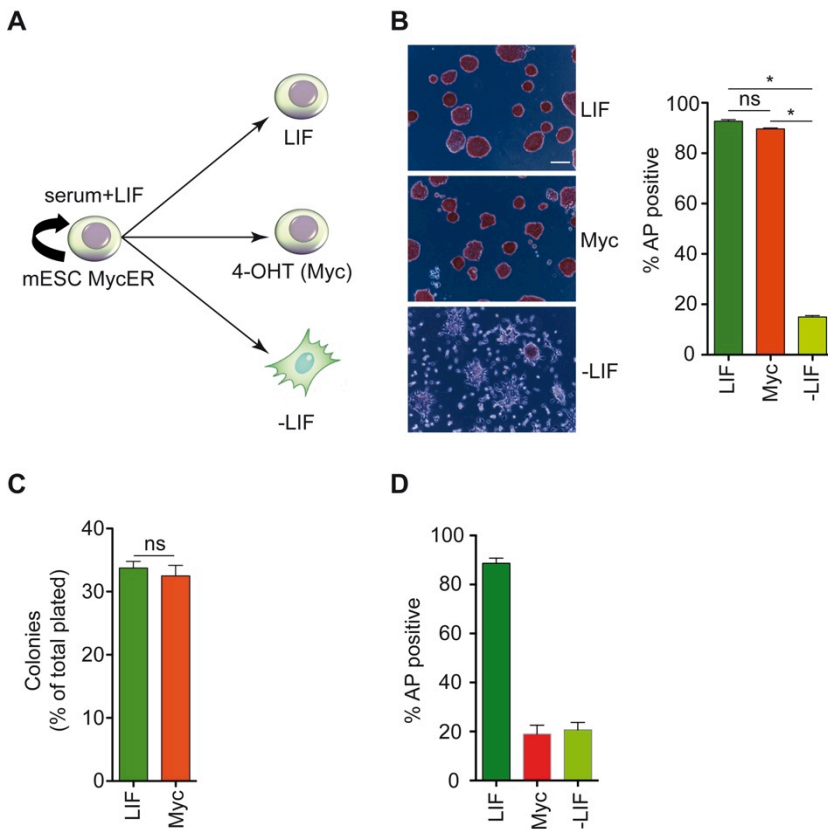
Figure 4.1 c-Myc sustains self-renewal of ES cells.
(A) Schematic representation of the experimental outline. (B) AP staining of ES cells MycER grown for three days in the indicated conditions and relative quantification of positive colonies are represented as percentage of the total colonies formed. Scale bar = 200 μm. (C) Single-cell clonogenic assay was performed and the relative number of colonies grown was quantified. (D) AP staining of R1 clone and relative quantification of positive colonies. Error bars represent standard deviation from 3 independent experiments. *p<0.05.

4.1.2 ES cells grown in a Myc-dependent manner maintain stem identity

Among several biological activities regulated by c-Myc, it plays a major role in the control of the cell cycle and cell proliferation [Ponzielli et al., 2005; Meyer and Penn, 2008]. In order to show that enforced expression of c-Myc does not affect the proliferation of ES cells, cells number was recorded at 24, 48 and 72h. The resulting growth curves demonstrated a comparable proliferation between LIF- and Myc-maintained ES cells, whereas cells grown without LIF and 4-OHT showed a reduction in proliferation (Figure 4.2A). Moreover, doubling time analysis confirmed previous results, showing a similar time of divisions between Myc- and LIF-maintained ES cells and increased time for –LIF ES cells (Figure 4.2B).
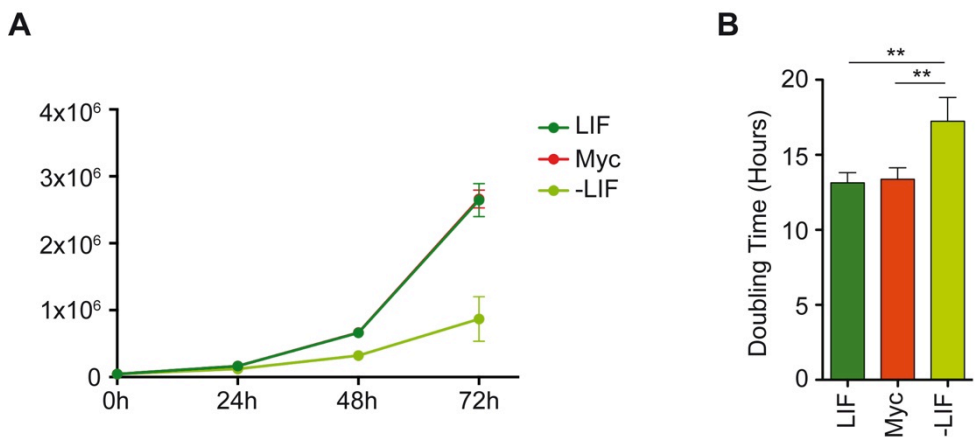
Figure 4.2 c-Myc maintains the proliferation of ES cells.
(A) Growth curve of ES cells MycER grown in LIF-, Myc- and –LIF-dependency for three days. (B) Quantification of the doubling time of MycER ES cells maintained in presence of 4-OHT, LIF or in absence of both LIF and 4-OHT. Error bars represent standard deviation from 3 independent experiments. **$p < 0.01$.

Single-cell tracking analyses confirmed that the LIF- and Myc-maintained ES cells have the same time of division. This analysis, suggests that Myc-dependent ES cells maintain a symmetrical pattern of cell division,

requirement of pluripotency (Figure 4.3A). Finally, FACS (Fluorescence Activated Cell Sorting) cell cycle analysis of the cells after three days of 4-OHT induction showed a cycle profiling comparable with that of cells grown in LIF containing media (Figure 4.3B).

Taken together, these data suggest that enforced expression of c-Myc not only is sufficient to sustain ES cells self-renewal, but also is able to maintain a stem cell identity similar to that of standard conditions, circumventing LIF/STAT3 signal.
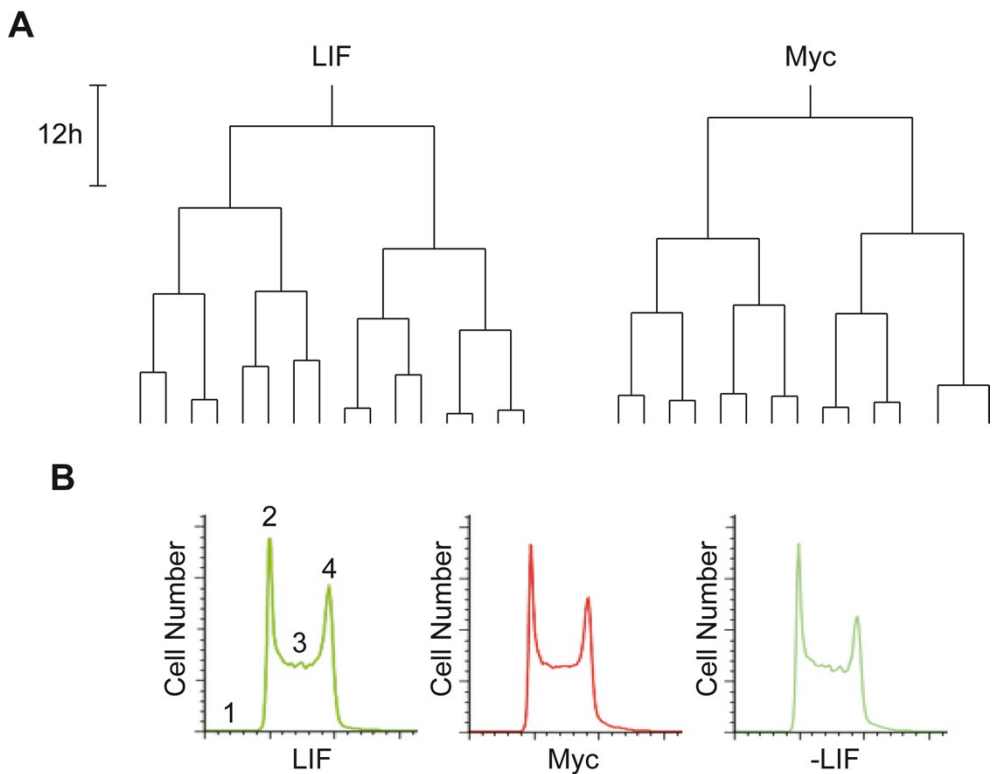
Figure 4.3 c-Myc sustains pluripotency of ES cells.
(A) Single-cell tracking of ES cells expressing H2B-eGFP. Lineage tree represent the pattern and timing of cell division of a single ES cell. (B) Cell cycle profile analysis to identify and quantify the different cell cycle phases: 1: Apoptotic cells (subG1); 2: G1; 3: S; 4: G2.

4.1.3 c-Myc activates an alternative regulatory circuit

To understand the molecular mechanisms through which c-Myc can support ES cells identity, we performed gene expression profile analyses of Myc- and LIF-ES cells, together with Epiblast Stem Cells (EpiSC), inserted as a control for a primed state of stemness. This analysis revealed that, in terms of gene expression profile, Myc-maintained ES cells clustered together with LIF-dependent ES cells and were distant from EpiSC. Despite the observed similarities, a specific gene expression signature distinguished the Myc- from the LIF-ES cells (Figure 4.4A). We experimentally validated this conclusion showing that Myc- and LIF-ES cells expressed high levels of pluripotency-specific markers and low levels of EpiSC-specific markers, when compared to EpiSC (Figure 4.4B). In order to gain insights on which geneset were differentially regulated by c-Myc, we interrogated Ingenuity Pathway Analysis (IPA), which indicated that ES cells pluripotency genes were enriched among the c-Myc up-regulated genes (Figure 4.5A). Subsequently, we retrieved an independent list of pluripotency-associated genes, represented by the Oct4/Sox2/Nanog/Tcf3 co-bound targets [Marson et al., 2008] and performed Gene Set Enrichment Analysis (GSEA). In accordance with IPA, GSEA suggests a relative enrichment of this geneset in Myc- with respect to LIF-maintained ES cells (Figure 4.5A). Altogether, these multiple bioinformatical approaches indicate that c-Myc potentiates pluripotency-associated genes in ES cells.
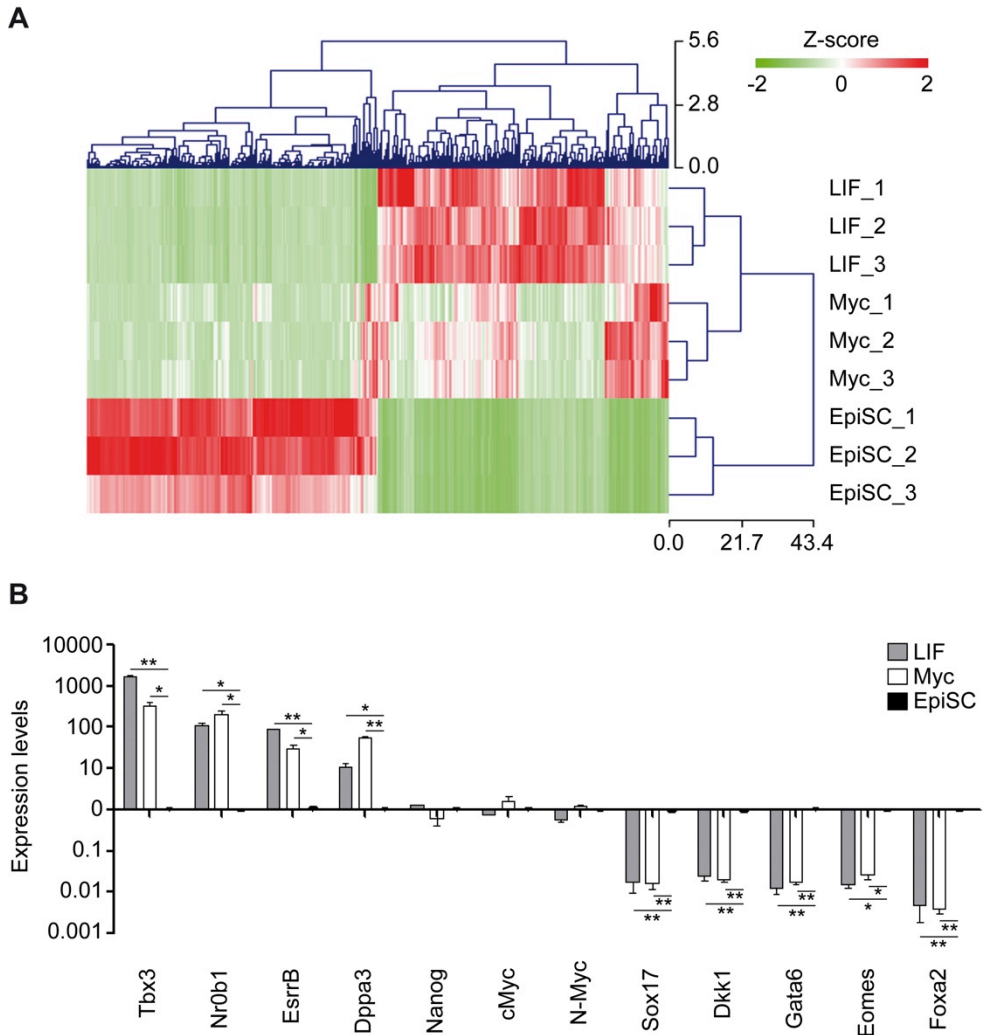
Figure 4.4 Myc ES cells maintain naïve pluripotent state.
(A) Heat map of the most differentially expressed genes (cut-off >1.5 fold change, 200 genes) between LIF-maintained ES cells and EpiSC. (B) The relative transcriptional level of some of ES cells and EpiSC specific genes were confirmed by qRT-PCR analysis in the indicated conditions. Error bars represent standard deviation from 3 independent experiments. *p<0.05; **p<0.01.

In order to assess whether Myc-maintained ES cells maintained their stemness identity, we analysed the core of TRN, Oct4, Sox2 and Nanog. To measure the level of TRN in Myc-dependent cells, a qPCR analysis of Oct4, Sox2 and Nanog mRNA was performed. The analysis showed that

expression levels of Oct4 and Sox2 were similar in LIF- and Myc-maintained ES cells; on the contrary, mRNA of Nanog decreased in Myc-maintained ES cells (Figure 4.5B). The observed reduction of Nanog at transcriptional and protein level, could be explained by the fact that Nanog is a downstream target of LIF/STAT3 pathway [Niwa et al., 2009]. Furthermore, a subset of pluripotency transcriptional regulators including Dppa3, Utf1, Nr0b1 and c-Myc [MacArthur et al., 2012] were transcriptionally up-regulated in Myc-maintained ES cells (Figure 5B). Taken together, this results indicate that c-Myc maintains ES cells identity by reinforcing a LIF-independent alternative core regulatory transcription circuit.

A

Myc up-regulated genes
IPA pathways

Term	P-value
Regulation of the Epithelial-Mesenchymal Transition Pathway	4.4E-05
Human Embryonic Stem Cell Pluripotency	7.9E-05
FGF Signaling	2.1E-04
Mouse Embryonic Stem Cell Pluripotency	2.5E-04
Germ Cell-Sertoli Cell Junction Signaling	7.8E-04
Integrin Signaling	8.1E-04
GADD45 Signaling	9.8E-04
Wnt/β-catenin Signaling	1.1E-03

Myc down-regulated genes
IPA pathways

Term	P-value
Role of NANOG in Mammalian Embryonic Stem Cell Pluripotency	1.6E-03
Regulation of the Epithelial-Mesenchymal Transition Pathway	1.7E-02
Role of JAK1, JAK2 and TYK2 in Interferon Signaling	1.7E-02
JAK/Stat Signaling	1.9E-02

B

Expression levels — genes: Dppa3, N-Myc, Nr0b1, Utf1, c-Myc, Mbd3, Oct3/4, Sox2, Fgf4, Jarid2, Nanog, Stat3, Tbx3, Klf4, Socs3; conditions: LIF, Myc.
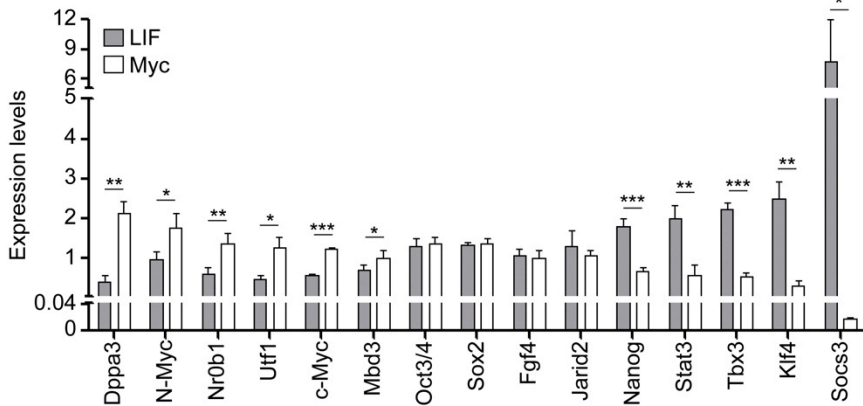
Figure 4.5 c-Myc activates an alternative pathway.
(A) Ingenuity Pathway Analysis (IPA) of differentially regulated genes between LIF- and Myc-maintained ES cells (n=3). (B) The relative transcriptional levels of some of the pluripotency genes were confirmed by qRT-PCR analysis in the indicated conditions. Error bars represent standard deviation from 3 independent experiments. *p<0.05; **p<0.01; ***p<0.001.

4.1.4 c-Myc potentiates Wnt pathway

Among the up-regulated pathway in Myc-maintained ES cells, we found the Wnt/β-Catenin signalling (Figure 4-5A). As recent works shown that Wnt signalling stimulate self-renewal and prevent ES cells differentiation [ten Berge et al., 2011; Merrill, 2012], we hypothesized that c-Myc can potentiate the Wnt/β-Catenin signalling to sustain ES cell identity. In order to understand how c-Myc sustains the Wnt pathway, we first performed protein level analysis, showing that Myc-dependent potentiation occurs at multiple stages (Figure 4.6A). At the cell membrane level, we observed activation of the Fzd/Lrp6 receptor complex resulting in the increased phosphorylation of Lrp6 in Myc-maintained ES cells. At the level of the destruction complex, which promotes β-Catenin degradation, we registered reduction of the rate-limiting factor of the complex Axin1. At the level of the nucleus we observe that the co-factors of Wnt pathway (Tcf and Lef family members) were up-regulated. Furthermore, in Myc-maintained ES cells we found an increased level of phosphorylation of Akt. The phosphorylation of Akt at Ser473 is believed to phosphorylate and inhibit Gsk3β [Cohen and Frame 2001], suggesting that c-Myc could potentiate Wnt pathway (Figure 4.6B). To further analyse the potentiation of Wnt pathway and to obtain insight into the mechanism of action of c-Myc, we performed qPCR analysis to measure the transcriptional level of members of Wnt pathway. The analysis showed that genes coding for receptors and co-receptors (Lrp and Fzd member family) are transcriptionally up-regulated; on the contrary genes coding for antagonists, such as Dkk1 and Sfrp1, are down-regulated in Myc-maintained ES cells (Figure 4.6C).
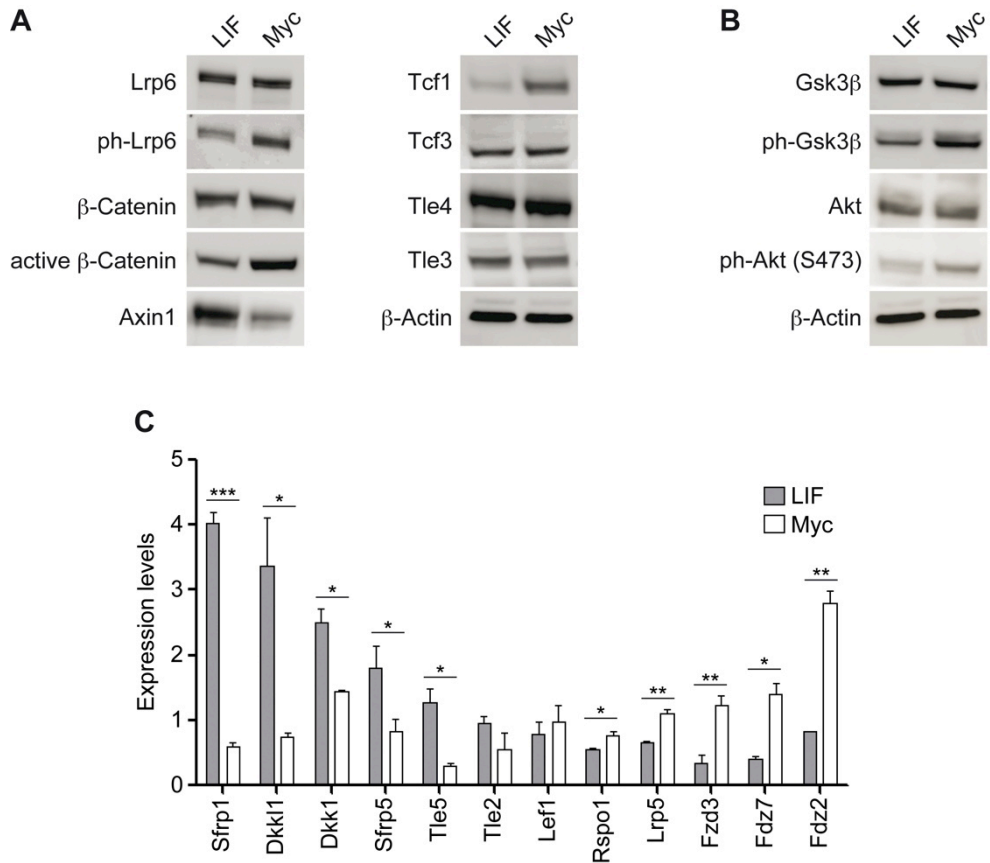
Figure 4.6 c-Myc activates Wnt/β-Catenin signalling.
(A) Western Blot analysis of Wnt/β-Catenin signaling pathway related proteins and (B) Western Blot analysis of Akt/Gsk3β pathway related proteins. Total protein extracts were collected from LIF and Myc-maintained ES cells, and immunostaining analysis was performed using the indicated antibodies; β-Actin was used as loading control. (C) The relative transcriptional level of some of the Wnt pathway associated genes was confirmed by qRT-PCR analysis in the indicated conditions. Error bars represent standard deviation from 3 independent experiments. *p<0.05; **p<0.01; ***p<0.001.

Since we observed that the destruction complex was inhibited in Myc-maintained ES cells, resulting in increased active β-Catenin, we hypothesized that it could move into the nucleus to activate the transcription of Wnt pathway target genes. To address this point, we measured the activity of Wnt pathway in Myc-maintained ES cells using Proximity Ligation Assay (PLA) method, that allows to detect and localize

direct protein interactions with a single molecule resolution. The results of PLA showed an increased translocation of β-Catenin into the nucleus and its association with downstream effectors Tcf1 and Tcf3 in Myc-maintained ES cells (Figure 4.7), suggesting that Myc-activated Wnt pathway could potentiate the transcriptional expression of Wnt target genes. Taken together, these data suggest that enforced c-Myc activity could reinforce the Wnt/β-Catenin signalling by repressing the antagonists of the pathway and preventing β-Catenin degradation through inhibition of destruction complex.
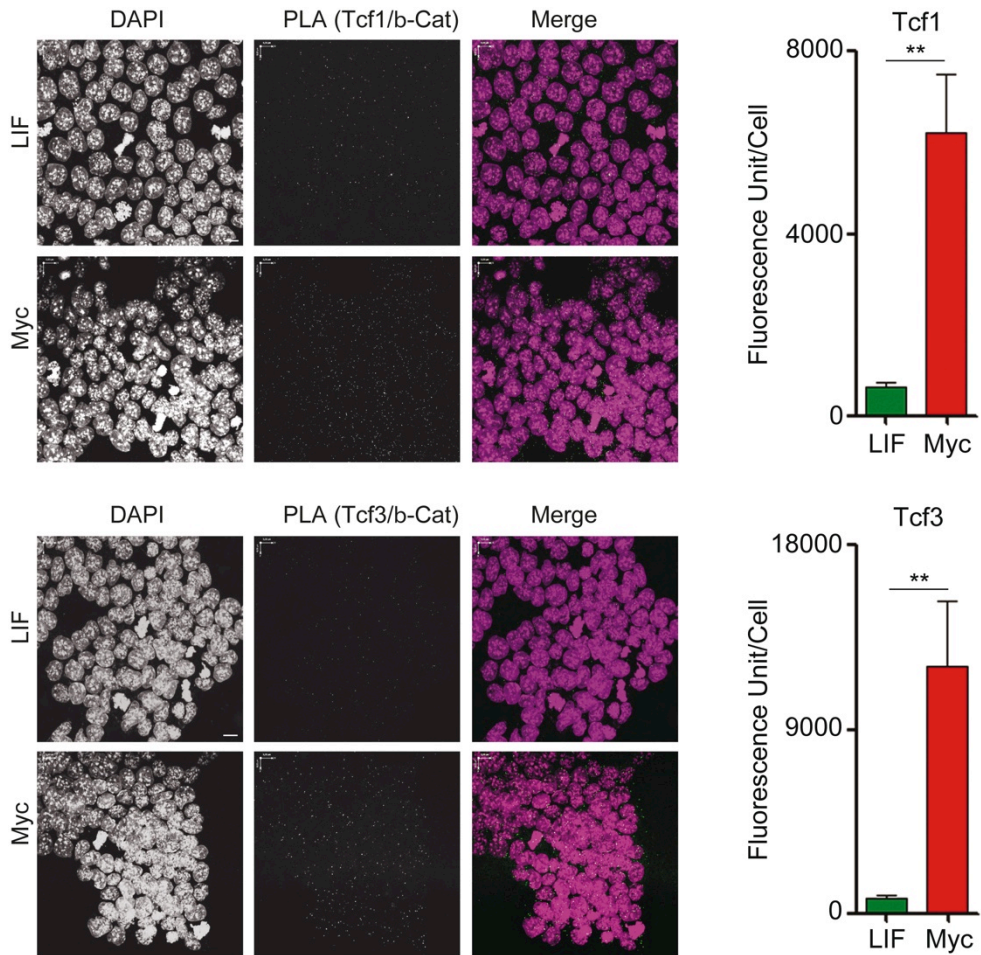
Figure 4.7 β-Catenin translocates in the nucleus and activates the expression of its target genes in Myc-maintained ES cells.

In situ Proximity Ligation assay (PLA) was performed to measure the proximity between Tcf1 or Tcf3 and β-Catenin within cell nuclei of LIF- and Myc-maintained ES cells. Representative images of PLA between Tcf1 or Tcf3 and β-Catenin within cell nuclei of LIF- and Myc-maintained ES cells and relative quantification; scale bar = 50 μm.

4.1.5 Wnt pathway activity is essential to sustain ES cell identity in Myc-maintained ES cells

The main negative regulators of Wnt pathway are the antagonists Dkk1 and Sfrp family member, which prevent the activation of the pathway by interfering with the receptor-ligand interaction. We hypothesized that Myc-maintained condition preserves the ES cell status by repression of Wnt antagonist. To test this hypothesis, we treated Myc-maintained ES cells with soluble Wnt inhibitors in order to complement their down-regulation. Upon Dkk1/Sfrp1 treatment, we found a change in cell morphology and a relative reduction of AP+ cells (Figure 4-8), indicating that a reduction of Wnt pathway activity is sufficient to start differentiation in Myc-maintained ES cells. Importantly, these effects were counteracted by ES cells stimulation with soluble Wnt3a (Figure 4.8).
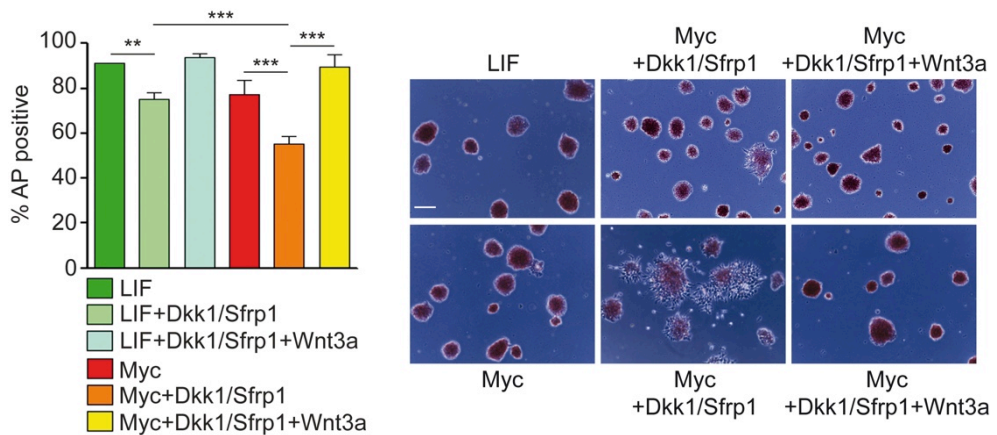
Figure 4.8 c-Myc requires active Wnt pathway to sustain ES cells self-renewal.
Alkaline Phosphatase (AP) staining of R1 ES MycER cells grown for three days in presence or absence of Wnt pathway inhibitors Dkk1 and Sfrp1 or the Wnt3a ligand, as indicated. Relative quantification of positive colonies is represented as percentage of the total colonies formed. Representative images of stained ES cells are shown. Scale bar = 200 μm. Error bars represent standard deviation from 3 independent experiments. **$p < 0.01$; ***$p < 0.001$.

Next, we evaluate whether c-Myc requires β-Catenin, the downstream effector of Wnt signalling, to sustain self-renewal in ES cells. To address this point, we generated a MycER β-Catenin knocked-down ES cells clone (shβ-Catenin ES cells), and we observed that it did not perturb self-renewal of ES cells grown in presence of LIF (Figure 4-9). In contrast, shβ-Catenin ES cells grown without LIF in presence of 4-OHT, started to differentiate, despite c-Myc was enforced, as shown by the changed colony morphology and the reduced number of AP+ colonies (Figure 4-9). Differently from what measured upon Dkk1 and Sfrp1 treatment, exogenous Wnt3a stimulation cannot revert the phenotype of Myc-maintained ES cells knockdown for β-Catenin (Figure 4.9).

Taken together, these data suggest that c-Myc, in order to exert its function on ES cells maintenance, requires the intact Wnt/ β-Catenin signalling.
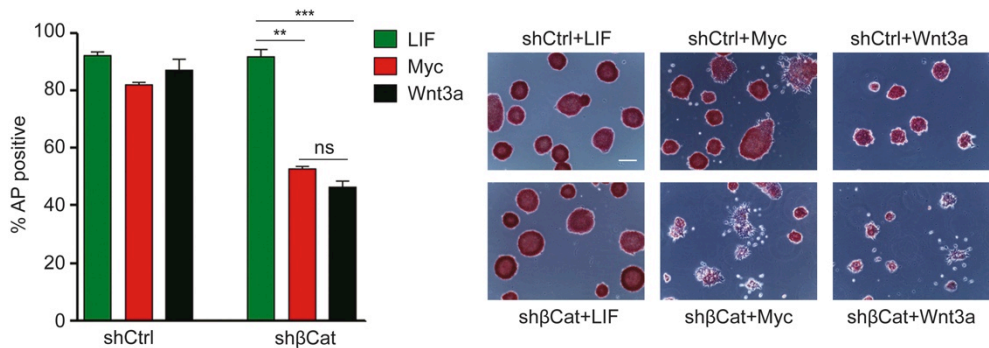
Figure 4.9 Active β-Catenin is essential in Myc-maintained ES cells.
AP staining of MycER ES cells clones expressing either a control shRNA (shCtrl) or a β-Catenin shRNAs (shβ−Cat) and grown for three days in the indicated conditions; relative quantification of positive colonies are represented as percentage of the total colonies formed. Representative images of stained ES cells grown in the different conditions are shown. Scale bar = 200 μm. Error bars represent standard deviation from 3 independent experiments. **p<0.01; ***p<0.001.

4.1.6 c-Myc directly associates with PRC2

In a previous work we showed that c-Myc is able to directly interact with the chromatin modifier Polycomb Repressive Complex 2 (PRC2), *in vitro*. Since the genes antagonists of the Wnt pathway such as Dkk and Sfrp family members are bivalent genes [Bernstein et al., 2006; Kurimoto et al., 2015] and Polycomb targets in ES cells [Leeb et al., 2010], we hypothesized that c-Myc could mediate the recruitment of PRC2 complex at their promoter in order to cause their repression. First of all, we confirmed that c-Myc directly interacts with PRC2 also in the cellular context. To assess this point, we used acceptor photobleaching Fluorescence Resonance Energy Transfer (apFRET). We cloned Eed and Aebp2 cDNA, which direct interact with c-Myc *in vitro*, in expression vectors that carried the fluorescent protein CFP (as described in methods). c-Myc cDNA instead was cloned in expression vector that carried the fluorescent protein YFP (Figure 3.1). Since we observed a low efficiency of co-transfection in mES cells, we performed this analysis in HEK 3T3 cells. To measure the fret efficiency we followed the protocol described in chapter 3.3.4. To analyse the association between Eed and c-Myc we used as positive control a construct expressing Ezh2 fused with YFP (Figure 3.1), while as negative control a construct expressing only YFP. apFRET results showed that EED is able to bound c-Myc also *in vivo* (Figure 4.10A).

Previous works suggest that Aebp2 interacts with Eed in PRC2 complex [Ciferri et al., 2012], then to quantify the association between Aebp2 and c-Myc, we used a construct expressing Eed fused with CFP as positive control. The results showed that Aebp2 directly interacted with c-MYC with high efficiency (Figure 4.10B). Furthermore, we tried to understand through which domain c-Myc could interact with Eed and Aebp2. Since Myc homology Box II (MBII) is involved in several interactions with a wide range of co-factors of c-Myc, essential for c-Myc activity, we cloned c-Myc protein deleted in the MBII domain (MycΔMBII) fused with YFP and we used the

same strategy to quantify association with EED and AEBP2. The results showed that the deletion of the MBII domain resulted in a reduction of the interaction with both EED and AEBP2 (Figure 4.10). These results suggest that c-Myc directly interacts with PRC2 in a cellular context and that its MBII domain is required for an efficient binding to the complex.
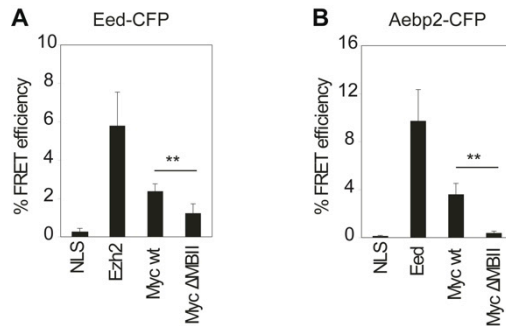
Figure 4.10 FRET efficiency.
The Fluorescence Resonance Energy Transfer (FRET) efficiency between Eed- or Aebp2-CFP and the indicated YFP-fusion proteins was calculated and the data are represented as the mean and the relative standard deviation obtained by analyzing 12 samples in three independent biological replicas. **p<0.01.

4.1.7 c-Myc requires PRC2 complex to repress Wnt pathway antagonists

To investigate whether Myc-PRC2 interaction was essential to sustain self-renewal in Myc-maintained ES cells, we generated stable MycER clones transduced with lentiviral vectors expressing Eed (shEed) or Ezh2 (shEzh2) short hairpin RNA. First, the knockdown efficiency of the shRNAs was determined measuring the protein level of Eed and Ezh2 in LIF- and Myc-maintained cells. Both the shRNAs had a good knockdown efficiency, as a reduction of Eed and Ezh2 protein levels was observed (Figure 4.12); in addition, in both knockdowns we observed a reduction of Suz12, confirming the inhibition of PRC2 complex (Figure 4.11).
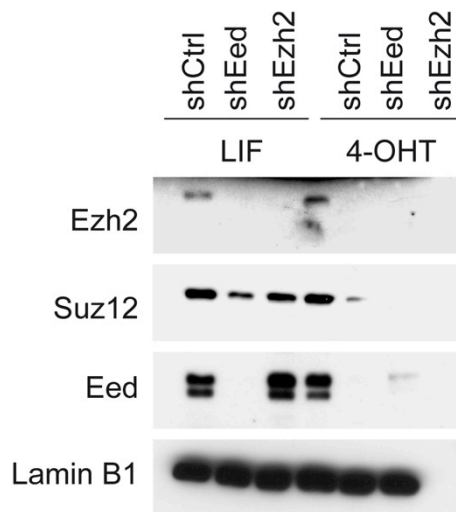
Figure 4.11 Eed and Ezh2 protein levels after knockdown.
ES cells were transduced with shRNAs against Eed and Ezh2 and 72h later PRC2 proteins levels were quantified by Western Blot.

Thereafter, we analyzed the capacity of Eed and Ezh2 knockdown-MycER cells to self renew in either a LIF-supplemented medium or in Myc-dependency. We observed that although c-Myc was enforced, in the absence of the PRC2 complex, ES cells started to differentiate, as shown by the changed morphology of the colonies and the reduced number of AP+ colonies (Figure 4.12) in both Eed and Ezh2 knockdown-cells. To evaluate whether the activation of Wnt pathway is a downstream effect of the interaction between c-Myc and PCR2 complex, we treated the Eed and Ezh2 knockdown-cells with recombinant Wnt3a. When Wnt/β-Catenin signalling was reactivated, Myc-maintained ES cells self-renewal was restored, as shown by the increased number of AP+ colonies (Figure 4.12). On the contrary, Dkk1/Sfrp1 supplementation even increased the negative effect of PRC2 knocking-down on Myc-dependent self-renewal capacity of ES cells (Figure 4.12).
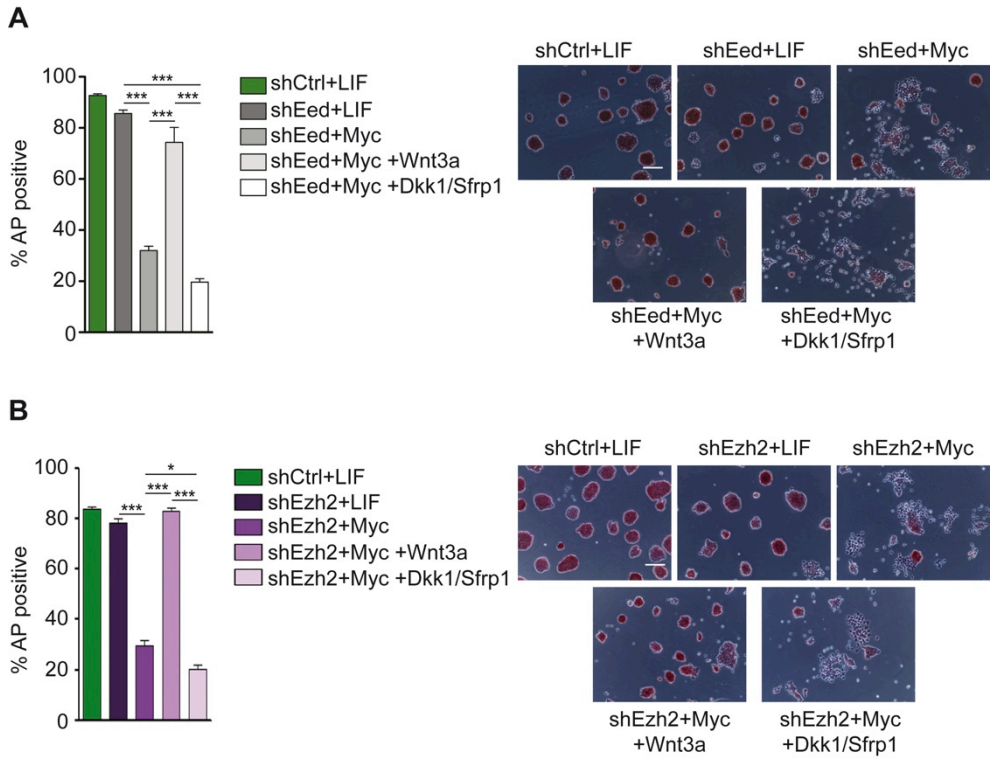
Figure 4.12 ES cells self-renewal upon Eed and Ezh2 knockdown.
AP staining of MycER ES cells clone expressing either a control shRNA (shCtrl), Eed shRNAs (shEed) or Ezh2 shRNAs (shEzh2) and grown for three days in the indicated conditions; relative quantification of positive colonies are represented as percentage of the total colonies formed. Representative images of stained ES cells grown in the different conditions are shown. Scale bar = 200 μm. Error bars represent standard deviation from 3 independent experiments. *$p<0.05$; **$p<0.01$; ***$p<0.001$.

To evaluate the effect of the interaction between c-Myc and PRC2, we performed Chromatin Immunoprecipitation (ChIP) experiments. To this end, we generated endogenous c- and N-Myc double Knocked-down in MycER ES cells (dKD), by transducing them with lentiviral vectors expressing either c- and N-Myc short hairpin RNAs. The established ES cells clone allowed the modulation of MycER protein level. Indeed, nuclear/cytoplasm fractionation showed that 16h after 4-OHT removal, MycER was completely export outside the nucleus and accumulated in the cytoplasm (Figure 4.13).
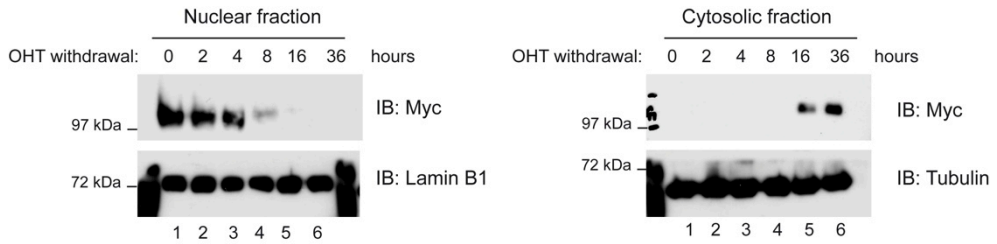
Figure 4.13 c-Myc protein levels after knockdown.
ES cells were transduced with shRNAs against c-Myc and N-Myc and 72h later nuclear/cytoplasm fractionation were performed and c-Myc proteins levels were quantified by Western Blot. Lamin B1 and Tubulin were used as loading control for nuclear and cytosolic fractionation respectively.

ChiP experiments showed that 16h after 4-OHT withdrawal, the loss of c-Myc binding led to reduction of H3K27me3 and Suz12 levels on Dkk1 and Sfrp1 promoters (Figure 4.14), while the levels of H3K4me3 were not affected. To evaluate that c-Myc directly recruits PRC2 on the promoters, after 16h without 4-OHT, we re-treated the ES cells with 4-OHT for 4h, and we observed an increase of Suz12 and H3K27me3 levels on the Dkk1 and Srp1 promoter. These results indicate that c-Myc could potentiate the Wnt pathway through PRC2 recruitment on Wnt antagonist promoter, therefore mediating their silencing.
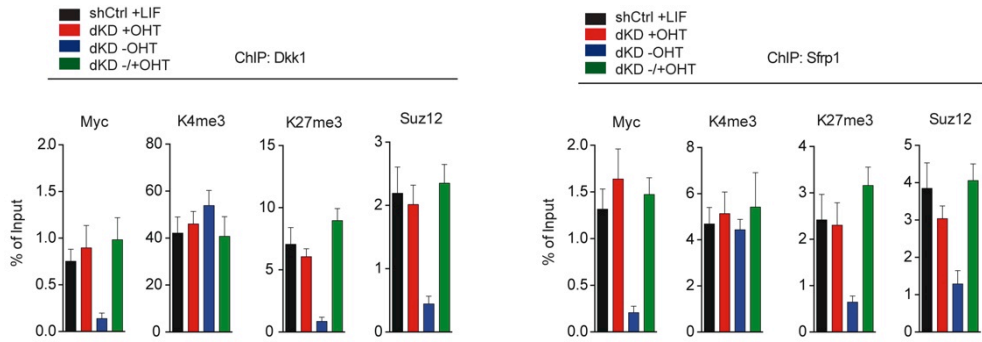
Figure 4.14 Binding of PRC2 and relative H3K27me3 histone mark on Dkk1 and Sfrp1 promoter.

Chromatin immunoprecipitation of PRC2 and H3K27me3 on the Dkk1 and Sfrp1 TSS in ES cells c-Myc/N-Myc (dKD) Knockdown. The shCtrl and the dKD ES cells were maintained respectively in LIF (black line) or in LIF in presence of 4-OHT (red line). After 56 h the dKD ES cells were either grown in the same conditions (+4-OHT, red line) or shifted to LIF only (-OHT, blu line) medium for the following 16 hours. Thereafter, the MycER protein was reactivated upon four hours treatment with 4-OHT (-/+ 4-OHT, green line).

4.2 c-Myc establishes an epigenetic memory in ES cells by generating a self-reinforcing positive feedback loop

4.2.1 c-Myc sustains ES cells self-renewal in long-term culture

We extended our analysis by assessing c-Myc ability to sustain ES cell self-renewal in long-term culture. To address this issue, we completely removed the LIF from the culture media and maintained ES cells only in the presence of MycER induction (Figure 4.15A). In agreement with a previous work [Cartwright et al., 2005], even after several passages in 4-OHT stimulation, Es cells maintained their identity, as shown by the number of AP+ colonies respect to LIF grown cells. Moreover Myc-maintained ES cells could proliferate indefinetly (Figure 4.15B). These results suggest that MycER activation can replace LIF activity in the long-term maintenance of ES cells.
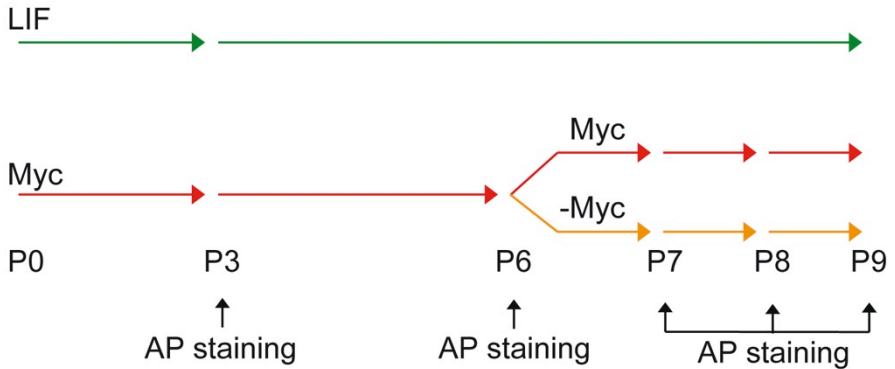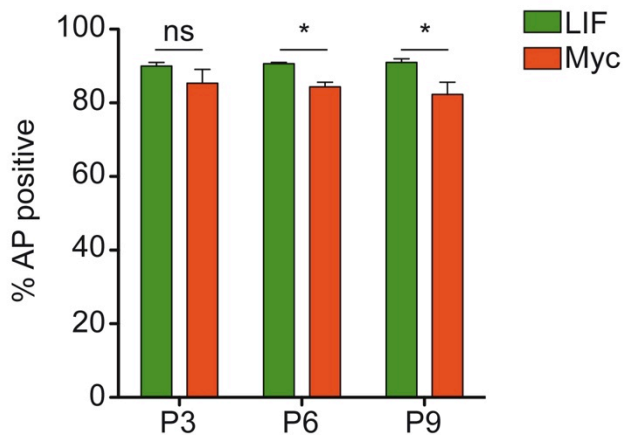
Figure 4.15 c-Myc sustains ES cells self-renewal in long-term culture.
(A) Schematic representation of the experimental outline. R1 MycER cells were grown either in presence of LIF (1000U/ml), as standard condition (named LIF, green line), or absence of LIF and in presence of 50 nM 4-OHT (named Myc, red line), or in absence of both LIF and 4-OHT (named -Myc, light red line). (B) Long-term colony forming assay was performed culturing cells in presence of LIF or 4-OHT (Myc) and the relative quantification of AP positive colonies was assessed at the indicated passages, until 18 days. Error bars represent standard deviation from 3 independent experiments. *p<0.05.

4.2.2 c-Myc establishes an epigenetic memory in ES cells

Environmental signals can induce changes in gene expression and chromatin structure. Such changes define cell identity and differentiation potential and can be maintained even in absence of initial signals, through many cell divisions [Bonasio et al., 2010]. We decided to test whether or not an environmental-induced epigenetic change could be heritable through mitosis. In order to test our hypothesis, we measured the self-renewal capacity of Myc-maintained ES cells following MycER inactivation upon 4-OHT withdrawal from the culture medium (call Myc-derived cells, -Myc) (Figure 15.A). We observed that upon only 6 days of culture with 4-OHT, if the environmental stimulus was removed, the ES cells started to differentiate. On the contrary, after twelve days of 4-OHT induction, despite a slight reduction in the first passages after stimulus removal, the morphology and the number of AP+ colonies were similar in LIF-, Myc-maintained and Myc-derived ES cells (Figure 4.16A). Furthermore, the rate of cellular proliferation shown that Myc-derived ES cells were able to expand indefinitely in the absence of both LIF and 4-OHT, yet maintaining their morphology (Figure 4.16B).
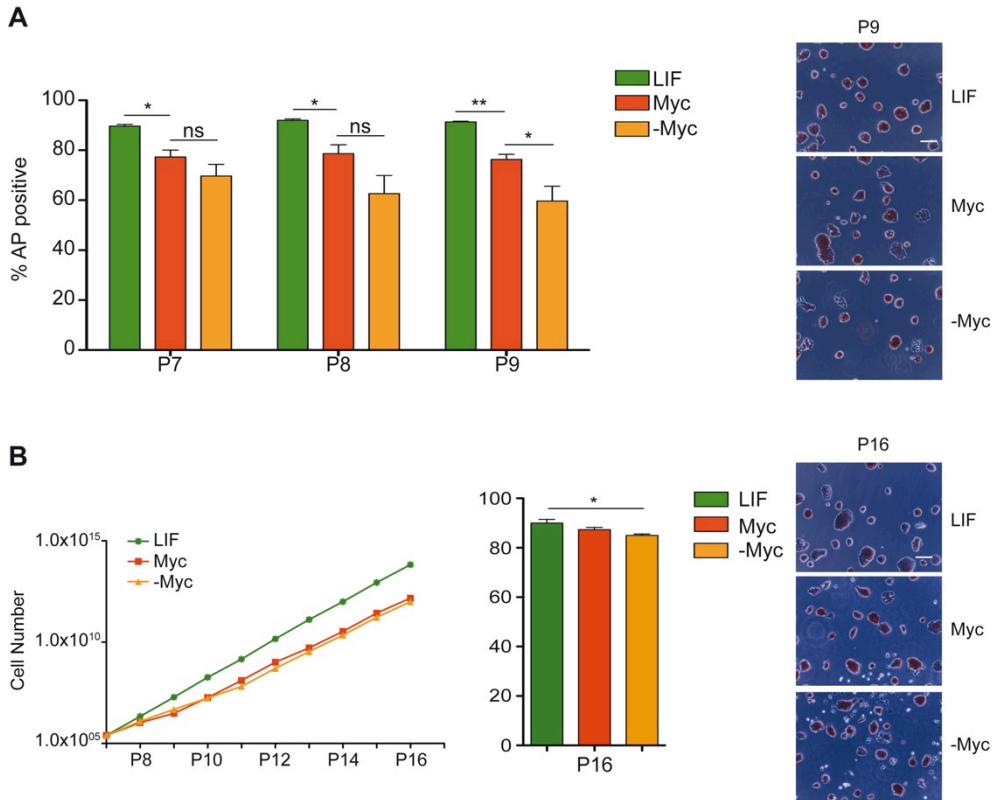
Figure 4.16 Myc-derived ES cells are able to self-renew and grow indefinitely.
(A) ES cells were grown for six passages in Myc-dependency (+4-OHT) and then were maintained in either the same culture condition (Myc) or they were grown in absence of both 4-OHT and LIF (-Myc). (B) Growth curve of LIF, Myc-maintained and Myc-derived ES cells. The relative quantification of AP positive colonies at each indicated passage were compared to ES cells grown in parallel in LIF-containing medium (LIF) and are represented as percentage of the total colonies formed. Representative images of stained ES cells at passages 9 and 16 are shown. Scale bar = 200 μm. Error bars represent standard deviation from 3 independent experiments. *p<0.05; **p<0.01.

To confirm that Myc-derived ES cells maintained a stem identity, we performed cell cycle profile and analysis of the timing of cell divisions. FACS analysis of Myc-derived cells showed that cell cycle is similar to LIF- and Myc-maintained cells (Figure 4.17A), and also the timing of divisions were comparable to LIF or Myc-maintained ES cells (Figure 4.17B).
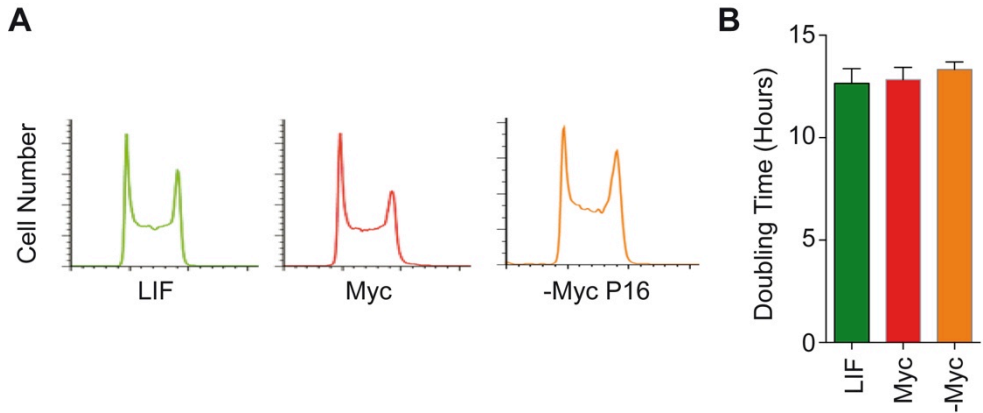
Figure 4.17 Cell cycle distribution and doubling time of ES cells upon 4-OHT withdrawal.
(A) ES cells were growth in LIF, Myc or –Myc manner and 48h later fixed and subjected to FACS. (B) Quantification of the doubling time of MycER^{T58A} ES cells maintained in presence of LIF, 4-OHT or in absence of both LIF and 4-OHT.

Finally, single cell tracking analysis confirm that the reduction of colonies in Myc-derived cells is attributable to increased cell death, however this cells showed a symmetrical pattern of division, suggesting that they maintained their pluripotency (Figure 4.18).
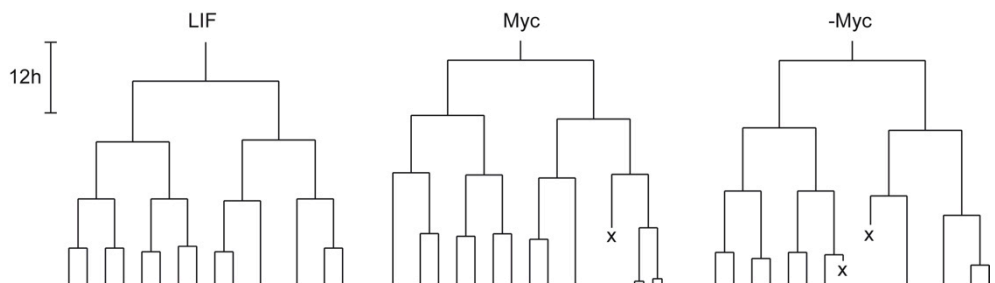
Figure 4.18 Single cell tracking analysis of LIF, Myc-maintained and Myc-derived ES cells expressing H2B-eGFP.
Lineage tree represents the pattern and timing of cell division of a single Embryonic Stem Cell grown in the indicated conditions.

To exclude the possibility that even in absence of 4-OHT induction, active form of MycER could be present in the Myc-derived ES cells, we performed nuclear/cytoplasm fractionation and analysed the localization of MycER. Despite a small amount of MycER was still present in the nucleus of Myc-derived cells at P7, this was completely absent in the subsequent passages (P8, P9 and P16) (Figure 4.19).
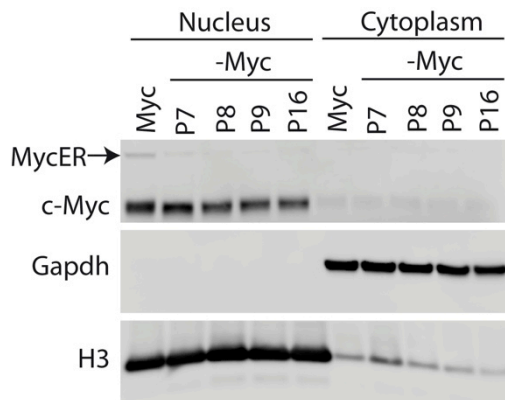
Figure 4.19 MycER protein levels in Myc-derived ES cells.
ES cells were harvested at different passages and nuclear/cytoplasm fractionation were performed and c-Myc proteins levels were quantified by Western Blot. Gapdh and histone H3 were used as loading control for cytosolic and nuclear fractionation respectively.

Taken together these results indicate that c-Myc not only sustains self-renewal in ES cells, but its prolonged over-expression induced by extern stimuli, can establish an epigenetic memory that would sustain ES cells self-renewal even in absence of further external stimuli.

4.2.3 The Myc-dependent epigenetic memory is not clone dependent

To examine whether the ability of c-Myc to establish an epigenetic memory could be ES Myc^{T58A}ER clone-dependent, we generated an independent ES cells clone, also expressing exogenous MycER (called A2 MycER clone) (Figure 4.20A). First of all, we investigated the cell pluripotency of MycER A2 clone, by measuring the protein levels of five genes implicated in pluripotency maintenance: Oct4, Nanog, Klf4, Sox2 and c-Myc (Figure 4.20A). Then, we compared A2 MycER cells grown in LIF or with 4-OHT induction and we measured a same number of dome-shaped AP+ colonies (Figure Figure 4.20B). Furthermore, their rate of proliferation, timing of division and cell cycle profile were comparable to LIF or Myc-maintained ES cells (Figure 4.21). Then, we measured the capacity of c-Myc to establish an epigenetic memory in A2 MycER clone. The cells were grown in absence of LIF with 4-OHT induction for 6 passages, then the 4-OHT was removed from the culture medium. We observed that also in an independent clone, Myc-derived ES cells maintained the same efficiency to give rise to round and AP+ colony similar to LIF-ES cells (Figure 4.22).
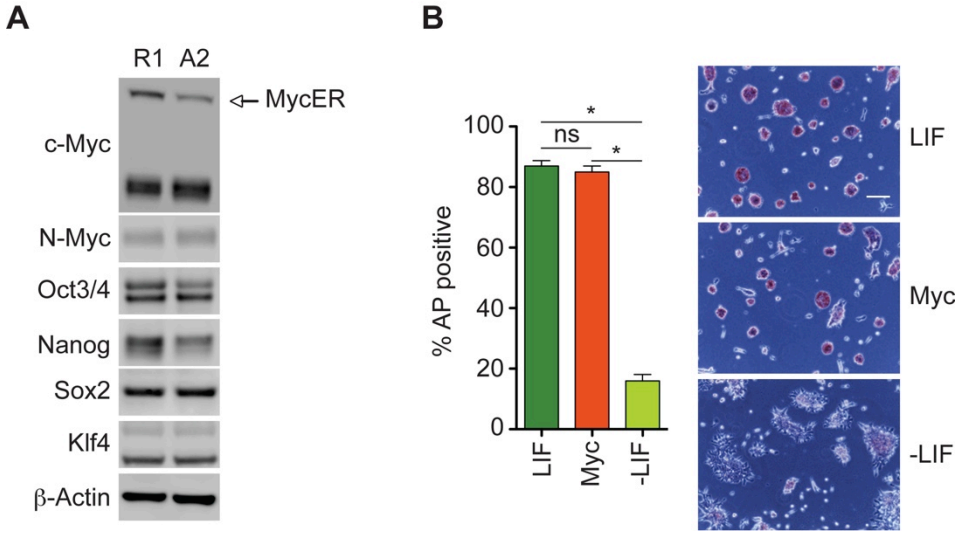
Figure 4.20 Characterization of the independently derived MycER ES cells A2 clone.
(A) Protein extracts were obtained from the MycER[T58A] ES cells clone R1 and from the newly derived MycER clone A2, maintained in presence of 4-OHT. Immunoblot analysis was performed with the indicated antibodies to measure the relative protein levels. The arrow indicates the MycER fusion protein. β-Actin was used as loading control. (B) Alkaline Phosphatase (AP) staining of the MycER A2 clone ES cells grown for three days in the indicated conditions and relative quantification of positive colonies are represented as percentage of the total colonies formed. Representative images of stained ES cells maintained for three days in LIF, 4-OHT (Myc) or in -LIF (middle panels). Scale bar = 200 μm. Error bars represent standard deviation from 3 independent experiments. *p<0.05; **p<0.01.
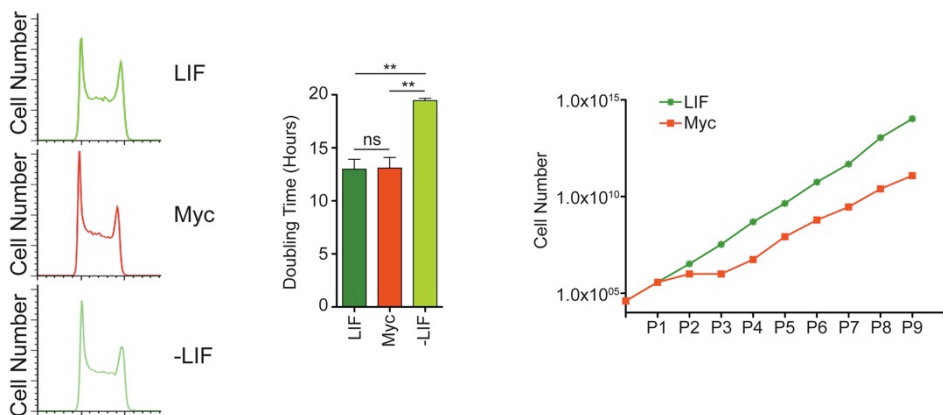
Figure 4.21 Cell cycle, doubling time and cell proliferation of A2 MycER clone.
Cell cycle profiles, doubling time and growth curve of A2 MycER clone. Error bars represent standard deviation from 3 independent experiments. **p<0.01.
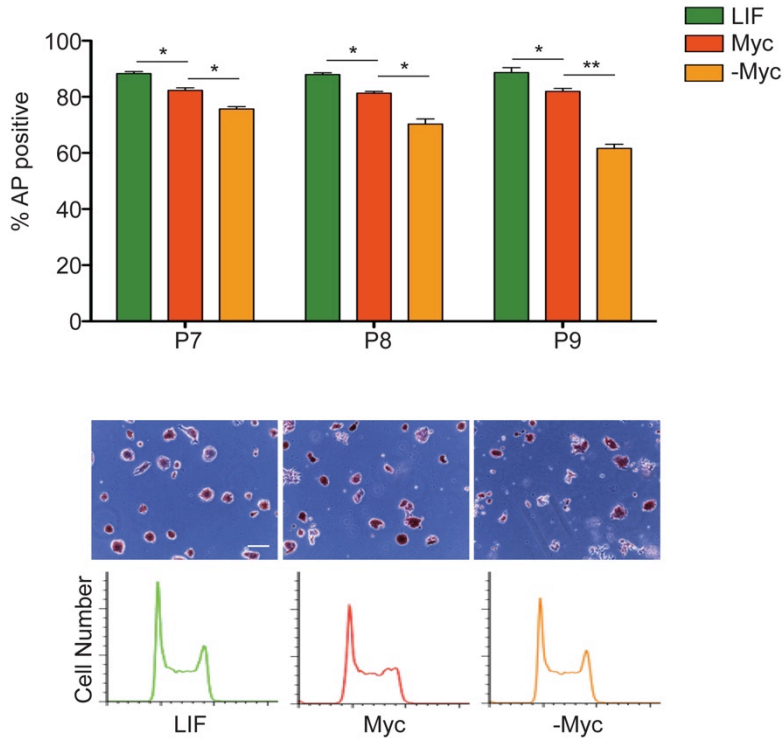
Figure 4.22 Myc-derived established from A2 MycER clone.

MycER A2 clone ES cells were grown for six passages in Myc-dependency (+4-OHT) and then were maintained for three more passages in either the same culture condition (+4-OHT) or grown in absence of both 4-OHT and LIF (- Myc). The relative quantification of AP positive colonies at each passage were compared to ES cells grown in parallel in LIF conditions and are represented as percentage of the total colonies formed. Representative images of stained ES cells maintained for three days in LIF, 4-OHT (Myc) or in -LIF/-4-OHT (-Myc) (middle panels) and the relative cell cycle profiles (lower panels) are shown. Scale bar = 200 μm. Error bars represent standard deviation from 3 independent experiments. *p<0.05; **p<0.01.

4.2.4 Myc-derived ES cells maintained pluripotency

Pluripotency is defined by the ability of cells to differentiate into derivatives of all the three embryonic germ layers: ectoderm, mesoderm and endoderm. A common tool to generate all three germ layers from ES cells *in vitro* is Embryoid Bodies (EBs) differentiation. To evaluate the differentiation potential of the Myc-derived ES cells we tried to aggregate Myc-derived ES cells in suspension, in order to form EBs. In this assay, the FBS was replaced by KnockOut Serum Replacement (KSR) to promote cell differentiation. In addition, we grew the cells into non-tissue culture-treated dishes to prevent their adherence to the plate. To examine the differentiation status of the cultured EBs, a qPCR analysis of lineage-specific genes was performed at different time point. We observed a similar expression of neuroectoderm (Pax6), endoderm (Gata6) and mesoderm (Pecam1) specific markers between LIF-, Myc-maintained and Myc-derived ES cells at day 8 of EBs differentiation, indicating that those cells can give rise to different germ layers *in vitro* (Figure 4.23).
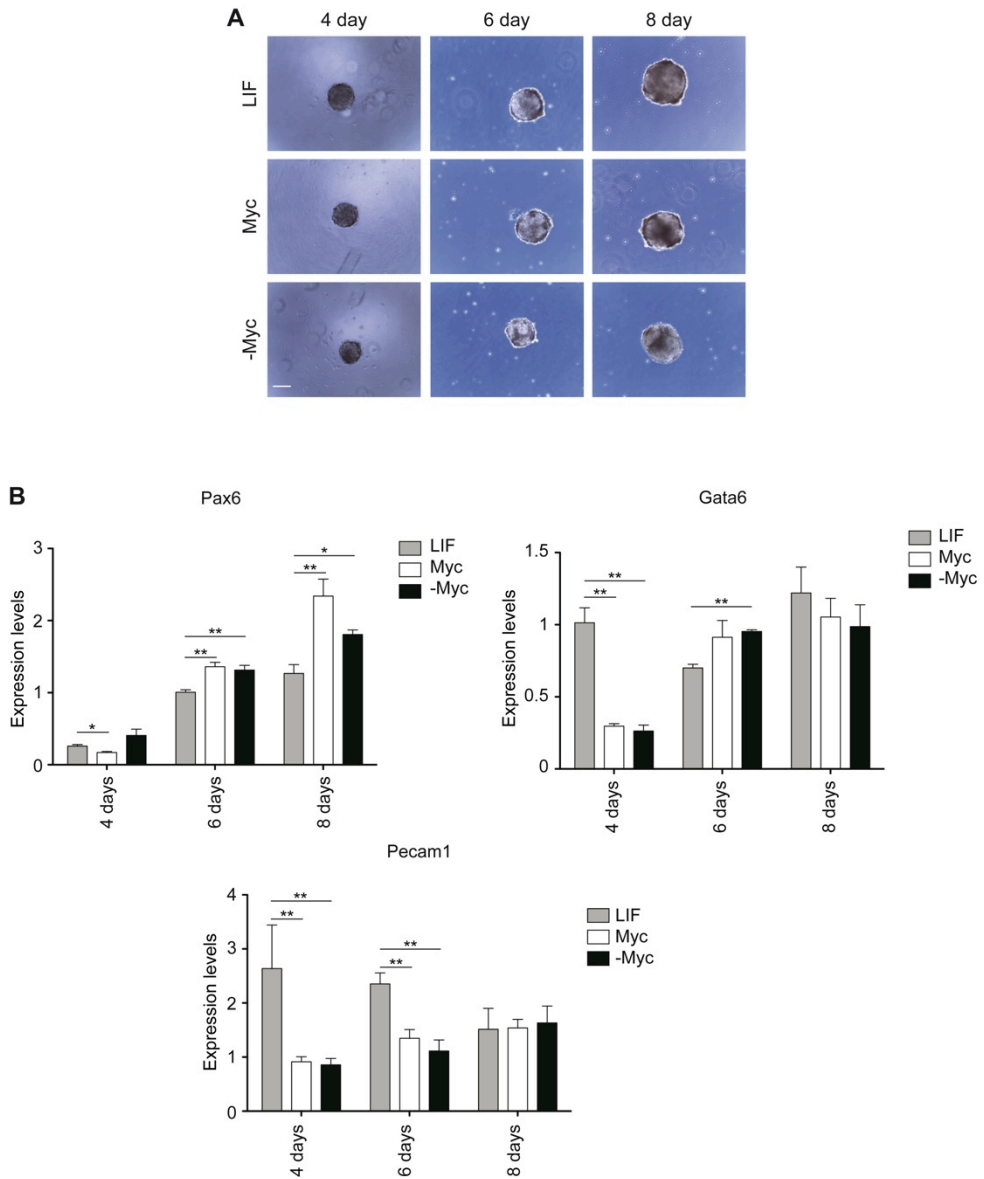
Figure 4.23 Embryoid bodies formation.

(A) LIF-, Myc-maintained or Myc-derived (-Myc) ES cells were grown for nine passages and then differentiated by inducing the formation of Embryoid Bodies (EBs). Representative images of forming EBs at 4, 6 and 8 days are shown. Scale bar = 200 μm. (B) The relative transcriptional level of lineage-restricted genes were quantified by qRT-PCR analysis in the formed EBs. Error bars represent standard deviation from 3 independent experiments. *p<0.05; **p<0.01.

In order to further investigate Myc-derived ES cell pluripotency, we tried to mimick the EpiSC transition *in vitro* from ES cells. First of all, we had to adapt ES cells to grow in a serum-free medium containing a MAPK inhibitor (PD0325901) and GSK3 inhibitor (CHIR99021) (2i medium), since under this conditions they are known for exhibiting a more homogeneous cell populations respect to normal culture medium. Then we derived EpiSC-like cells (EpiLCs) by culturing ES cells for 3 days in N2B27 medium supplemented with Activin A, basic fibroblast growth factor (bFGF) and KSR. In those conditions we observed a uniform differentiation of ES cells into flattened epithelial colonies that mimicked the epiblast structure (Figure 4.24).
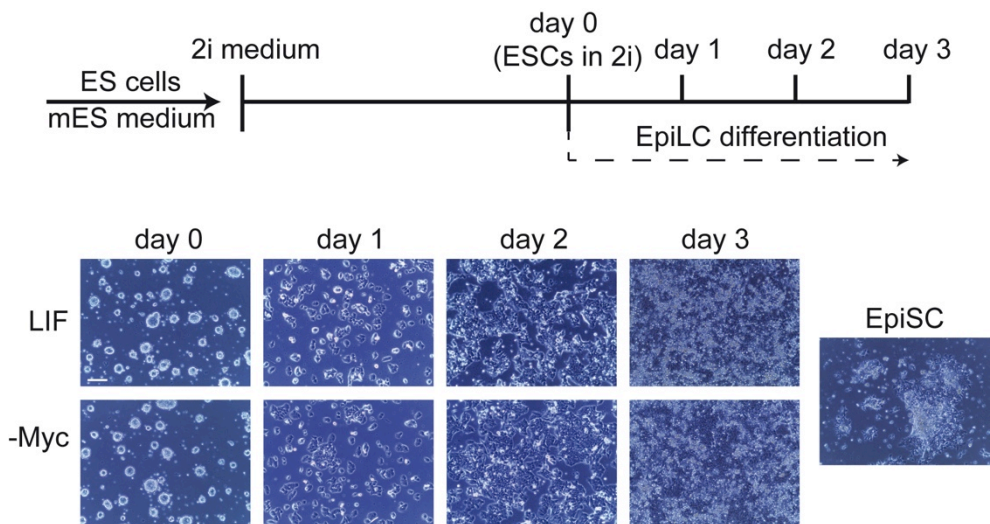
Figure 4.24 Epiblast-like cell transition.
Work outline and bright-field images of EpiLC induction from LIF-maintained and Myc-derived ES cells. EpiSC were used as control. Scal bar = 200 μm.

In order to measure the EpiSC transition, we quantified the expression of EpiSCs specific genes in the EpiLCs at 3 different days of differentiation,

and we used EpiSCs as positive control. In agreement with previous results [Hayashi et al., 2011], the expression level analysis showed that both in LIF-maintained and in Myc-derived ES cells, the level of Oct4 did not change during EpiLC transition, whereas genes more associated with the naïve state, such as Sox2 and Klf2, were down-regulated, similarly to EpiSC. Finally, during the transition, the expression level of genes associated with the primed state, such as Fgf5 and Dnmt3b were up-regulated similarly to EpiSC (Figure 4.25). These results confirmed that Myc-derived ES cells retain their naïve pluripotent state.
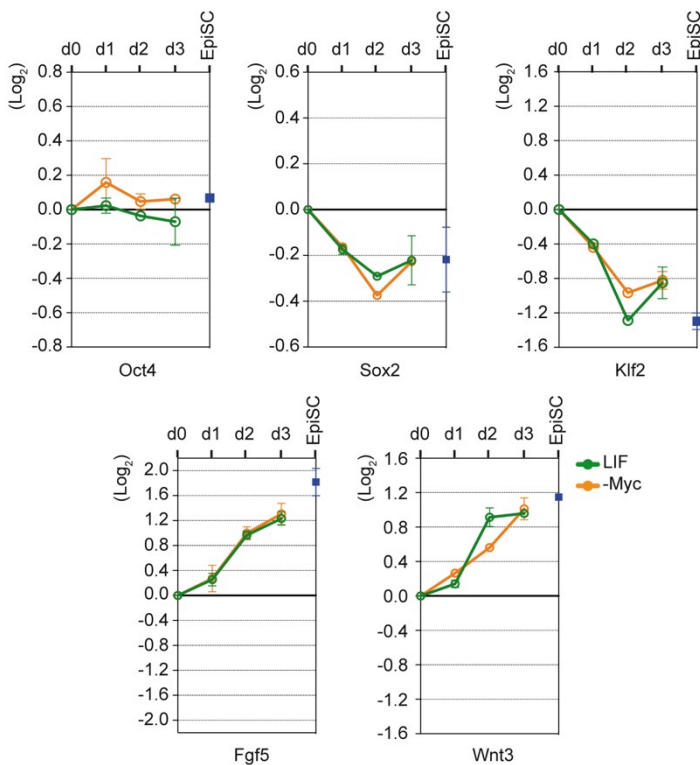
Figure 4.25 Gene expression profiles during EpiLC transition.
mRNA at different time point was measured by qPCR. EpiSCs were used as control. For each gene examined, the ΔCT from the average CT values of the two independent housekeeping genes Actin and Gapdh was calculated. The value was set as 0. For each point, the average value from three experiments is shown on the $\log_2$ scale.

Most importantly, Myc-derived ES cells pluripotency was corroborated by the fact that they were able to form teratomas once injected in *Nude* mice (Figure 4.26A). Haematoxylin/Eosin staining showed mesodermal-, ectodermal- and endoderml-derived cells, demonstrating that Myc-derived ES cells are able to differentiate into the three germ layers *in vivo*, similarly to LIF and Myc-maintained ES cells [Cartwright et al., 2005] (Figure 4.26B). Taken together, these results suggest that Myc-derived ES cells maintain their pluripotency, as they are able to differentiate into the three germ layers both *in vitro* and *in vivo*.
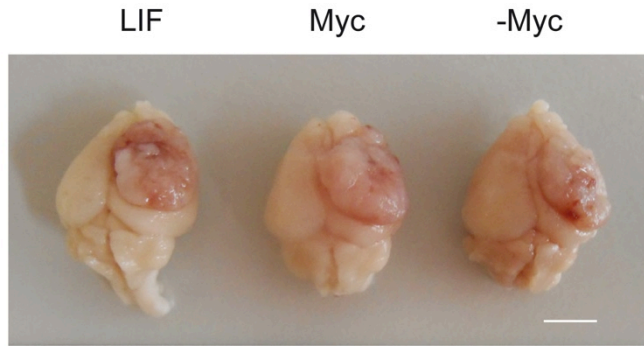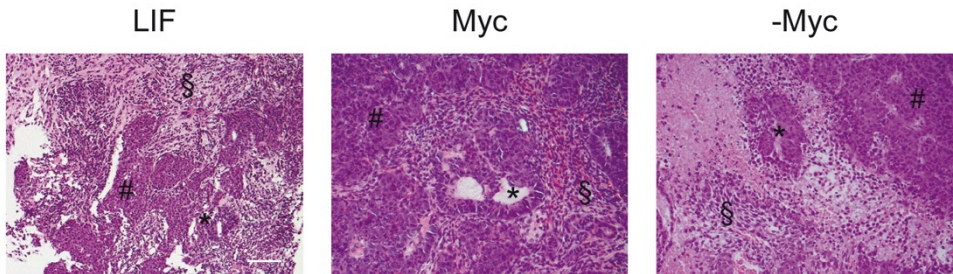
Figure 4.26 Myc-derived ES cells form teratomas upon injected in *nude* mice.
Teratoma assay assessing the pluripotency of LIF- (LIF), Myc-maintained (Myc) and Myc-derived (-Myc) ES cells upon injection into Nude mice. (A)Animals were sacrificed 24 days after injections and the whole brain were removed to measure the presence and size of teratomas. Scale bar = 5 mm. (B) Haematoxylin/Eosin staining showed mesodermal- (mesenchymal-like; §), ectodermal- (epithelial-like; #) and endodermal-derived (gut-like; *) cell types in each teratoma. Scale bar = 200 μm.

4.2.7 c-Myc sustains a self-reinforcing positive feedback loop

To evaluate the molecular mechanisms through which c-Myc could establish an epigenetic memory in ES cells, we investigated the Wnt pathway targets that could have a role on ES cells identity. To identify the downstream effectors of the Wnt pathway that are required for Myc-dependent self-renewal maintenance, we crossed the geneset of pluripotency factors [Marks et al., 2012; MacArthur et al., 2012] with the Oct4/Sox2/Nanog and Tcf3 co-bound targets, and analysed their expression profile in Myc- versus LIF-maintained ES cells. We found that both the endogenous c- and N-Myc genes are downstream effectors of the Wnt pathway and that their regulation depends on the MycER-driven reinforcement of Wnt signalling (Figure 4.27A). In fact, treatment of Myc-maintained ES cells with soluble Dkk1/Sfrp1 strongly inhibited the MycER-dependent transcriptional activation of both c- an N-Myc.

Thereafter, we evaluated whether endogenous Myc proteins are required to sustain Myc-dependent self-renewal capacity. In order to address this issue, we transduced MycER ES cells with lentivirus expressing inducible shRNA for both c- and N-Myc (called i-dKD), thus allowing us to tightly control the level and timing of gene silencing (Figure 4.27B). We observed that reduction of about 50% of the total amount of Myc proteins was sufficient to block the MycER-dependent self-renewing circuit in Myc- but not in LIF-maintained ES cells (Figure 4.27C). The role of endogenous Myc as downstream targets of the Wnt pathway was further highlighted by the finding that while control ES cells responded in a dose-dependent manner to Wnt3a-induced self-renewal, the Myc i-dKD cells did not.

Taken together, these findings show that activation of MycER establishes a positive feedback loop by sustaining the Wnt signalling, which in turn triggers the transcriptional activation of the endogenous c- and N-Myc genes. This self-reinforcing circuit plays a pivotal role in maintaining the identity of Myc-dependent ES cells.
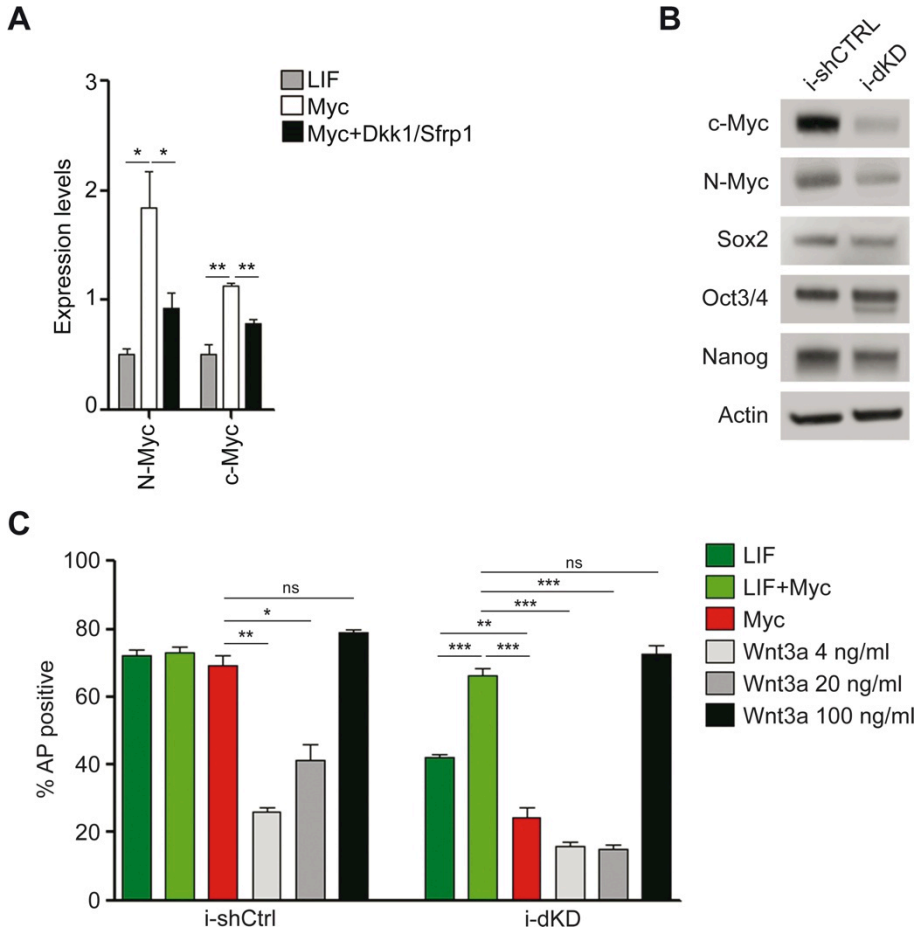
Figure 4.27 Myc sustains a self-reinforcing positive feedback loop.
(A) The relative transcriptional level of endogenous c- and N-Myc was confirmed by qRT-PCR analysis on RNAs extracted from ES cells grown in the indicated conditions for three days. (B) Western Blot analysis of proteins extracted from MycER ES cells expressing an IPTG-inducible control (shCtrl) or IPTG-inducible double c- and N-Myc shRNAs (dKD). Immunostaining (IB) analysis was performed using the indicated antibodies; β-Actin was used as loading control. (C) AP staining of MycER ES cell expressing either an IPTG-inducible control (shCtrl) or an IPTG-inducible c-Myc and N-Myc shRNAs (dKD) and grown in the indicated conditions for three days; relative quantification of positive colonies are represented as percentage of the total colonies formed. Error bars represent standard deviation from 3 independent experiments. *p<0.05; **p<0.01.

4.2.8 Myc-derived cells acquire a PRC2-dependent epigenetic memory

We asked whether the self-reinforcing regulatory circuit, triggered by prolonged MycER activation, could be maintained by the epigenetic silencing of Wnt antagonist through PRC2 recruitment. To assess this point, we treated ES cells with two different inhibitors of Ezh2 methyltransferase activity, EPZ and GSK126, and in both cases we observed a strong reduction of dome-shaped and AP+ colonies (Figure 4.28), suggesting that Myc-derived cells required an active PRC2 complex to self-renew. Importantly, the PRC2 inhibition could be reverted by treating the cells with exogenous Wnt3a (Figure 4.28), suggesting that Myc-derived cells require the PRC2 complex to activate the Wnt signalling through repression of its antagonists, as occur in Myc-maintained cells.

Hence, to further analyse the silencing of Wnt antagonists, we performed ChIP experiments to quantify the binding of endogenous c- and N-Myc on the promoter of Dkk1 and Sfrp1. The same levels of c-Myc and higher N-Myc levels were detected in Myc-derived ES cells compared to LIF-maintained ES cells. (Figure 4.29). Furthermore, no significant changes in the amount of PRC2 complex or H3K27me3 levels on the promoter of Dkk1 and Sfrp1 could be detected among LIF and Myc-derived ES cells (Figure 4.29). Taken together, these results suggest that Wnt antagonists are kept repressed by endogenous Myc proteins through PRC2 recruitment. This leads to reinforcement of the autocrine Wnt signalling, which sustains the expression of endogenous c- and N-Myc genes. This positive feedback loop could sustain self-renewal capacity of ES cells even in absence of environmental cues.
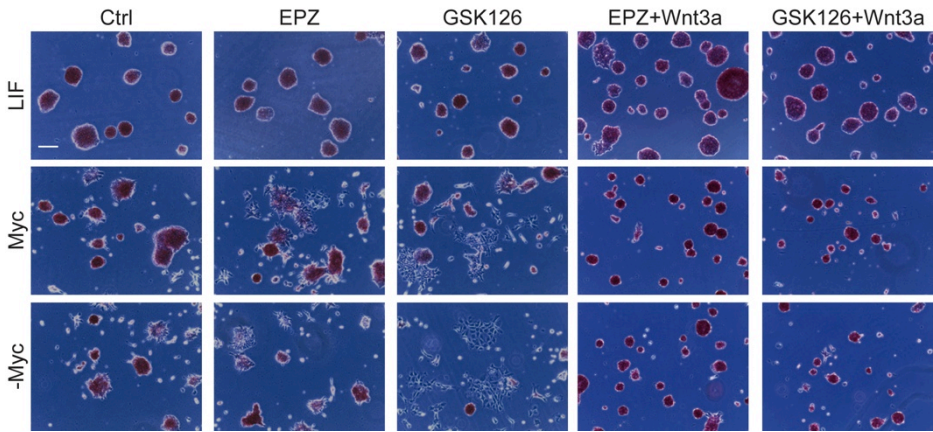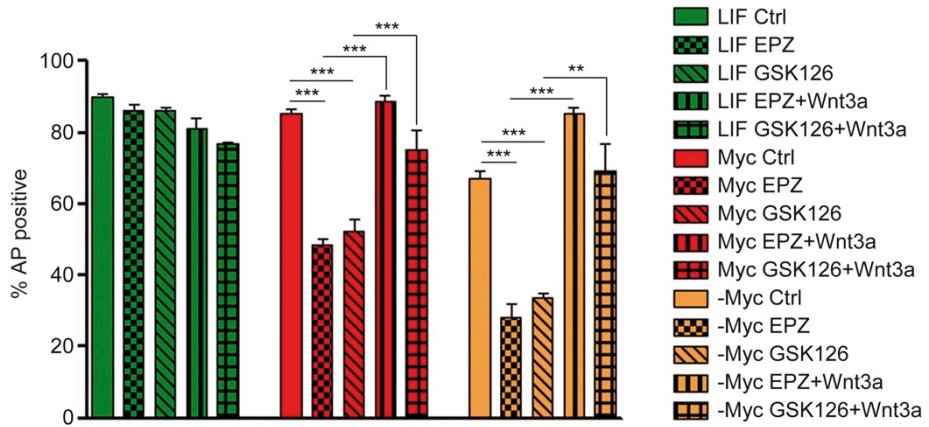
Figure 4.28 PRC2 biochemical activity is required to sustain self-renewal in Myc-derived ES cells.

AP staining of MycER ES cells grown for three days in the indicated conditions and relative quantification of positive colonies are represented as percentage of the total colonies formed. Representative images of stained ES cells are shown. Scale bar = 200 μm. Error bars represent standard deviation from 3 independent experiments. *p<0.05; **p<0.01.
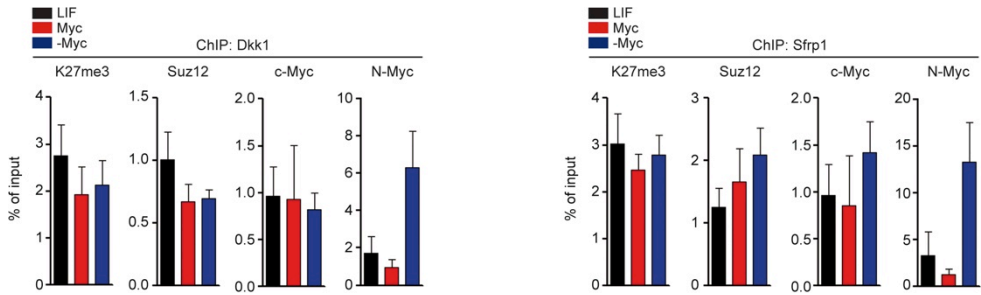
Figure 4.29 Myc-derived ES cells have PRC2 on Wnt antagonists promoters.
Chromatin extracts were obtained from either the MycER ES cells maintained in LIF- or Myc-dependency or the Myc-derived ES cells (-Myc). The level of H3K27me3 and the binding of Myc, N-Myc and Suz12 at the TSS of the indicated genes were measured by ChIP assay, (n=4).

To exclude the possibility that self-renewal and pluripotency ability of Myc-derived ES cells was due to genetic modification, we performed a karyotype analysis, which showed that Myc-derived cells remain euploid after prolonged culture, since they showed a proper set of chromosomes (n=40) (Figure 4.30A).

Moreover, upon reverse adaptation to grow in LIF containing medium, the Myc-derived ES cells (called LIF-reprogrammed, rLIF) returned sensitive to the LIF/Stat3 pathway, as observed by the strongly reduction of AP+ colonies when treated with two different inhibitors of the JAK pathway, AG490 and Jaki1 (Figure 4.30B). On the other hand, they returned to be unresponsive both to the functional activity of PRC2, if treated with EPZ and GSK126 inhibitors, and to Wnt pathway activity, if treated with XAV939 and Dkk1/Sfrp1inhibitors (Figure 4.30B).
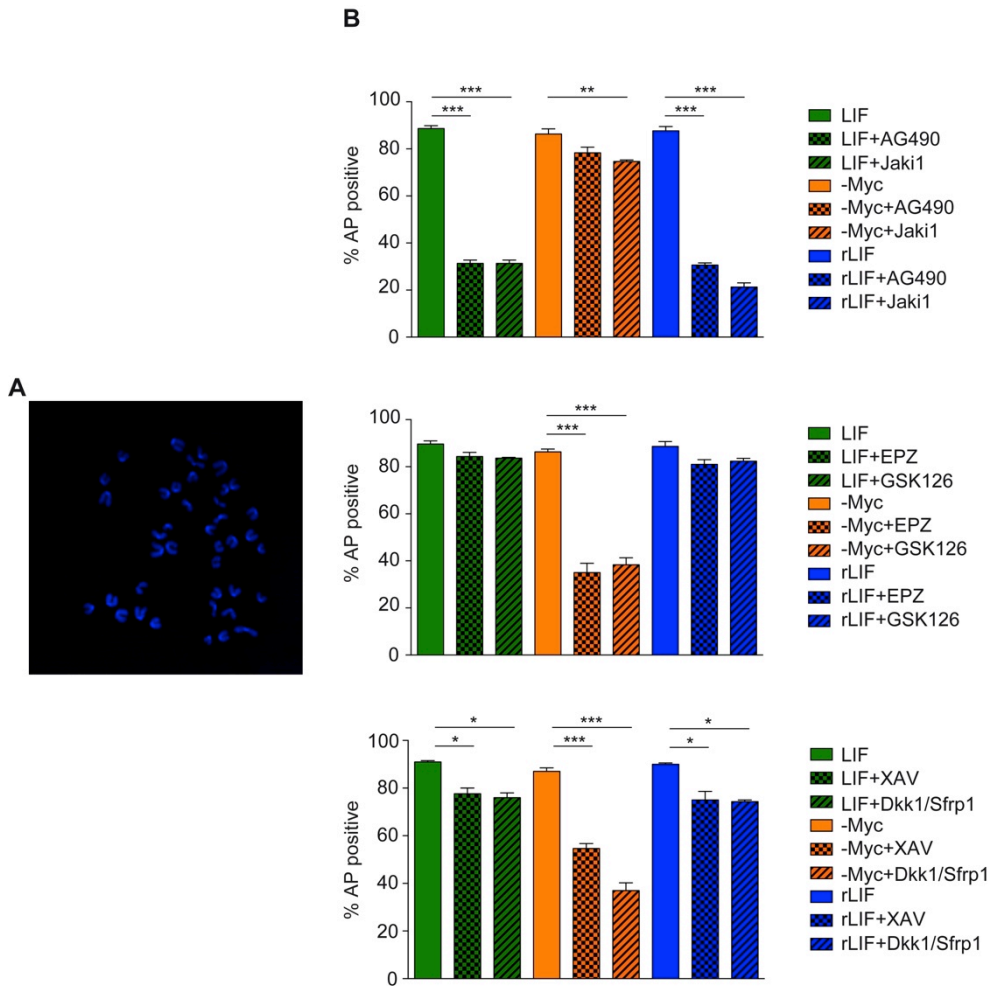
Figure 4.30 Myc-derived ES cells are euploid and are able to revert into a LIF-dependent state.
(A) karyotype analysis of Myc-derived ES cells at passage 30. (B) AP staining of MycER ES cells grown for three days in the indicated conditions and relative quantification of positive colonies are represented as percentage of the total colonies formed. Error bars represent standard deviation from 3 independent experiments. *p<0.05; **p<0.01; ***p<0.001.

Finally, we measured the transcriptional levels of Wnt antagonists, Dkk1 and Sfrp1, in LIF-reprogrammed ES cells in order to confirm the reversion of the self-reinforcing positive feed-back loop. qPCR analysis showed that gene expression levels of Dkk1 and Sfrp1 were up-regulated at similar levels to LIF-maintained ES cells (Figure 4.31). Taken together, these

results showed that in order to establish a positive feedback loop, c-Myc requires the biological activity of PRC2, and that this self-reinforcing circuit can be reverted upon treatment with LIF.
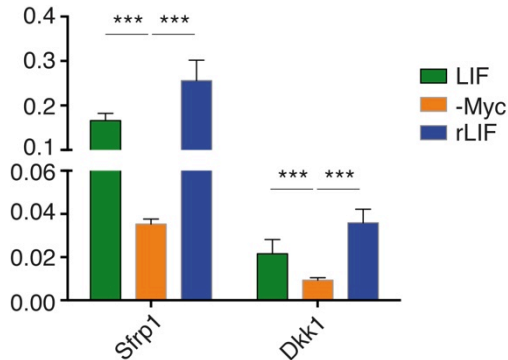
Figure 4.31 Dkk1 and Sfrp1 expression levels.
The relative transcriptional level of Dkk1 and Sfrp1 was confirmed by qRT-PCR analysis on RNAs extracted from ES cells grown in the indicated conditions for three days. Error bars represent standard deviation from 3 independent experiments. ***p<0.001.

4.3 c-MYC acts as tumor reprogramming factor in human mammary epithelial cells by inducing stem cell-like fate

Recent findings shown the existence on neoplastic tissues of a subpopulation of tumor cells, called Cancer Stem Cells (CSCs), that carries similar properties to those that characterize normal stem cells. Despite their attractiveness, the molecular mechanisms underlying their formation are poorly understood. Several works have shown evidences implicating progenitor cells as targets of neoplastic transformation, induced by the reacquisition of self-renewal capacity, through accumulation of a number of genetic and epigenetic modifications [Cozzio et al., 2003; Krivtsov et al., 2006]. Furthermore, recent works demonstrated that TFs network play an important role in establishing cellular states, including the SC state [Polytarchou et al., 2012; Rheinbay et al., 2013].

Given the previous considerations, we hypothesized that c-MYC over-expression in committed mammary epithelial cells could induce their reprogramming to a stem cell-like state.

To address this issue, as model we used a human hTERT-immortalized mammary epithelial cell (IMEC) line in which we induced constitutive c-MYC over-expression (IMEC MYC) (Figure 4.32A). We observed that constitutive c-MYC over-expression in IMEC induced loss of the typical epithelial phenotype. In fact, after the first divisions, cells started to detach and grew as semi-adherent spheroids (mammospheres) (Figure 4.32B). In particular, while IMEC WT cells divide parallel to the culture plane, about 50% of cells over-expressing c-MYC divide by tilting their mitotic spindle until to 25°C (Figure 4.32C).

Further analysis indicated that this loss of cell polarity is combined to a disorganization of adherent junctions, in term of β-Catenin distribution and to a general reduction of β-Catenin and Cadherin protein levels (Figure 4.33).
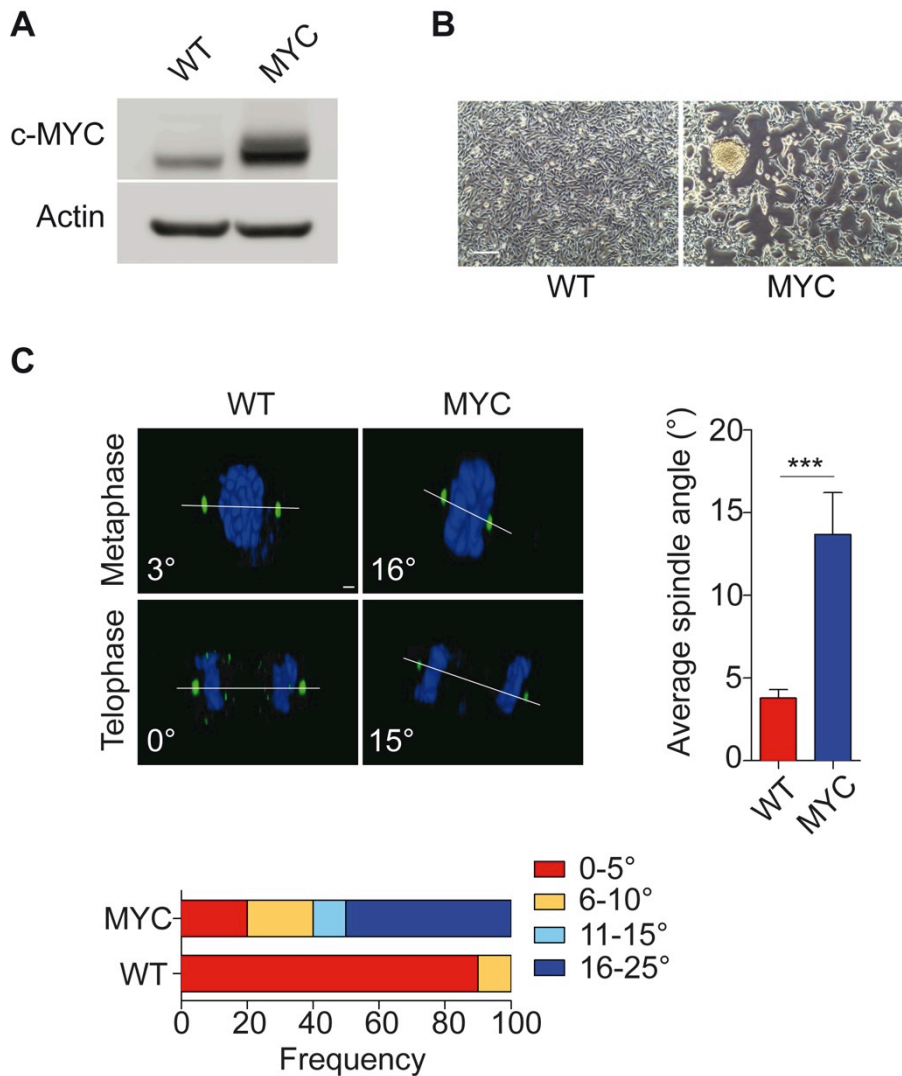
Figure 4.32 c-MYC over-expression causes loss of cell polarity in IMEC.
(A) Western Blot analysis of proteins extracted from both IMEC WT and c-MYC. Immunostaining (IB) analysis was performed using the indicated antibodies; Actin was used as loading control. (B) Morphology of IMEC WT and c-MYC cells. Scale bar = 200 μm. (C) Immunofluorescence images and angle analysis of mitotic spindle. γ-Tubulin (poles) and DAPI (chromosomes) are shown. Scale bar = 10 μm.
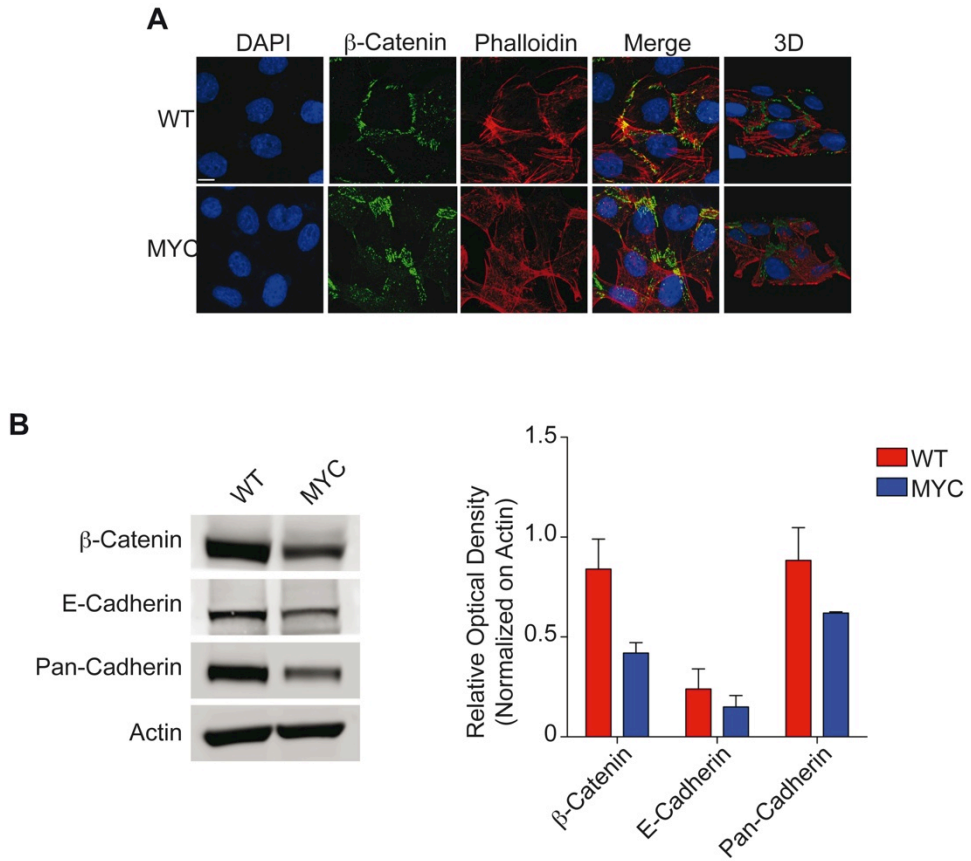
Figure 4.33 Loss of adherent junctions in IMEC MYC.
(A) Immunofluorescence images of the IMEC WT and MYC stained with β-Catenin and Phalloidin to highlight the cytoplasm. Scale bar = 100 μm. (B) Immunostaining (IB) analysis was performed using the indicated antibodies; Actin was used as loading control. (C) Histone quantification from Immunostaining analysis.

5. DISCUSSION

5.1 c-Myc sustains self-renewal and pluripotency of ES cells

Pluripotent stem cells are poised to differentiate into essentially all cell types in response to different environmental stimuli. In this context, the chromatin acts as molecular sensor of cellular signaling pathways activated in response to physiological and environmental stimuli and allows changes in gene expression pattern that can be stably maintained during cell division, therefore establishing a defined cell identity.

A well-known signaling pathway, with a crucial role in Embryonic Stem (ES) cells maintenance, is initiated by the cytokine Leukemia Inhibitory Factor (LIF). LIF acts via the glycoprotein-130 receptor, to promote a JAK-STAT3 signaling cascade [Raz et al., 1999], which integrates into the core of the Transcriptional Regulatory Network (TRN) by co-occupying enhancers bound by Oct4, Sox2 and Nanog [Chen et al., 2008]. More recently, it has been shown that dual inhibition of Erk and Gsk3b signaling pathways is able to prevent ES cells differentiation [Ying et al., 2008]. The ES cells dependency on LIF-STAT3 pathway could be circumvented by enforced expression of pluripotency factors [Chambers et al., 2003; Niwa et al., 2009; Cartwright et al., 2005]. Among these, the Myc family members, c-Myc and N-Myc have been described to modulate self-renewal and pluripotency of ES cells. Despite numerous studies have demonstrated the crucial role of c-Myc in sustaining pluripotency [Cartwright et al., 2005; Neri et al., 2012; Smith et al., 2010], its mechanisms of action are still not completely described. Until now, it has been proposed that c-Myc can sustain self-renewal and cell proliferation of ES cells by regulating specific set of genes from those regulated by the TRN [Chen et al., 2008; Kim et al., 2010]. Moreover, it has been proposed that c-Myc acts as universal

amplifier by binding to the promoter regions of its target genes that cause a redistribution of RNA polymerase [Lin et al., 2012; Nie et al., 2012]. However, c-Myc not only acts as a transcriptional activator, but about 35% of its target genes are repressed. In fact, c-Myc can suppress primitive endoderm differentiation of pluripotent stem cells, by inhibiting the master regulator Gata6 [Smith et al., 2010] and, through miR-17-92 cluster, can suppress the expression of chromatin regulatory genes, to promote cell proliferation [Li et al., 2014]. Although it is very tempting to conclude that c-Myc has a crucial role in sustaining ES cells self-renewal, those works still did not prove the molecular mechanisms that underlie the Myc-dependent transcriptional repression. This study describes a new model in which Myc-dependent self-renewal maintenance of ES cells is ensured by the Myc-dependent repression of genes encoding for Wnt antagonists, in cooperation with the PRC2 complex.

In our work, we used mouse ES cells which express a steroid-activable MycER construct [Cartwright et al., 2005]. We propose that controlling the amount of c-Myc, through 4-OHT induction, is crucial for the maintenance of ES cells self-renewal and pluripotency. Our data are in agreement with previous studies, showing that elevated activity of c-Myc can replace the LIF/Stat3 signaling in ES cells [Cartwright et al., 2005].

Gene expression profile analyses of Myc-maintained and LIF-dependent ES cells, together with Epiblast Stem cells (EpiSCs), used as control for a primed state of stemness, revealed that Myc-maintained ES cells cluster together with LIF-ES cells and are distant from EpiSCs. However, despite the observed similarities, a specific gene expression pattern distinguished Myc- from LIF-maintained ES cells. Ingenuity Patway Analysis (IPA) showed that JAK/Stat3 and Mapk pathway are over-represented in LIF, while the Wnt/β-Catenin signaling is enriched in Myc-maintained ES cells. One of the aims of this work was to determine whether c-Myc required the activation of Wnt pathway to support the pluripotency of ES cells. In fact,

several studies have demonstrated that the Wnt pathway can act as a niche factor to support the self-renewal of ES cells [Reya et al., 2003].

Our data indicated a Myc-mediated reinforcement of the Wnt autocrine loop, including activation of the Fzd/Lrp receptor complex resulting in the phosphorylation of Lrp6. Moreover we showed that MycER activity significantly affects the protein levels of active β-Catenin. This could be the result of inhibition of the β-Catenin destruction complex, due to reduction of the rate-limiting component Axin1 and of Gsk3β, via Akt-mediated phosphorylation [Li et al., 2012; Kim et al., 2013]. These results are consistent with a previous study in which it was shown how, after inhibition of the function of β-Catenin negative regulators, Wnt signaling can promote the undifferentiated phenotype of mouse ES cells [Kielman et al., 2002] through active β-Catenin, that moves to the nucleus and binds the downstream effectors Tcf1 and Tcf3 [Nusse, 2005]. Moreover, we demonstrated that c-Myc represses transcription of the Wnt antagonists Dkk1 and Sfrp1, therefore reinforcing the Wnt pathway activity. Several studies showed that Dkk1 and Sfrp1 promoters contain bivalent domains and are Polycomb targets [Trenkmann et al., 2011; Kaur and Cole, 2013]. Furthermore, it was observed that a subset of Polycomb target genes, with bivalent histone methylation patterns, are bound and regulated in response to altered c-Myc levels [Lin et al., 2009]. Given those findings, we propose that c-Myc can recruit Polycomb complex on the promoters of these genes to keep them repressed. In this work we demonstrated, by using different approaches, that c-Myc associates with the PRC2 complex through direct interaction with the core proteins Eed and Aebp2. Interestingly, among the PcG proteins, Aebp2 is the only transcription factor, which has been shown to have some degree of specificity in DNA binding [Kim et al., 2009]. The close association of c-Myc with Aebp2 within the PRC2 complex invokes the possibility of a synergism in the DNA-

binding recognition of the PRC2 complex, thus favoring the selection for specific loci. We show that c-Myc interacts with the Polycomb members Eed and Aebp2 through the MBII domain. This is a notable finding, since it has been shown that this domain is required for Myc-dependent cell transformation, because of its crucial role in the recruitment of multiprotein enzymatic complexes [Adhikary and Eilers, 2005]. Considering that Myc-dependent recruitment of the proper cofactor to a specific target gene is crucial for the transcriptional outcome, it is likely that a combination of events, including intracellular signaling that induce post-translational modifications, may play an important role in the selection of alternative complexes. The functional analysis reported in this work, based on shRNA-knockdowns, demonstrate that the integrity and biochemical activity of the PRC2 is required for Myc-mediated repression. Importantly, we showed that PRC2-dependent impairment of Myc-maintained ES cell self-renewal was restored upon reactivation of Wnt pathway. Our study is the first to report that c-Myc causes transcriptional repression by directly recruiting histone modifier on its target genes.

Although we do not exclude the possibility that c-Myc participates in recruiting PRC2 to other Polycomb target genes, involved in cell lineage commitment, our findings suggest an alternative role of PRC2 in ES cells. In fact, PRC2 has been described until now as a player in lineage priming with mild effects on self-renewal capacity [Leeb et al., 2010; Di Croce and Helin, 2013]. Here we show that PRC2 actually participate in the fine-tuning of Wnt signaling, thus sustaining self-renew of Myc-maintained ES cells. The apparent discrepancy between our findings and previous reports could be explained by considering that the role of PRC2 in self-renewal have been evaluated in ES cells grown in LIF-dependency [Boyer et al., 2006; Leeb et al., 2010] or in 2i medium [Riising et al., 2014], where other signaling cascades counterbalance the improper inhibition of the autocrine Wnt/β-Catenin pathway, as consequence of PRC2 inactivation.

We have shown a critical interplay between c-Myc activation and the autocrine Wnt/β-Catenin signaling, which drives the onset of a positive feedback loop through the transcriptional activation of the endogenous c- and N-Myc genes. This network motif stabilizes the TRN by counteracting the transcriptional repression activity of Tcf3, possibly through its association with β-Catenin, thus recapitulating the ground state of ES cells [Ying et al., 2008] (Figure 5.1).
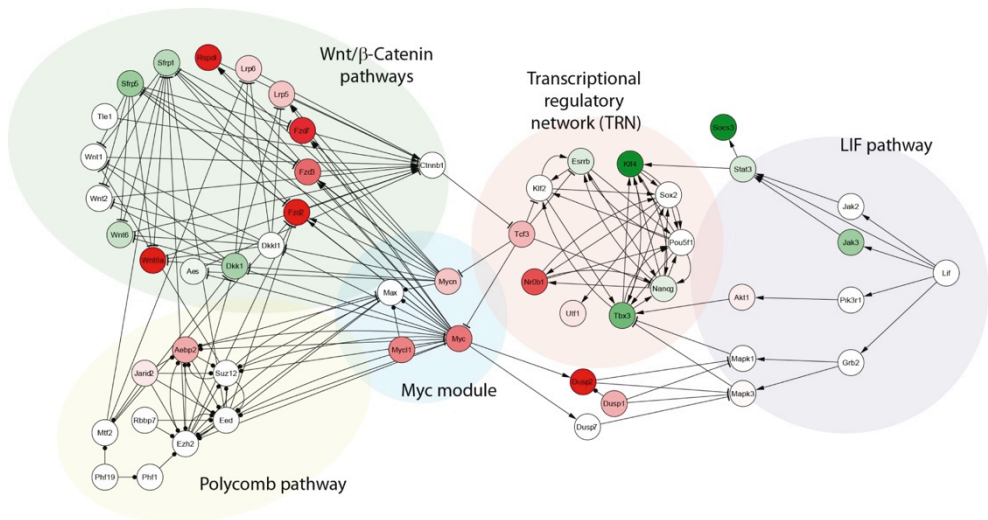
Figure 5.1 Network visualization of the Myc-mediated machinery to sustain ES cells self-renewal.

Three main molecular modules are shown, from right to left: the LIF signal transduction module, the core Transcriptional Regulatory Network (TRN), the Wnt/β-Catenin pathways and the Polycomb module. Network edges were manually curated according to literature knowledge, lab findings and completed querying interaction repositories: they indicate activation (arrowheads), inhibitions (T-shaped heads) and physical interactions (circle-shaped head).

5.2 c-Myc establishes an epigenetic memory in ES cells generating a self-reinforcing positive feedback motif

Many signaling pathways activated by environmental stimuli can establish Transcription Factors (TFs) networks, called "network motifs" [Shen-Orr et al., 2002; Milo et al., 2002]. Each motif has distinct properties, whose dynamic functions are achieved efficiently [Alon, 2007]. Although the specific components of corresponding networks motifs may vary greatly from one system to another, networks motifs represent the basic building block for the formation of cellular memory [Han et al., 2007]. Although it has been demonstrated that TFs networks are involved in establishing of cellular memory in prokaryotic cells, the molecular mechanisms through which they are able to act in eukaryotic cells have not been elucidated. In this work we report the central role of c-Myc in establishing an epigenetic memory in ES cells. Our data show that activation of MycER, by an external stimulus, establishes a positive feedback loop, by repressing the Wnt antagonists via PRC2 recruitment, thus sustaining Wnt signaling, which triggers the transcriptional activation of the endogenous c- and N-Myc genes (Figure 5.2A).

Several lines of evidence suggest that PRC-dependent silencing of Wnt antagonists is the main mediator of Myc-driven epigenetic memory in ES cells. First, the inhibition of Ezh2 methyltransferase activity shows that the biochemical function of the PRC2 is necessary to sustain ES cell self-renewal. Furthermore, activation of Wnt pathway, by exogenous Wnt3a, is able to compensate for the PRC2 inhibition. Second, the expression of endogenous c- and N-Myc is dependent from Wnt signaling activation. Third, even in the absence of environmental stimuli, c-Myc is able to recruit PRC2 on the promoters of Wnt antagonists, Dkk1 and Sfrp1.

Additional evidence for a role of c-Myc in establishing an epigenetic memory was obtained by reverse adaptation to the original culture

conditions. We find that, in agreement with general perspective of dynamic and reversible nature of histone post-translational modifications [Bernstein et al., 2007], the gene repression of Wnt antagonists in our system is highly specific and plastic, reverting back to the original steady state when given the appropriate environmental cues. Furthermore, upon reverse adaptation to growth in LIF containing medium, Myc-derived ES cells return sensitive to the LIF/Stat3 pathway, while returning to be unresponsive to the functional activity of PRC2 and Wnt pathway.

If c-Myc establishes an epigenetic memory and ES cells are able to self-renew in absence of further inputs, from either the ectopically expressed MycER protein or from exogenous LIF signaling, we would expect that Myc-derived ES cell were able to differentiate into all three germ layers. Indeed, we found that expression of lineage-specific genes increased when Myc-derived ES cells were induced to EBs differentiation. Therefore, Myc-derived ES cells were able to generate EpiSC in culture, a pivotal event in cellular differentiation [ten Berge et al., 2011]. Our results not only demonstrate that Myc-derived ES cells differentiate in vitro, but also that they are able to generate teratomas once injected in *Nude* mice.

As revealed in this study, for a cellular memory to be established, cells must be subjected to a prolonged stimulus for the required period (Figure 5.2B). Our data are in agreement with previous studies showing that if the feedback is weak, in response to a short stimulus the system returns to the basal level. As the feedback strength increases, the response to a stimulus can become irreversible and upon decreasing the stimulus to zero, the system still remains active [Xiong and Ferrell, 2003].
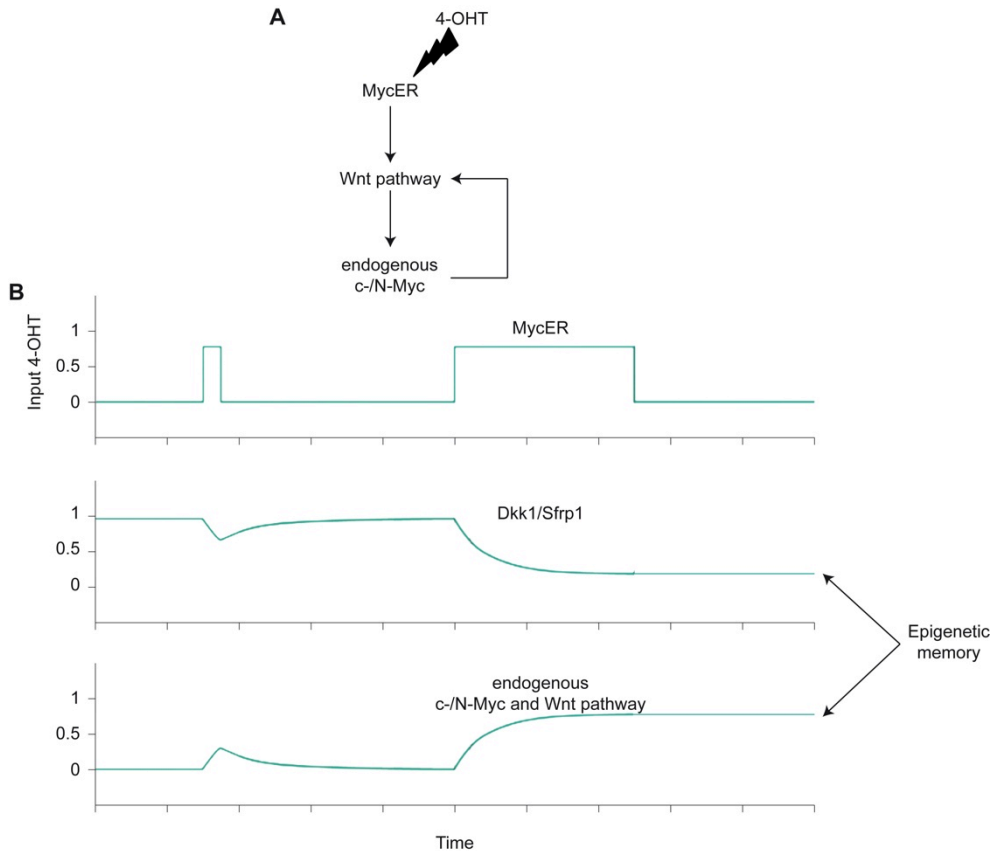
Figure 5.2 Schematic representation of experimental data.
(A) Signaling module composed of a positive feedback motif. (B) Response of a signaling module after different timing of stimulation.

5.3 c-MYC acts as tumor reprogramming factor in human mammary epithelial cells by inducing stem cell-like fate

Breast cancer is the most common cancer in woman with a mortality rate of 17% of all deaths due to cancer. About 12% of woman will develop invasive breast cancer during their lifetime [National Cancer Institute, NIH]. Cancer is both a genetic and epigenetic disease and epigenetic allows the genome to intrinsically integrate with environmental signals [Jaenisch and Bird, 2003]. These three determinants represent the major driving forces of tumorigenesis and they cause the functional heterogeneity observed in most of the cancer types. Evidence is accumulating that both normal and fully neoplastic cell populations harbor subpopulations of stem cells, which can both self-renew and spawn more differentiated progeny, that in the case of Cancer Stem Cells (CSCs) form the great bulk of many tumors [Chaffer and Weinberg, 2015]. However, the regulators that control the adult stem cells state are poorly understood, particularly in epithelial tissues. Given the previous considerations, along with the fact that SCs have a longer lifespan than more differentiated cells, the current view depicts normal SCs as the initial targets of oncogenic transformation. Accordingly, the population of normal SCs would accumulate a number of genetic alterations, until the CSCs population arises in a highly malignant tumor. However, this model is affected by at least two inconsistences: normal SCs population is too small and too rarely dividing to have the chance to accumulate more stochastic changes that confer advantage phenotype [Chaffer and Weinberg, 2015]. An alternative process seems to suggest a more likely model of how multistep tumor progression really proceeds. In this model transit amplifying progenitor cells, that are mitotically more active and more numerous than SCs, may serve as targets of somatic and epigenetic aberrations that can cause their alteration and de-differentiation to SCs. So, hierarchically organized cell populations

result more plastic than previously imagined [Chaffer and Weinberg, 2015]. In this view, cell transformation can be described as a cell reprogramming process towards a stem cell-like state in which a committed cell has to overcome a number of epigenetic barriers in order to alter its identity.

Moreover, developmental studies have demonstrated that TFs play an important role in establishing cellular states, including the SC state [Polytarchou et al., 2012; Rheinbay et al., 2013].

Here we report the central role of c-MYC in inducing reprogramming to a stem cell-like state in committed mammary epithelial cells. In particular, over-expression of c-MYC is sufficient to induce loss of both the typical epithelial cell phenotype and cell polarity, as the cells start to grow as non-adherent spheroids. In agreement with the results obtained with ES cells, preliminary data suggest that it could happen through hyper activation of the autocrine Wnt pathway, caused by MYC-driven epigenetic silencing of two major inhibitors of the wnt pathway, Dkk1 and Sfrp1 (Figure 5.3).
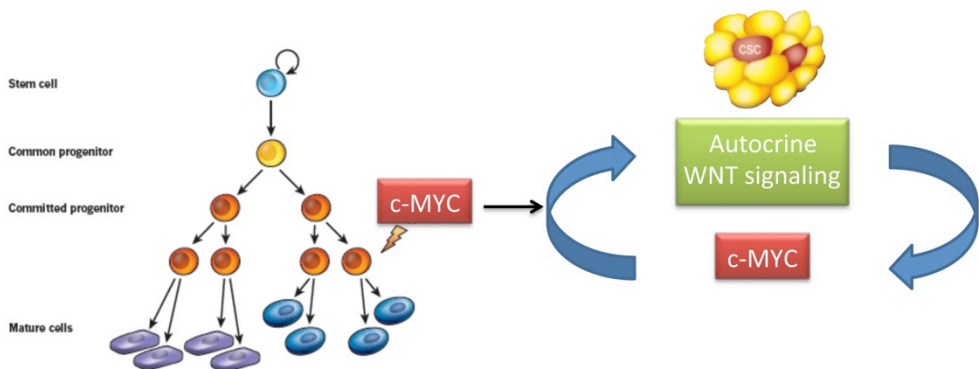
Figure 5.3 Schematic representation of experimental data.
[Modified from Visvader, 2011]

6. CONCLUSION

This work addressed the suspected role of the c-Myc protein in the regulation of self-renewal and pluripotency in mouse ES cells and it describes a molecular mechanism that can explain this ability. Our findings expose new evidence for Myc-induced transcriptional repression and for the first time it is shown that this occurs through the direct interaction between c-Myc and histone modifiers.

Although our study requires additional experiments in order to finalize some important results, it seems likely that cross-talk between environmental stimuli and TFs network motifs are the basis for the formation of cellular memories.

It is hoped that this work will stimulate further interest to study how differently TFs network motifs can interact and change or maintain a specific cell identity in response to different environmental stimuli. For instance, translating these studies to human ES cells would represent an enormous promise for regenerative medicine. However, how the epigenetic stability of hES cells is maintained in xeno-free culture conditions was poorly investigated so far.

Furthermore, the deregulation of TFs, concomitantly with epigenetic alterations, plays an important role in many types of cancer. However how the TFs interconnect between environmental stimuli and determine the reprogramming to SC-like state in tumor are poorly understood. A characterization of these networks could be of significance importance in order to identify new therapeutic targets, since treatment failure is often the result of CSCs escape from traditional therapies.

REFERENCES

1. Adhikary, S. and M. Eilers (2005). "Transcriptional regulation and transformation by Myc proteins." Nat Rev Mol Cell Biol **6**(8): 635-645.
2. Alon, U. (2007). "Network motifs: theory and experimental approaches." Nat Rev Genet **8**(6): 450-461.
3. Amati, B., M. W. Brooks, N. Levy, T. D. Littlewood, G. I. Evan and H. Land (1993). "Oncogenic activity of the c-Myc protein requires dimerization with Max." Cell **72**(2): 233-245.
4. Arney, K. L. and A. G. Fisher (2004). "Epigenetic aspects of differentiation." J Cell Sci **117**(Pt 19): 4355-4363.
5. Arnold, H. K., X. Zhang, C. J. Daniel, D. Tibbitts, J. Escamilla-Powers, A. Farrell, S. Tokarz, C. Morgan and R. C. Sears (2009). "The Axin1 scaffold protein promotes formation of a degradation complex for c-Myc." EMBO J **28**(5): 500-512.
6. Bannister, A. J. and T. Kouzarides (2011). "Regulation of chromatin by histone modifications." Cell Res **21**(3): 381-395.
7. Bernstein, B. E., A. Meissner and E. S. Lander (2007). "The mammalian epigenome." Cell **128**(4): 669-681.
8. Bernstein, B. E., T. S. Mikkelsen, X. Xie, M. Kamal, D. J. Huebert, J. Cuff, B. Fry, A. Meissner, M. Wernig, K. Plath, R. Jaenisch, A. Wagschal, R. Feil, S. L. Schreiber and E. S. Lander (2006). "A bivalent chromatin structure marks key developmental genes in embryonic stem cells." Cell **125**(2): 315-326.
9. Bird, A. and S. Tweedie (1995). "Transcriptional noise and the evolution of gene number." Philos Trans R Soc Lond B Biol Sci **349**(1329): 249-253.
10. Blackwell, T. K., L. Kretzner, E. M. Blackwood, R. N. Eisenman and H. Weintraub (1990). "Sequence-specific DNA binding by the c-Myc protein." Science **250**(4984): 1149-1151.
11. Bonasio, R., S. Tu and D. Reinberg (2010). "Molecular signals of epigenetic states." Science **330**(6004): 612-616.
12. Boyer, L. A., K. Plath, J. Zeitlinger, T. Brambrink, L. A. Medeiros, T. I. Lee, S. S. Levine, M. Wernig, A. Tajonar, M. K. Ray, G. W. Bell, A. P. Otte, M. Vidal, D. K. Gifford, R. A. Young and R. Jaenisch (2006). "Polycomb complexes repress developmental regulators in murine embryonic stem cells." Nature **441**(7091): 349-353.
13. Bracken, A. P., N. Dietrich, D. Pasini, K. H. Hansen and K. Helin (2006). "Genome-wide mapping of Polycomb target genes unravels their roles in cell fate transitions." Genes Dev **20**(9): 1123-1136.
14. Bruggeman, S. W., D. Hulsman, E. Tanger, T. Buckle, M. Blom, J. Zevenhoven, O. van Tellingen and M. van Lohuizen (2007). "Bmi1 controls tumor development in an Ink4a/Arf-independent manner in a mouse model for glioma." Cancer Cell **12**(4): 328-341.

15.	Buchwald, G., P. van der Stoop, O. Weichenrieder, A. Perrakis, M. van Lohuizen and T. K. Sixma (2006). "Structure and E3-ligase activity of the Ring-Ring complex of polycomb proteins Bmi1 and Ring1b." EMBO J **25**(11): 2465-2474.

16.	Cao, R., Y. Tsukada and Y. Zhang (2005). "Role of Bmi-1 and Ring1A in H2A ubiquitylation and Hox gene silencing." Mol Cell **20**(6): 845-854.

17.	Cao, R., L. Wang, H. Wang, L. Xia, H. Erdjument-Bromage, P. Tempst, R. S. Jones and Y. Zhang (2002). "Role of histone H3 lysine 27 methylation in Polycomb-group silencing." Science **298**(5595): 1039-1043.

18.	Capecchi, M. R. (2005). "Gene targeting in mice: functional analysis of the mammalian genome for the twenty-first century." Nat Rev Genet **6**(6): 507-512.

19.	Cartwright, P., C. McLean, A. Sheppard, D. Rivett, K. Jones and S. Dalton (2005). "LIF/STAT3 controls ES cell self-renewal and pluripotency by a Myc-dependent mechanism." Development **132**(5): 885-896.

20.	Chaffer, C. L. and R. A. Weinberg (2015). "How does multistep tumorigenesis really proceed?" Cancer Discov **5**(1): 22-24.

21.	Chambers, I., D. Colby, M. Robertson, J. Nichols, S. Lee, S. Tweedie and A. Smith (2003). "Functional expression cloning of Nanog, a pluripotency sustaining factor in embryonic stem cells." Cell **113**(5): 643-655.

22.	Chen, X., H. Xu, P. Yuan, F. Fang, M. Huss, V. B. Vega, E. Wong, Y. L. Orlov, W. Zhang, J. Jiang, Y. H. Loh, H. C. Yeo, Z. X. Yeo, V. Narang, K. R. Govindarajan, B. Leong, A. Shahab, Y. Ruan, G. Bourque, W. K. Sung, N. D. Clarke, C. L. Wei and H. H. Ng (2008). "Integration of external signaling pathways with the core transcriptional network in embryonic stem cells." Cell **133**(6): 1106-1117.

23.	Ciferri, C., G. C. Lander, A. Maiolica, F. Herzog, R. Aebersold and E. Nogales (2012). "Molecular architecture of human polycomb repressive complex 2." Elife **1**: e00005.

24.	Clapier, C. R. and B. R. Cairns (2009). "The biology of chromatin remodeling complexes." Annu Rev Biochem **78**: 273-304.

25.	Cohen, P. and S. Frame (2001). "The renaissance of GSK3." Nat Rev Mol Cell Biol **2**(10): 769-776.

26.	Cowling, V. H. and M. D. Cole (2006). "Mechanism of transcriptional activation by the Myc oncoproteins." Semin Cancer Biol **16**(4): 242-252.

27.	Cozzio, A., E. Passegue, P. M. Ayton, H. Karsunky, M. L. Cleary and I. L. Weissman (2003). "Similar MLL-associated leukemias arising from self-renewing stem cells and short-lived myeloid progenitors."

Genes Dev **17**(24): 3029-3035.

28. Cross, S. H. and A. P. Bird (1995). "CpG islands and genes." <u>Curr Opin Genet Dev</u> **5**(3): 309-314.

29. Czermin, B., R. Melfi, D. McCabe, V. Seitz, A. Imhof and V. Pirrotta (2002). "Drosophila enhancer of Zeste/ESC complexes have a histone H3 methyltransferase activity that marks chromosomal Polycomb sites." <u>Cell</u> **111**(2): 185-196.

30. Danielian, P. S., R. White, S. A. Hoare, S. E. Fawell and M. G. Parker (1993). "Identification of residues in the estrogen receptor that confer differential sensitivity to estrogen and hydroxytamoxifen." <u>Mol Endocrinol</u> **7**(2): 232-240.

31. Davis, A. C., M. Wims, G. D. Spotts, S. R. Hann and A. Bradley (1993). "A null c-myc mutation causes lethality before 10.5 days of gestation in homozygotes and reduced fertility in heterozygous female mice." <u>Genes Dev</u> **7**(4): 671-682.

32. Delaval, K. and R. Feil (2004). "Epigenetic regulation of mammalian genomic imprinting." <u>Curr Opin Genet Dev</u> **14**(2): 188-195.

33. Di Croce, L. and K. Helin (2013). "Transcriptional regulation by Polycomb group proteins." <u>Nat Struct Mol Biol</u> **20**(10): 1147-1155.

34. DiRenzo, J., S. Signoretti, N. Nakamura, R. Rivera-Gonzalez, W. Sellers, M. Loda and M. Brown (2002). "Growth factor requirements and basal phenotype of an immortalized mammary epithelial cell line." <u>Cancer Res</u> **62**(1): 89-98.

35. Eberhardy, S. R. and P. J. Farnham (2001). "c-Myc mediates activation of the cad promoter via a post-RNA polymerase II recruitment mechanism." <u>J Biol Chem</u> **276**(51): 48562-48571.

36. Eilers, M. and R. N. Eisenman (2008). "Myc's broad reach." <u>Genes Dev</u> **22**(20): 2755-2766.

37. Ezhkova, E., H. A. Pasolli, J. S. Parker, N. Stokes, I. H. Su, G. Hannon, A. Tarakhovsky and E. Fuchs (2009). "Ezh2 orchestrates gene expression for the stepwise differentiation of tissue-specific stem cells." <u>Cell</u> **136**(6): 1122-1135.

38. Frank, S. R., T. Parisi, S. Taubert, P. Fernandez, M. Fuchs, H. M. Chan, D. M. Livingston and B. Amati (2003). "MYC recruits the TIP60 histone acetyltransferase complex to chromatin." <u>EMBO Rep</u> **4**(6): 575-580.

39. Gil, J., D. Bernard and G. Peters (2005). "Role of polycomb group proteins in stem cell self-renewal and cancer." <u>DNA Cell Biol</u> **24**(2): 117-125.

40. Gregory, M. A., Y. Qi and S. R. Hann (2003). "Phosphorylation by glycogen synthase kinase-3 controls c-myc proteolysis and subnuclear localization." <u>J Biol Chem</u> **278**(51): 51606-51612.

41. Han, Z., T. M. Vondriska, L. Yang, W. Robb MacLellan, J. N. Weiss and Z. Qu (2007). "Signal transduction network motifs and biological

memory." <u>J Theor Biol</u> **246**(4): 755-761.

42. Hann, S. R. (2006). "Role of post-translational modifications in regulating c-Myc proteolysis, transcriptional activity and biological function." <u>Semin Cancer Biol</u> **16**(4): 288-302.

43. Hann, S. R. and R. N. Eisenman (1984). "Proteins encoded by the human c-myc oncogene: differential expression in neoplastic cells." <u>Mol Cell Biol</u> **4**(11): 2486-2497.

44. Hayashi, K., H. Ohta, K. Kurimoto, S. Aramaki and M. Saitou (2011). "Reconstitution of the mouse germ cell specification pathway in culture by pluripotent stem cells." <u>Cell</u> **146**(4): 519-532.

45. Heard, E. (2005). "Delving into the diversity of facultative heterochromatin: the epigenetics of the inactive X chromosome." <u>Curr Opin Genet Dev</u> **15**(5): 482-489.

46. Holliday, R. (2006). "Epigenetics: a historical overview." <u>Epigenetics</u> **1**(2): 76-80.

47. Hydbring, P., F. Bahram, Y. Su, S. Tronnersjo, K. Hogstrand, N. von der Lehr, H. R. Sharifi, R. Lilischkis, N. Hein, S. Wu, J. Vervoorts, M. Henriksson, A. Grandien, B. Luscher and L. G. Larsson (2010). "Phosphorylation by Cdk2 is required for Myc to repress Ras-induced senescence in cotransformation." <u>Proc Natl Acad Sci U S A</u> **107**(1): 58-63.

48. Ideraabdullah, F. Y., S. Vigneau and M. S. Bartolomei (2008). "Genomic imprinting mechanisms in mammals." <u>Mutat Res</u> **647**(1-2): 77-85.

49. Izzo, A. and R. Schneider (2010). "Chatting histone modifications in mammals." <u>Brief Funct Genomics</u> **9**(5-6): 429-443.

50. Jaenisch, R. and A. Bird (2003). "Epigenetic regulation of gene expression: how the genome integrates intrinsic and environmental signals." <u>Nat Genet</u> **33 Suppl**: 245-254.

51. Jaenisch, R. and R. Young (2008). "Stem cells, the molecular circuitry of pluripotency and nuclear reprogramming." <u>Cell</u> **132**(4): 567-582.

52. Jenuwein, T. and C. D. Allis (2001). "Translating the histone code." <u>Science</u> **293**(5532): 1074-1080.

53. Kaji, K., I. M. Caballero, R. MacLeod, J. Nichols, V. A. Wilson and B. Hendrich (2006). "The NuRD component Mbd3 is required for pluripotency of embryonic stem cells." <u>Nat Cell Biol</u> **8**(3): 285-292.

54. Kaur, M. and M. D. Cole (2013). "MYC acts via the PTEN tumor suppressor to elicit autoregulation and genome-wide gene repression by activation of the Ezh2 methyltransferase." <u>Cancer Res</u> **73**(2): 695-705.

55. Kielman, M. F., M. Rindapaa, C. Gaspar, N. van Poppel, C. Breukel, S. van Leeuwen, M. M. Taketo, S. Roberts, R. Smits and R. Fodde (2002). "Apc modulates embryonic stem-cell differentiation by

controlling the dosage of beta-catenin signaling." Nat Genet **32**(4): 594-605.

56. Kim, H., K. Kang and J. Kim (2009). "AEBP2 as a potential targeting protein for Polycomb Repression Complex PRC2." Nucleic Acids Res **37**(9): 2940-2950.

57. Kim, J., A. J. Woo, J. Chu, J. W. Snow, Y. Fujiwara, C. G. Kim, A. B. Cantor and S. H. Orkin (2010). "A Myc network accounts for similarities between embryonic stem and cancer cell transcription programs." Cell **143**(2): 313-324.

58. Kim, S. E., H. Huang, M. Zhao, X. Zhang, A. Zhang, M. V. Semonov, B. T. MacDonald, X. Zhang, J. Garcia Abreu, L. Peng and X. He (2013). "Wnt stabilization of beta-catenin reveals principles for morphogen receptor-scaffold assemblies." Science **340**(6134): 867-870.

59. Kirmizis, A., S. M. Bartley and P. J. Farnham (2003). "Identification of the polycomb group protein SU(Z)12 as a potential molecular target for human cancer therapy." Mol Cancer Ther **2**(1): 113-121.

60. Kleer, C. G., Q. Cao, S. Varambally, R. Shen, I. Ota, S. A. Tomlins, D. Ghosh, R. G. Sewalt, A. P. Otte, D. F. Hayes, M. S. Sabel, D. Livant, S. J. Weiss, M. A. Rubin and A. M. Chinnaiyan (2003). "EZH2 is a marker of aggressive breast cancer and promotes neoplastic transformation of breast epithelial cells." Proc Natl Acad Sci U S A **100**(20): 11606-11611.

61. Kouzarides, T. (2007). "Chromatin modifications and their function." Cell **128**(4): 693-705.

62. Krivtsov, A. V., D. Twomey, Z. Feng, M. C. Stubbs, Y. Wang, J. Faber, J. E. Levine, J. Wang, W. C. Hahn, D. G. Gilliland, T. R. Golub and S. A. Armstrong (2006). "Transformation from committed progenitor to leukaemia stem cell initiated by MLL-AF9." Nature **442**(7104): 818-822.

63. Kurimoto, K., Y. Yabuta, K. Hayashi, H. Ohta, H. Kiyonari, T. Mitani, Y. Moritoki, K. Kohri, H. Kimura, T. Yamamoto, Y. Katou, K. Shirahige and M. Saitou (2015). "Quantitative Dynamics of Chromatin Remodeling during Germ Cell Specification from Mouse Embryonic Stem Cells." Cell Stem Cell **16**(5): 517-532.

64. Kuzmichev, A., R. Margueron, A. Vaquero, T. S. Preissner, M. Scher, A. Kirmizis, X. Ouyang, N. Brockdorff, C. Abate-Shen, P. Farnham and D. Reinberg (2005). "Composition and histone substrates of polycomb repressive group complexes change during cellular differentiation." Proc Natl Acad Sci U S A **102**(6): 1859-1864.

65. Kuzmichev, A., K. Nishioka, H. Erdjument-Bromage, P. Tempst and D. Reinberg (2002). "Histone methyltransferase activity associated with a human multiprotein complex containing the Enhancer of Zeste protein." Genes Dev **16**(22): 2893-2905.

66.   Lee, T. I., R. G. Jenner, L. A. Boyer, M. G. Guenther, S. S. Levine, R. M. Kumar, B. Chevalier, S. E. Johnstone, M. F. Cole, K. Isono, H. Koseki, T. Fuchikami, K. Abe, H. L. Murray, J. P. Zucker, B. Yuan, G. W. Bell, E. Herbolsheimer, N. M. Hannett, K. Sun, D. T. Odom, A. P. Otte, T. L. Volkert, D. P. Bartel, D. A. Melton, D. K. Gifford, R. Jaenisch and R. A. Young (2006). "Control of developmental regulators by Polycomb in human embryonic stem cells." Cell 125(2): 301-313.

67.   Leeb, M., D. Pasini, M. Novatchkova, M. Jaritz, K. Helin and A. Wutz (2010). "Polycomb complexes act redundantly to repress genomic repeats and genes." Genes Dev 24(3): 265-276.

68.   Levens, D. (2010). "You Don't Muck with MYC." Genes Cancer 1(6): 547-554.

69.   Levine, S. S., A. Weiss, H. Erdjument-Bromage, Z. Shao, P. Tempst and R. E. Kingston (2002). "The core of the polycomb repressive complex is compositionally and functionally conserved in flies and humans." Mol Cell Biol 22(17): 6070-6078.

70.   Lewis, E. B. (1978). "A gene complex controlling segmentation in Drosophila." Nature 276(5688): 565-570.

71.   Li, V. S., S. S. Ng, P. J. Boersema, T. Y. Low, W. R. Karthaus, J. P. Gerlach, S. Mohammed, A. J. Heck, M. M. Maurice, T. Mahmoudi and H. Clevers (2012). "Wnt signaling through inhibition of beta-catenin degradation in an intact Axin1 complex." Cell 149(6): 1245-1256.

72.   Li, Y., P. S. Choi, S. C. Casey, D. L. Dill and D. W. Felsher (2014). "MYC through miR-17-92 suppresses specific target genes to maintain survival, autonomous proliferation, and a neoplastic state." Cancer Cell 26(2): 262-272.

73.   Lin, C. H., C. Lin, H. Tanaka, M. L. Fero and R. N. Eisenman (2009). "Gene regulation and epigenetic remodeling in murine embryonic stem cells by c-Myc." PLoS One 4(11): e7839.

74.   Lin, C. Y., J. Loven, P. B. Rahl, R. M. Paranal, C. B. Burge, J. E. Bradner, T. I. Lee and R. A. Young (2012). "Transcriptional amplification in tumor cells with elevated c-Myc." Cell 151(1): 56-67.

75.   Luger, K., A. W. Mader, R. K. Richmond, D. F. Sargent and T. J. Richmond (1997). "Crystal structure of the nucleosome core particle at 2.8 A resolution." Nature 389(6648): 251-260.

76.   Lutterbach, B. and S. R. Hann (1994). "Hierarchical phosphorylation at N-terminal transformation-sensitive sites in c-Myc protein is regulated by mitogens and in mitosis." Mol Cell Biol 14(8): 5510-5522.

77.   MacArthur, B. D., A. Sevilla, M. Lenz, F. J. Muller, B. M. Schuldt, A. A. Schuppert, S. J. Ridden, P. S. Stumpf, M. Fidalgo, A. Ma'ayan, J. Wang and I. R. Lemischka (2012). "Nanog-dependent feedback loops

regulate murine embryonic stem cell heterogeneity." Nat Cell Biol **14**(11): 1139-1147.

78. Margueron, R. and D. Reinberg (2011). "The Polycomb complex PRC2 and its mark in life." Nature **469**(7330): 343-349.

79. Marks, H., T. Kalkan, R. Menafra, S. Denissov, K. Jones, H. Hofemeister, J. Nichols, A. Kranz, A. F. Stewart, A. Smith and H. G. Stunnenberg (2012). "The transcriptional and epigenomic foundations of ground state pluripotency." Cell **149**(3): 590-604.

80. Marson, A., S. S. Levine, M. F. Cole, G. M. Frampton, T. Brambrink, S. Johnstone, M. G. Guenther, W. K. Johnston, M. Wernig, J. Newman, J. M. Calabrese, L. M. Dennis, T. L. Volkert, S. Gupta, J. Love, N. Hannett, P. A. Sharp, D. P. Bartel, R. Jaenisch and R. A. Young (2008). "Connecting microRNA genes to the core transcriptional regulatory circuitry of embryonic stem cells." Cell **134**(3): 521-533.

81. Martinez, A. M. and G. Cavalli (2006). "The role of polycomb group proteins in cell cycle regulation during development." Cell Cycle **5**(11): 1189-1197.

82. McMahon, S. B., M. A. Wood and M. D. Cole (2000). "The essential cofactor TRRAP recruits the histone acetyltransferase hGCN5 to c-Myc." Mol Cell Biol **20**(2): 556-562.

83. Merrill, B. J. (2012). "Wnt pathway regulation of embryonic stem cell self-renewal." Cold Spring Harb Perspect Biol **4**(9): a007971.

84. Meshorer, E., D. Yellajoshula, E. George, P. J. Scambler, D. T. Brown and T. Misteli (2006). "Hyperdynamic plasticity of chromatin proteins in pluripotent embryonic stem cells." Dev Cell **10**(1): 105-116.

85. Meyer, N. and L. Z. Penn (2008). "Reflecting on 25 years with MYC." Nat Rev Cancer **8**(12): 976-990.

86. Milo, R., S. Shen-Orr, S. Itzkovitz, N. Kashtan, D. Chklovskii and U. Alon (2002). "Network motifs: simple building blocks of complex networks." Science **298**(5594): 824-827.

87. Mitsui, K., Y. Tokuzawa, H. Itoh, K. Segawa, M. Murakami, K. Takahashi, M. Maruyama, M. Maeda and S. Yamanaka (2003). "The homeoprotein Nanog is required for maintenance of pluripotency in mouse epiblast and ES cells." Cell **113**(5): 631-642.

88. Mohammad, H. P. and S. B. Baylin (2010). "Linking cell signaling and the epigenetic machinery." Nat Biotechnol **28**(10): 1033-1038.

89. Murry, C. E. and G. Keller (2008). "Differentiation of embryonic stem cells to clinically relevant populations: lessons from embryonic development." Cell **132**(4): 661-680.

90. Nekrasov, M., B. Wild and J. Muller (2005). "Nucleosome binding and histone methyltransferase activity of Drosophila PRC2." EMBO Rep **6**(4): 348-353.

91. Neri, F., A. Zippo, A. Krepelova, A. Cherubini, M. Rocchigiani and S. Oliviero (2012). "Myc regulates the transcription of the PRC2 gene to control the expression of developmental genes in embryonic stem cells." Mol Cell Biol **32**(4): 840-851.

92. Ng, J., C. M. Hart, K. Morgan and J. A. Simon (2000). "A Drosophila ESC-E(Z) protein complex is distinct from other polycomb group complexes and contains covalently modified ESC." Mol Cell Biol **20**(9): 3069-3078.

93. Nie, Z., G. Hu, G. Wei, K. Cui, A. Yamane, W. Resch, R. Wang, D. R. Green, L. Tessarollo, R. Casellas, K. Zhao and D. Levens (2012). "c-Myc is a universal amplifier of expressed genes in lymphocytes and embryonic stem cells." Cell **151**(1): 68-79.

94. Niwa, H., T. Burdon, I. Chambers and A. Smith (1998). "Self-renewal of pluripotent embryonic stem cells is mediated via activation of STAT3." Genes Dev **12**(13): 2048-2060.

95. Niwa, H., K. Ogawa, D. Shimosato and K. Adachi (2009). "A parallel circuit of LIF signalling pathways maintains pluripotency of mouse ES cells." Nature **460**(7251): 118-122.

96. Nusse, R. (2005). "Wnt signaling in disease and in development." Cell Res **15**(1): 28-32.

97. Orkin, S. H. and K. Hochedlinger (2011). "Chromatin connections to pluripotency and cellular reprogramming." Cell **145**(6): 835-850.

98. Pasini, D., A. P. Bracken, M. R. Jensen, E. Lazzerini Denchi and K. Helin (2004). "Suz12 is essential for mouse development and for EZH2 histone methyltransferase activity." EMBO J **23**(20): 4061-4071.

99. Polytarchou, C., D. Iliopoulos and K. Struhl (2012). "An integrated transcriptional regulatory circuit that reinforces the breast cancer stem cell state." Proc Natl Acad Sci U S A **109**(36): 14470-14475.

100. Ponzielli, R., S. Katz, D. Barsyte-Lovejoy and L. Z. Penn (2005). "Cancer therapeutics: targeting the dark side of Myc." Eur J Cancer **41**(16): 2485-2501.

101. Ramsahoye, B. H., D. Biniszkiewicz, F. Lyko, V. Clark, A. P. Bird and R. Jaenisch (2000). "Non-CpG methylation is prevalent in embryonic stem cells and may be mediated by DNA methyltransferase 3a." Proc Natl Acad Sci U S A **97**(10): 5237-5242.

102. Raz, R., C. K. Lee, L. A. Cannizzaro, P. d'Eustachio and D. E. Levy (1999). "Essential role of STAT3 for embryonic stem cell pluripotency." Proc Natl Acad Sci U S A **96**(6): 2846-2851.

103. Reya, T., A. W. Duncan, L. Ailles, J. Domen, D. C. Scherer, K. Willert, L. Hintz, R. Nusse and I. L. Weissman (2003). "A role for Wnt signalling in self-renewal of haematopoietic stem cells." Nature **423**(6938): 409-414.

104. Rheinbay, E., M. L. Suva, S. M. Gillespie, H. Wakimoto, A. P. Patel,

M. Shahid, O. Oksuz, S. D. Rabkin, R. L. Martuza, M. N. Rivera, D. N. Louis, S. Kasif, A. S. Chi and B. E. Bernstein (2013). "An aberrant transcription factor network essential for Wnt signaling and stem cell maintenance in glioblastoma." <u>Cell Rep</u> **3**(5): 1567-1579.

105. Rieger, M. A. and T. Schroeder (2009). "Instruction of lineage choice by hematopoietic cytokines." <u>Cell Cycle</u> **8**(24): 4019-4020.

106. Riising, E. M., I. Comet, B. Leblanc, X. Wu, J. V. Johansen and K. Helin (2014). "Gene silencing triggers polycomb repressive complex 2 recruitment to CpG islands genome wide." <u>Mol Cell</u> **55**(3): 347-360.

107. Ringrose, L. and R. Paro (2007). "Polycomb/Trithorax response elements and epigenetic memory of cell identity." <u>Development</u> **134**(2): 223-232.

108. Ryan, K. M. and G. D. Birnie (1996). "Myc oncogenes: the enigmatic family." <u>Biochem J</u> **314 (Pt 3)**: 713-721.

109. Sauvageau, M. and G. Sauvageau (2010). "Polycomb group proteins: multi-faceted regulators of somatic stem cells and cancer." <u>Cell Stem Cell</u> **7**(3): 299-313.

110. Schuettengruber, B., D. Chourrout, M. Vervoort, B. Leblanc and G. Cavalli (2007). "Genome regulation by polycomb and trithorax proteins." <u>Cell</u> **128**(4): 735-745.

111. Schwartz, Y. B. and V. Pirrotta (2007). "Polycomb silencing mechanisms and the management of genomic programmes." <u>Nat Rev Genet</u> **8**(1): 9-22.

112. Schwartz, Y. B. and V. Pirrotta (2008). "Polycomb complexes and epigenetic states." <u>Curr Opin Cell Biol</u> **20**(3): 266-273.

113. Sears, R., F. Nuckolls, E. Haura, Y. Taya, K. Tamai and J. R. Nevins (2000). "Multiple Ras-dependent phosphorylation pathways regulate Myc protein stability." <u>Genes Dev</u> **14**(19): 2501-2514.

114. Shao, Z., F. Raible, R. Mollaaghababa, J. R. Guyon, C. T. Wu, W. Bender and R. E. Kingston (1999). "Stabilization of chromatin structure by PRC1, a Polycomb complex." <u>Cell</u> **98**(1): 37-46.

115. Shen, X., Y. Liu, Y. J. Hsu, Y. Fujiwara, J. Kim, X. Mao, G. C. Yuan and S. H. Orkin (2008). "EZH1 mediates methylation on histone H3 lysine 27 and complements EZH2 in maintaining stem cell identity and executing pluripotency." <u>Mol Cell</u> **32**(4): 491-502.

116. Shen-Orr, S. S., R. Milo, S. Mangan and U. Alon (2002). "Network motifs in the transcriptional regulation network of Escherichia coli." <u>Nat Genet</u> **31**(1): 64-68.

117. Silva, J. and A. Smith (2008). "Capturing pluripotency." <u>Cell</u> **132**(4): 532-536.

118. Smith, K. N., A. M. Singh and S. Dalton (2010). "Myc represses primitive endoderm differentiation in pluripotent stem cells." <u>Cell Stem Cell</u> **7**(3): 343-354.

119. Soufi, A., G. Donahue and K. S. Zaret (2012). "Facilitators and

impediments of the pluripotency reprogramming factors' initial engagement with the genome." Cell **151**(5): 994-1004.

120. Sparmann, A. and M. van Lohuizen (2006). "Polycomb silencers control cell fate, development and cancer." Nat Rev Cancer **6**(11): 846-856.

121. Spotswood, H. T. and B. M. Turner (2002). "An increasingly complex code." J Clin Invest **110**(5): 577-582.

122. Sridharan, R., J. Tchieu, M. J. Mason, R. Yachechko, E. Kuoy, S. Horvath, Q. Zhou and K. Plath (2009). "Role of the murine reprogramming factors in the induction of pluripotency." Cell **136**(2): 364-377.

123. Staller, P., K. Peukert, A. Kiermaier, J. Seoane, J. Lukas, H. Karsunky, T. Moroy, J. Bartek, J. Massague, F. Hanel and M. Eilers (2001). "Repression of p15INK4b expression by Myc through association with Miz-1." Nat Cell Biol **3**(4): 392-399.

124. Stock, J. K., S. Giadrossi, M. Casanova, E. Brookes, M. Vidal, H. Koseki, N. Brockdorff, A. G. Fisher and A. Pombo (2007). "Ring1-mediated ubiquitination of H2A restrains poised RNA polymerase II at bivalent genes in mouse ES cells." Nat Cell Biol **9**(12): 1428-1435.

125. Suzuki, M. M. and A. Bird (2008). "DNA methylation landscapes: provocative insights from epigenomics." Nat Rev Genet **9**(6): 465-476.

126. Takahashi, K. and S. Yamanaka (2006). "Induction of pluripotent stem cells from mouse embryonic and adult fibroblast cultures by defined factors." Cell **126**(4): 663-676.

127. Taverna, S. D., H. Li, A. J. Ruthenburg, C. D. Allis and D. J. Patel (2007). "How chromatin-binding modules interpret histone modifications: lessons from professional pocket pickers." Nat Struct Mol Biol **14**(11): 1025-1040.

128. ten Berge, D., D. Kurek, T. Blauwkamp, W. Koole, A. Maas, E. Eroglu, R. K. Siu and R. Nusse (2011). "Embryonic stem cells require Wnt proteins to prevent differentiation to epiblast stem cells." Nat Cell Biol **13**(9): 1070-1075.

129. Trenkmann, M., M. Brock, R. E. Gay, C. Kolling, R. Speich, B. A. Michel, S. Gay and L. C. Huber (2011). "Expression and function of EZH2 in synovial fibroblasts: epigenetic repression of the Wnt inhibitor SFRP1 in rheumatoid arthritis." Ann Rheum Dis **70**(8): 1482-1488.

130. Tse, C., T. Sera, A. P. Wolffe and J. C. Hansen (1998). "Disruption of higher-order folding by core histone acetylation dramatically enhances transcription of nucleosomal arrays by RNA polymerase III." Mol Cell Biol **18**(8): 4629-4638.

131. Turner, B. M. (2009). "Epigenetic responses to environmental change and their evolutionary implications." Philos Trans R Soc Lond B Biol

Sci **364**(1534): 3403-3418.

132. Vennstrom, B., D. Sheiness, J. Zabielski and J. M. Bishop (1982). "Isolation and characterization of c-myc, a cellular homolog of the oncogene (v-myc) of avian myelocytomatosis virus strain 29." J Virol **42**(3): 773-779.

133. Visvader, J. E. (2011). "Cells of origin in cancer." Nature **469**(7330): 314-322.

134. Wang, H., L. Wang, H. Erdjument-Bromage, M. Vidal, P. Tempst, R. S. Jones and Y. Zhang (2004). "Role of histone H2A ubiquitination in Polycomb silencing." Nature **431**(7010): 873-878.

135. Whitcomb, S. J., A. Basu, C. D. Allis and E. Bernstein (2007). "Polycomb Group proteins: an evolutionary perspective." Trends Genet **23**(10): 494-502.

136. Xiong, W. and J. E. Ferrell, Jr. (2003). "A positive-feedback-based bistable 'memory module' that governs a cell fate decision." Nature **426**(6965): 460-465.

137. Ying, Q. L., J. Wray, J. Nichols, L. Batlle-Morera, B. Doble, J. Woodgett, P. Cohen and A. Smith (2008). "The ground state of embryonic stem cell self-renewal." Nature **453**(7194): 519-523.

138. Young, R. A. (2011). "Control of the embryonic stem cell state." Cell **144**(6): 940-954.

139. Zippo, A., A. De Robertis, R. Serafini and S. Oliviero (2007). "PIM1-dependent phosphorylation of histone H3 at serine 10 is required for MYC-dependent transcriptional activation and oncogenic transformation." Nat Cell Biol **9**(8): 932-944.

APPENDIX

A. List of Primers

Primer	Sequence	Application
Sfrp1 Fwd	CCGGCCCATCTACCCGTGTC	qPCR
Sfrp1 Rev	ACCGTTGTGCCTTGGGGCTT	qPCR
Dkkl1 Fwd	GAACACCTCCGGGTTCCT	qPCR
Dkkl1 Rev	TCCAGGTCTCGTAGCAGGTC	qPCR
Dkk1 Fwd	CCGGGAACTACTGCAAAAAT	qPCR
Dkk1 Rev	CCAAGGTTTTCAATGATGCTT	qPCR
Sfrp5 Fwd	GATCTGTGCCCAGTGTGAGA	qPCR
Sfrp5 Rev	TTAATGCGCATCTTGACCAC	qPCR
Tle5 Fwd	CGCGACTGACATGATGTTTC	qPCR
Tle5 Rev	GAGTCGGAGGTGGTGAACTT	qPCR
Tle2 Fwd	TGGCACCAGCTATCCACAC	qPCR
Tle2 Rev	AGGCGTTTCACAATCTCAGC	qPCR
Lef1 Fwd	TCCTGAAATCCCCACCTTCT	qPCR
Lef1 Rev	TGGGATAAACAGGCTGACCT	qPCR
Rspo1 Fwd	CGACATGAACAAATGCATCA	qPCR
Rspo1 Rev	CTCCTGACACTTGGTGCAGA	qPCR
Lrp5 Fwd	CATGGACATCCAAGTGCTGA	qPCR
Lrp5 Rev	TTGTCCTCCTCGCATGGT	qPCR
Fzd3 Fwd	GCAGCCTCCACAGGTCAC	qPCR
Fzd3 Rev	ACATGCTGCCGTGAGGTAG	qPCR
Fzd7 Fwd	GCCATTTGACTTGAAACTTGG	qPCR
Fzd7 Rev	TCCGCCTTCTCTCCTTGAG	qPCR
Fzd2 Fwd	ATCTGGTCCGGCAAGACA	qPCR
Fzd2 Rev	GCTGTTGGTGAGACGAGTGTAG	qPCR

Dkk1 promoter Fwd	AGAGGGCTTGCTTTTGATCC	ChIP
Dkk1 promoter Rev	TTCCTCCTGTCCTGTCCTGT	ChIP
Sfrp1 promoter Fwd	CACCCAGGTCTTCCTCTGTT	ChIP
Sfrp1 promoter Rev	AGCGACACGGGTAGATGG	ChIP
Pax6 Fwd	CACCAGACTCACCTGACACC	qPCR
Pax6 Rev	ACCGCCCTTGGTTAAAGTC	qPCR
Gata6 Fwd	GGTCTCTACAGCAAGATGAAT GG	qPCR
Gata6 Rev	TGGCACAGGACAGTCCAAG	qPCR
Pecam1 Fwd	CAAAGTGGAATCAAACCGTAT CT	qPCR
Pecam1 Rev	CTACAGGTGTGCCCGAG	qPCR
Oct4 Fwd	TGGGGGCAGAGAAGATGGTTG	qPCR
Oct4 Rev	AAGGCAGCGACTTGGAAGCC	qPCR
Sox2 Fwd	TTTTCGTTTTTAGGGTAAGGTA CTGGGAAG	qPCR
Sox2 Rev	CCACGTGAATAATCCTATATGC ATCACAAT	qPCR
Klf2 Fwd	TCGAGGCTAGATGCCTTGTGA	qPCR
Klf2 Rev	AAACGAAGCAGGCGGCAGA	qPCR
Fgf5 Fwd	AAAACCTGGTGCACCCTAGA	qPCR
Fgf5 Rev	CATCACATTCCCGAATTAAGC	qPCR
Wnt3 Fwd	CAGTGCCTGAGTGGGAGATT	qPCR
Wnt3 Rev	AGGGACTTCAGACCCGAGAT	qPCR
N-Myc Fwd	CCTCCGGAGAGGATACCTTG	qPCR
N-Myc Rev	TCTCTACGGTGACCACATCG	qPCR
c-Myc Fwd	CCTAGTGCTGCATGAGGAGA	qPCR
c-Myc Rev	TCCACAGACACCACATCAATTT	qPCR
Nanog Fwd	GCCTCCAGCAGATGCAAG	qPCR
Nanog Rev	GGTTTTGAAACCAGGTCTTAAC C	qPCR
Fwd_XhoI Eed	CATACTCGAGATGTCCGAGAG	Cloning

	GGAAGTGTC	
Rev_BamHI Eed	TATTGGATCCTTATCGAAGTCG ATCCCAGCG	Cloning
Fwd_XhoI Ezh2	CATACTCGAGATGGGCCAGAC TGGGAAGA	Cloning
Rev_BamHI Ezh2	TATTGGATCCTCAAGGGATTTC CATTTCTCTTTC	Cloning
Fwd_XhoI Aebp2	AGATCTCGAGATGGCCGCCGC TATCACC	Cloning
Rev_EcoRI Aebp2	TGCAGAATTCCCTCTTCAACCT CTTCTG	Cloning
Fwd_XhoI c-Myc	AGATCTCGAGCTGGATTTTTTT CGGGTA	Cloning
Rev_BamHI c-Myc	GGTGGATCCTTACGCACAAGA GTTCCGT	Cloning

B. List of Antibodies

Antibody	Code	Seller	Application
p44/42 (Erk1/2)	9102	Cell Signaling	WB
ph-p44/4 (Erk1/2) (Thr202/Tyr204) (D13.14.4E)	4370	Cell Signaling	WB
LRP6 (C47E12)	3395	Cell Signaling	WB
ph-LRP6 (Ser1490)	2568	Cell Signaling	WB
β−Catenin	8480	Cell Signaling	WB
Active β-Catenin (D13A1)	8814	Cell Signaling	WB
Axin1 (C76H11)	2087	Cell Signaling	WB
Tcf1 (C63D9)	2203	Cell Signaling	WB, PLA
Tcf3	SAB2102977	Sigma	WB, PLA
Tle3 (M-201)	sc-9124	Santa Cruz	WB
Tle4 (E-10)	sc-365406	Santa Cruz	WB
Gsk-3β (27C10)	9315	Cell Signaling	WB
Phospho-Gsk-3β (Ser9) (5B3)	9323	Cell Signaling	WB
Akt (pan) (40D4)	2920	Cell Signaling	WB
ph-Akt (Ser473) (D9E)	4060	Cell Signaling	WB
Ezh2 (AC22)	3147	Cell Signaling	WB
Suz12 (D39F6)	3737	Cell Signaling	WB, ChIP
Eed (AA19)	05-1320	Millipore	WB
Lamin B (B-10)	sc-374015	Santa Cruz	WB
β−Catenin	610153	BD	PLA
c-Myc (D84C12)	5605	Cell Signaling	WB, ChIP
β-Tubulin (H-235)	sc-9104	Santa Cruz	WB
Histone H3-trimethyl-K27	07-449	Millipore	ChIP
Histone H3-trimethyl-K4	07-473	Millipore	ChIP

Histone H3	9715	Cell Signaling	WB
Gapdh (6C5)	sc-32233	Santa Cruz	WB
Oct-3/4 (C-10)	sc-5279	Santa Cruz	WB
Sox-2 (Y-17)	sc-17320	Santa Cruz	WB
Nanog	A300-397A	Bethyl	WB
Klf4 (H-180)	sc-20691	Santa Cruz	WB
β−actina	A5441	Sigma	WB
N-Myc (NCM II 100)	OP13	Calbiochem	WB, ChIP
γ-Tubulin	T6557	Sigma	IF
E-Cadherin	610182	BD Pharingen	IF, WB
Pan-Cadherin	Ab6528	abcam	WB
Phalloidin	P1951	Sigma	IF